US011179076B2

(12) **United States Patent**
Abdolahad et al.

(10) **Patent No.: US 11,179,076 B2**
(45) **Date of Patent: *Nov. 23, 2021**

(54) **ELECTROCHEMICAL PROBE FOR CANCER DIAGNOSIS**

(71) Applicants: **Mohammad Abdolahad**, Tehran (IR); **Zohreh Sadat Miripour**, Tehran (IR); **Hadi Ghafari**, Tehran (IR); **Fereshteh Abbasvandi**, Tehran (IR); **Pooneh Mohaghegh**, Shiraz (IR); **Parisa Aghaee**, Tehran (IR); **Mahsa Faramarzpour Darzini**, Tehran (IR)

(72) Inventors: **Mohammad Abdolahad**, Tehran (IR); **Zohreh Sadat Miripour**, Tehran (IR); **Hadi Ghafari**, Tehran (IR); **Fereshteh Abbasvandi**, Tehran (IR); **Pooneh Mohaghegh**, Shiraz (IR); **Parisa Aghaee**, Tehran (IR); **Mahsa Faramarzpour Darzini**, Tehran (IR)

(*) Notice: Subject to any disclaimer, the term of this patent is extended or adjusted under 35 U.S.C. 154(b) by 0 days.

This patent is subject to a terminal disclaimer.

(21) Appl. No.: **17/035,663**

(22) Filed: **Sep. 28, 2020**

(65) **Prior Publication Data**

US 2021/0022650 A1 Jan. 28, 2021

Related U.S. Application Data

(63) Continuation of application No. 16/857,428, filed on Apr. 24, 2020, now Pat. No. 10,786,188, which is a (Continued)

(51) **Int. Cl.**
C12Q 1/02 (2006.01)
A61B 5/1459 (2006.01)
(Continued)

(52) **U.S. Cl.**
CPC ***A61B 5/1459*** (2013.01); ***A61B 5/6848*** (2013.01); ***C23C 14/14*** (2013.01);
(Continued)

(58) **Field of Classification Search**
CPC . A61B 5/1459; A61B 5/6848; C23C 16/0272; C23C 14/30; C23C 16/26;
(Continued)

(56) **References Cited**

U.S. PATENT DOCUMENTS

7,939,734 B1 * 5/2011 Li G01N 27/3277 435/6.1
2009/0061451 A1 * 3/2009 Achim G01N 33/5438 435/6.11

(Continued)

OTHER PUBLICATIONS

Wikipedia contributors. "America wire gauge." Wikipedia, The Free Encyclopedia, https://web.archive.org/web/20071103232133/http://en.Wikipedia.org:80/wiki/American_wire_gauge#Table_of_AWGs_and_approximate_corresponding_sizes, Nov. 3, 2007. Accessed Oct. 29, 2020 (Year: 2007).*

Primary Examiner — Andrey Shostak
(74) *Attorney, Agent, or Firm* — Bajwa IP Law Firm; Haris Zaheer Bajwa

(57) **ABSTRACT**

An electrochemical probe for in-vivo measurement of H_2O_2 oxidation within a living tissue. The electrochemical probe includes a sensing part and a handle. The sensing part includes a working electrode including a first biocompatible conductive needle, a counter electrode including a second biocompatible conductive needle, and a reference electrode including a third biocompatible conductive needle. The working electrode, the counter electrode, and the reference electrode are configured to be put in contact with the living tissue by inserting the sensing part into the living tissue. The handle includes an insertion part that may be configured to
(Continued)

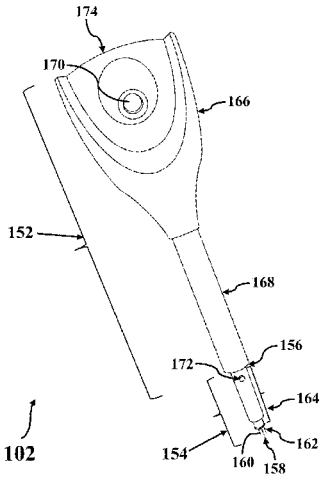

insert the sensing part into the living tissue. The sensing part is attached to the insertion part.

5 Claims, 75 Drawing Sheets

Related U.S. Application Data

continuation-in-part of application No. 16/010,510, filed on Jun. 17, 2018.

(60) Provisional application No. 62/522,115, filed on Jun. 20, 2017, provisional application No. 62/563,673, filed on Sep. 27, 2017.

(51) **Int. Cl.**

C23C 14/14	(2006.01)
C23C 14/30	(2006.01)
C23C 14/58	(2006.01)
G01N 33/50	(2006.01)
C23C 16/02	(2006.01)
C23C 16/26	(2006.01)
A61B 5/00	(2006.01)
G01N 33/574	(2006.01)

(52) **U.S. Cl.**

CPC ***C23C 14/30*** (2013.01); ***C23C 14/5806*** (2013.01); ***C23C 14/5846*** (2013.01); ***C23C 16/0272*** (2013.01); ***C23C 16/26*** (2013.01); ***G01N 33/5091*** (2013.01); ***G01N 33/574*** (2013.01)

(58) **Field of Classification Search**

CPC . C23C 14/5806; C23C 14/5846; C23C 14/14; G01N 33/5091; G01N 33/574

See application file for complete search history.

(56) **References Cited**

U.S. PATENT DOCUMENTS

2009/0076496	A1*	3/2009	Azure	A61B 18/1485 606/34
2013/0102027	A1	4/2013	Mohajerzadeh et al.	
2015/0005788	A1*	1/2015	Sniffin	A61B 17/068 606/139
2016/0095585	A1*	4/2016	Zergiebel	A61B 17/07207 606/1
2016/0258899	A1	9/2016	Patolsky et al.	
2019/0227028	A1	7/2019	Patolsky et al.	

* cited by examiner

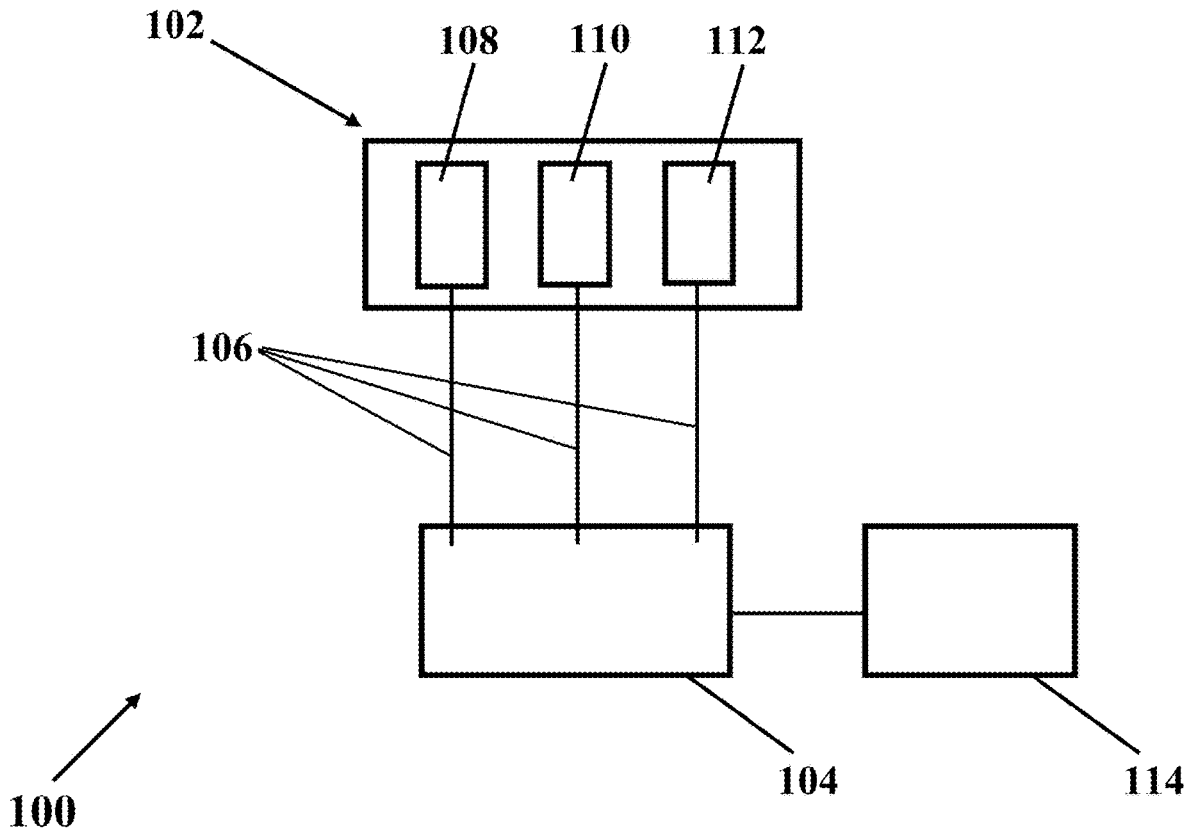

FIG. 1A

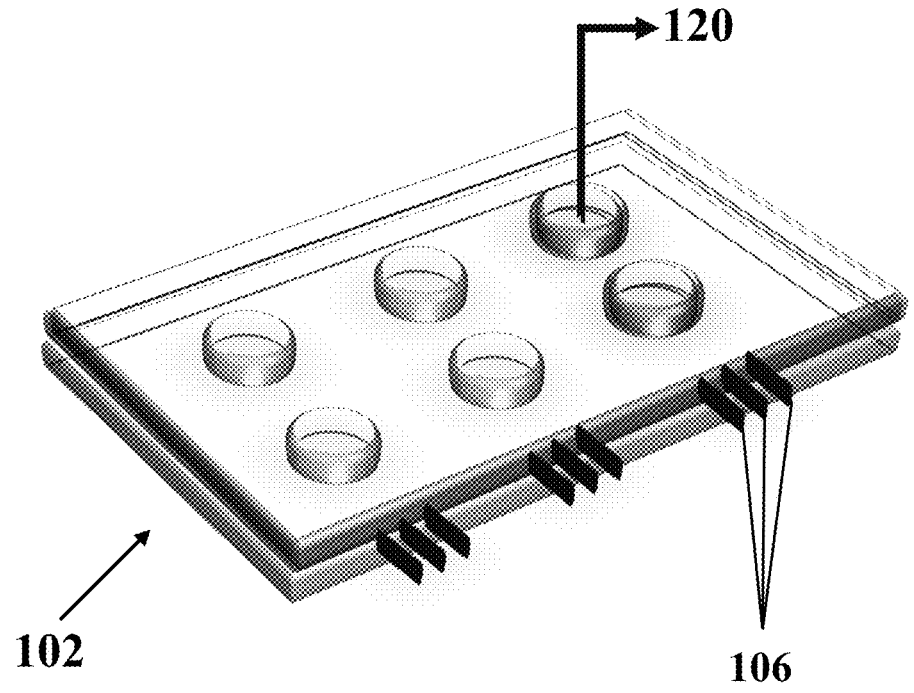

FIG. 1B

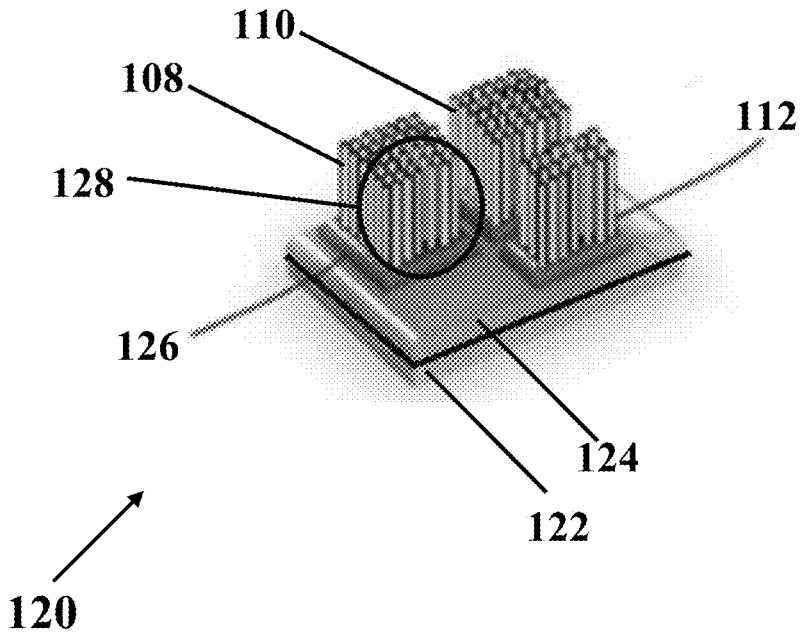

FIG. 1C

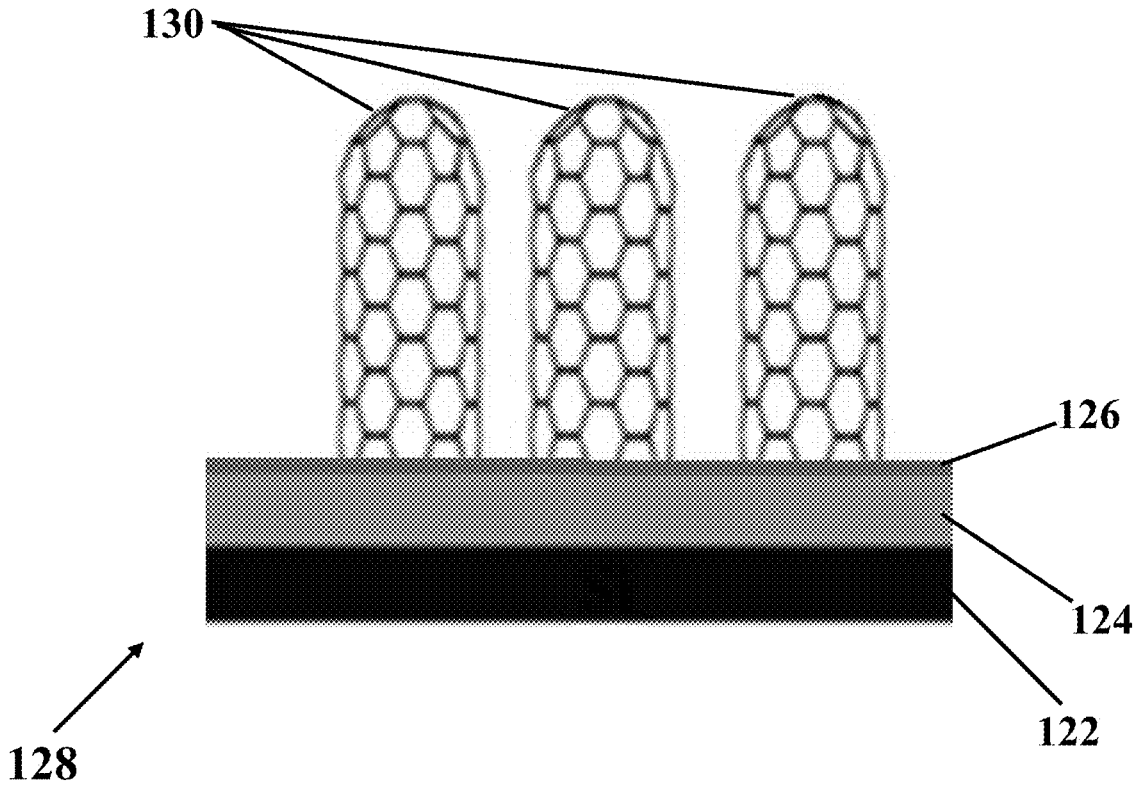

FIG. 1D

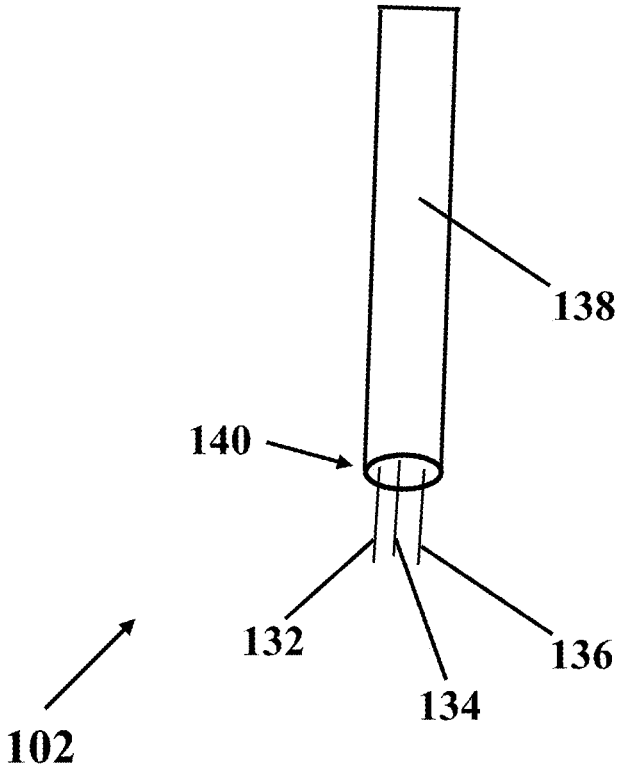

FIG. 1E

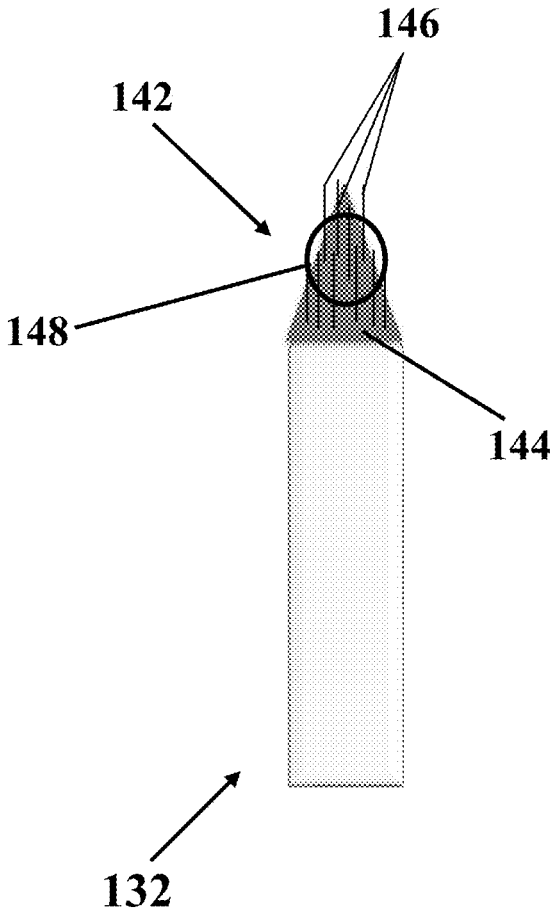

FIG. 1F

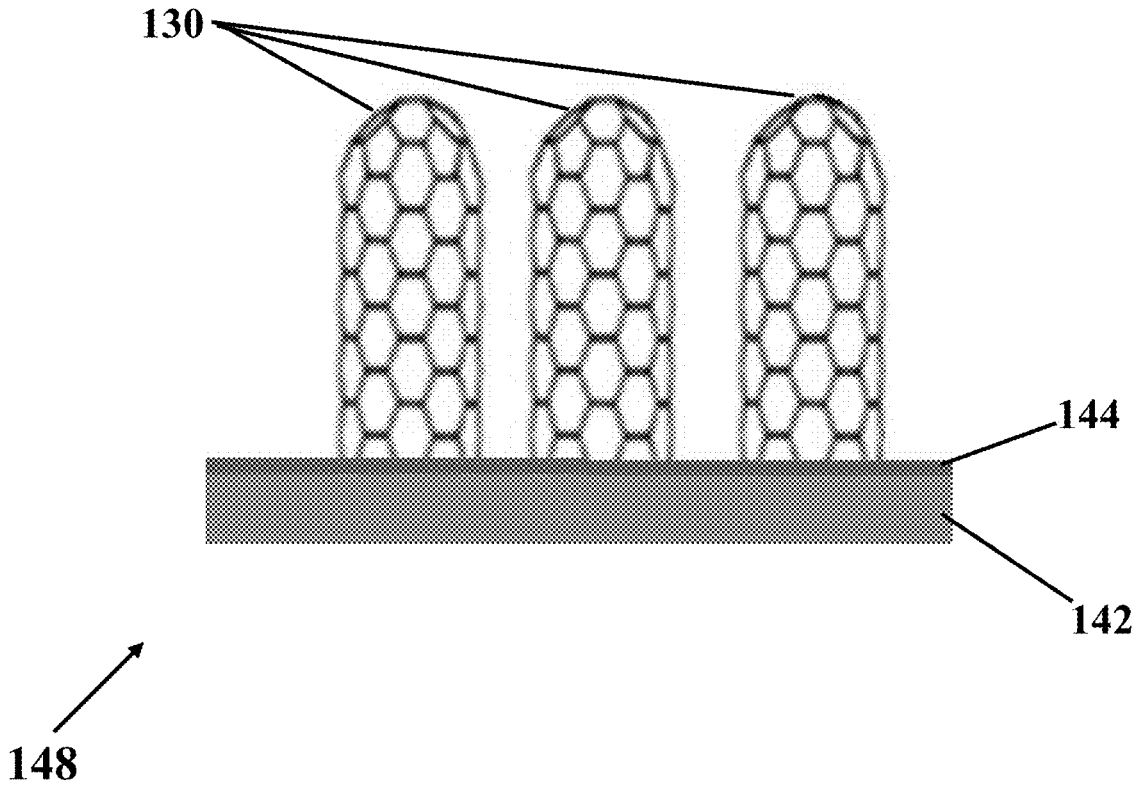

FIG. 1G

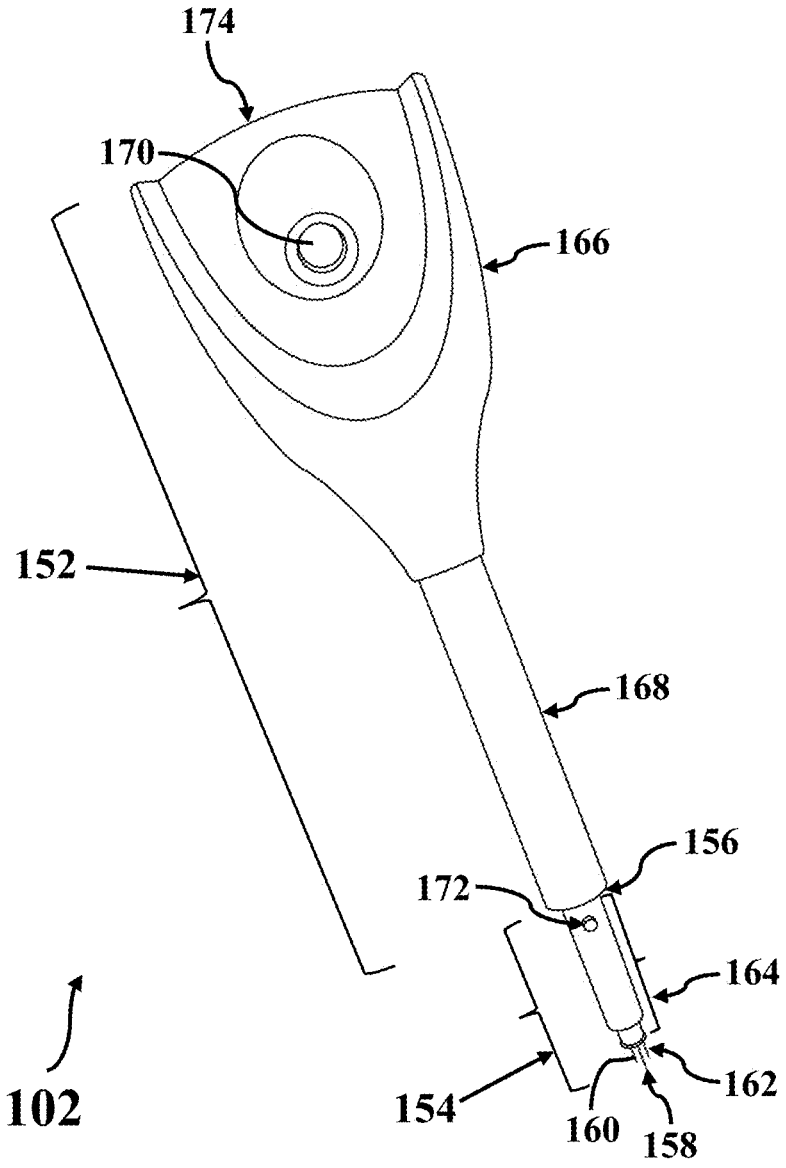

FIG. 1H

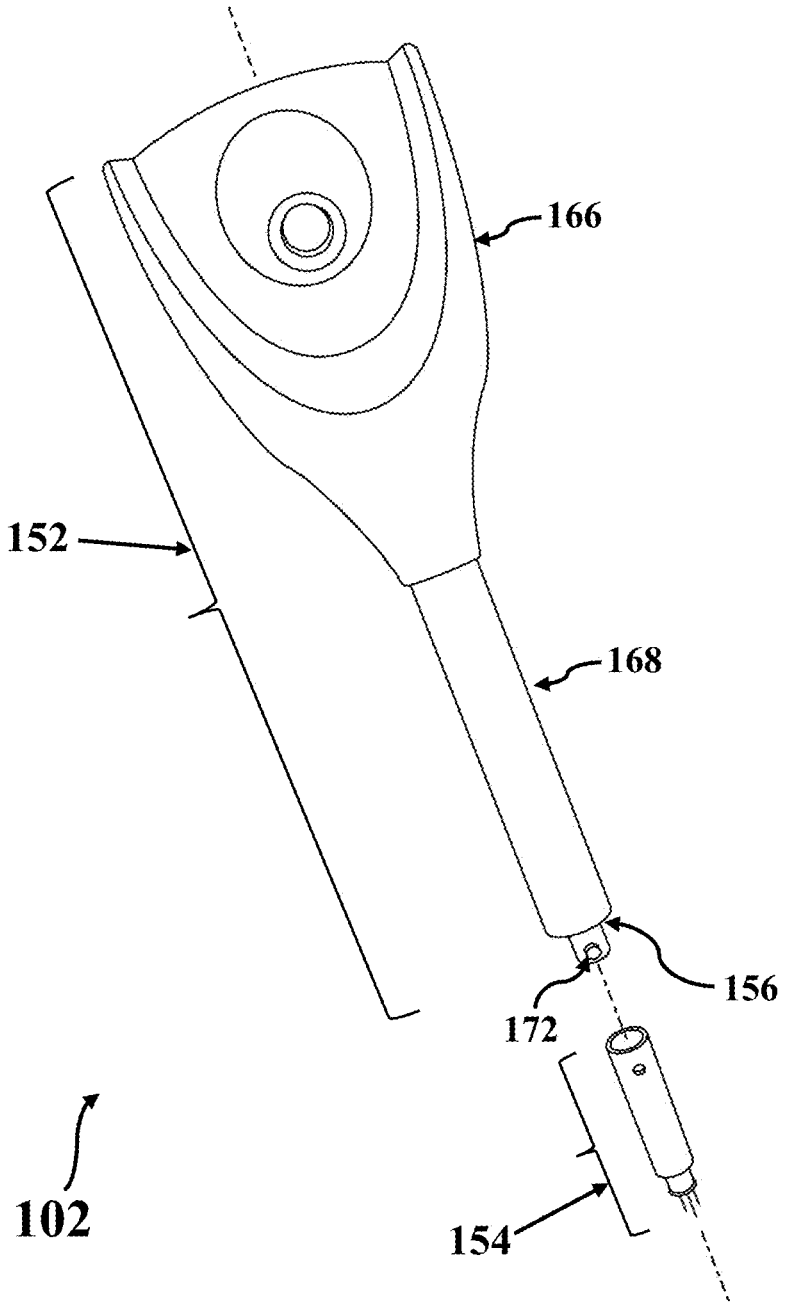

FIG. 1I

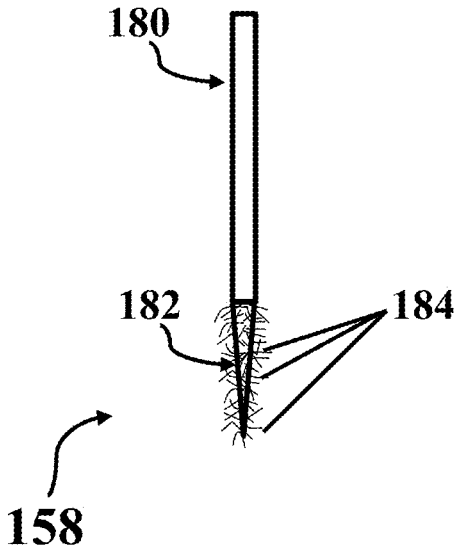

FIG. 1J

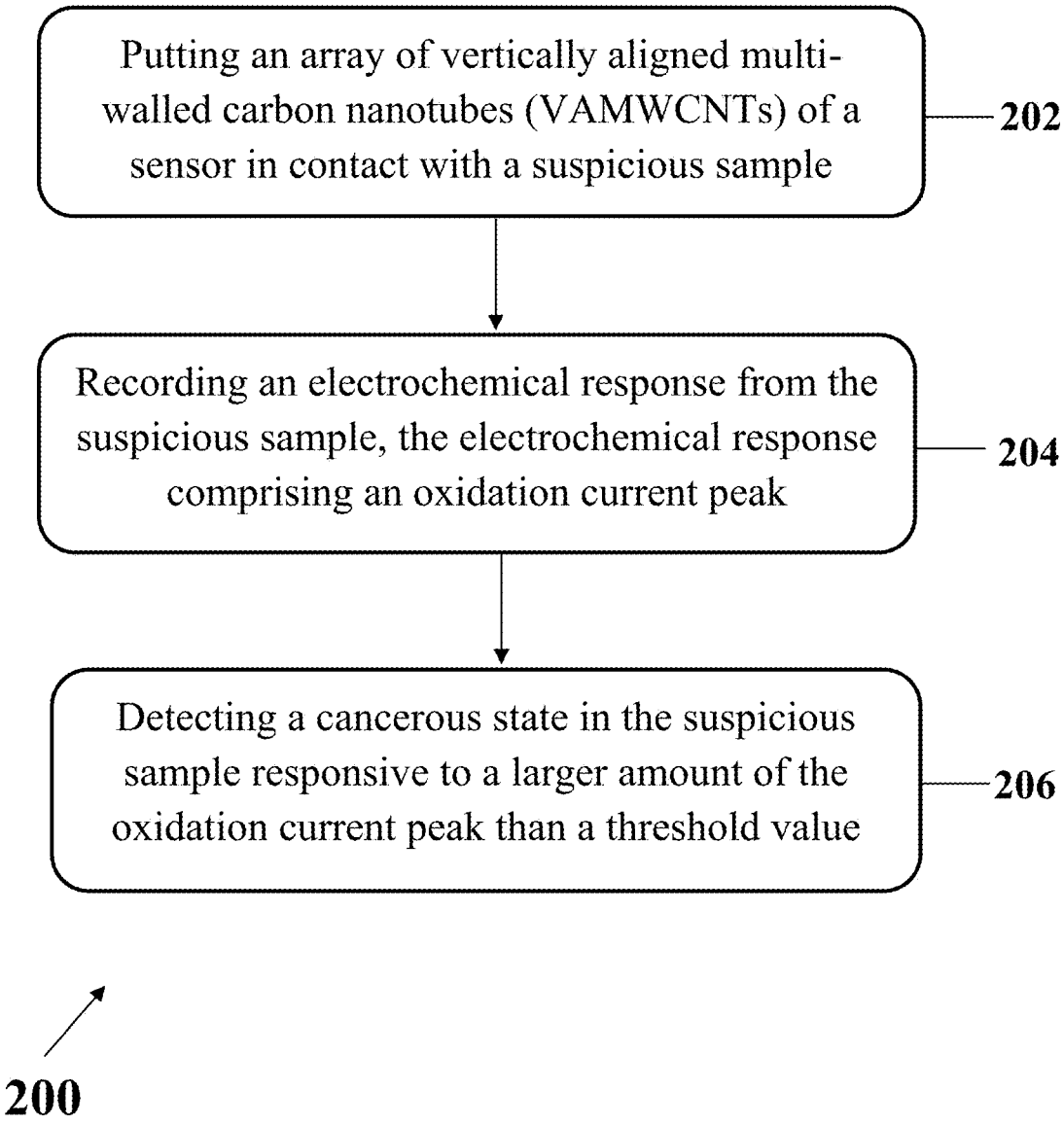
Putting an array of vertically aligned multi-walled carbon nanotubes (VAMWCNTs) of a sensor in contact with a suspicious sample
202
Recording an electrochemical response from the suspicious sample, the electrochemical response comprising an oxidation current peak
204
Detecting a cancerous state in the suspicious sample responsive to a larger amount of the oxidation current peak than a threshold value
206
200

FIG. 2A

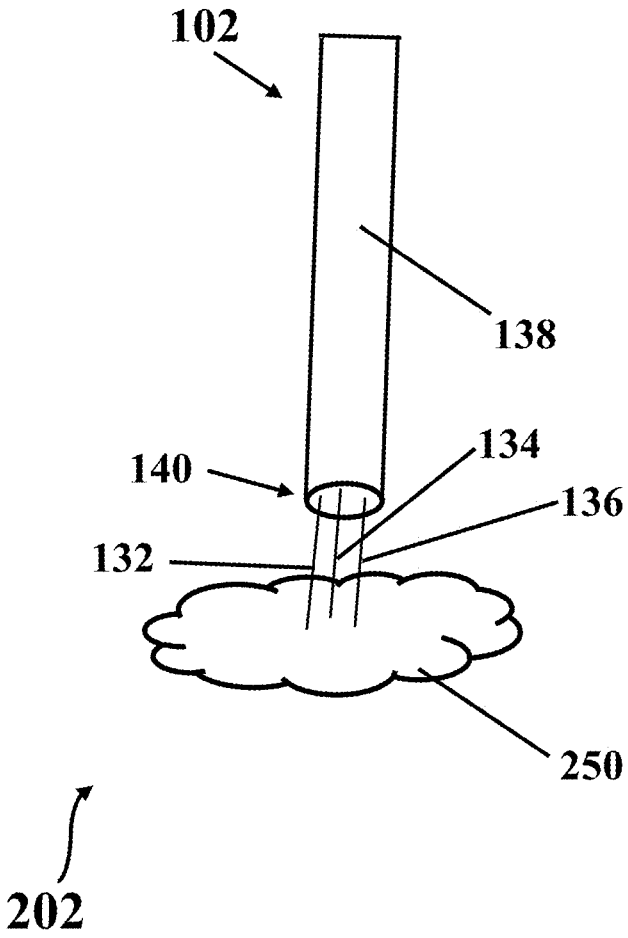

FIG. 2B

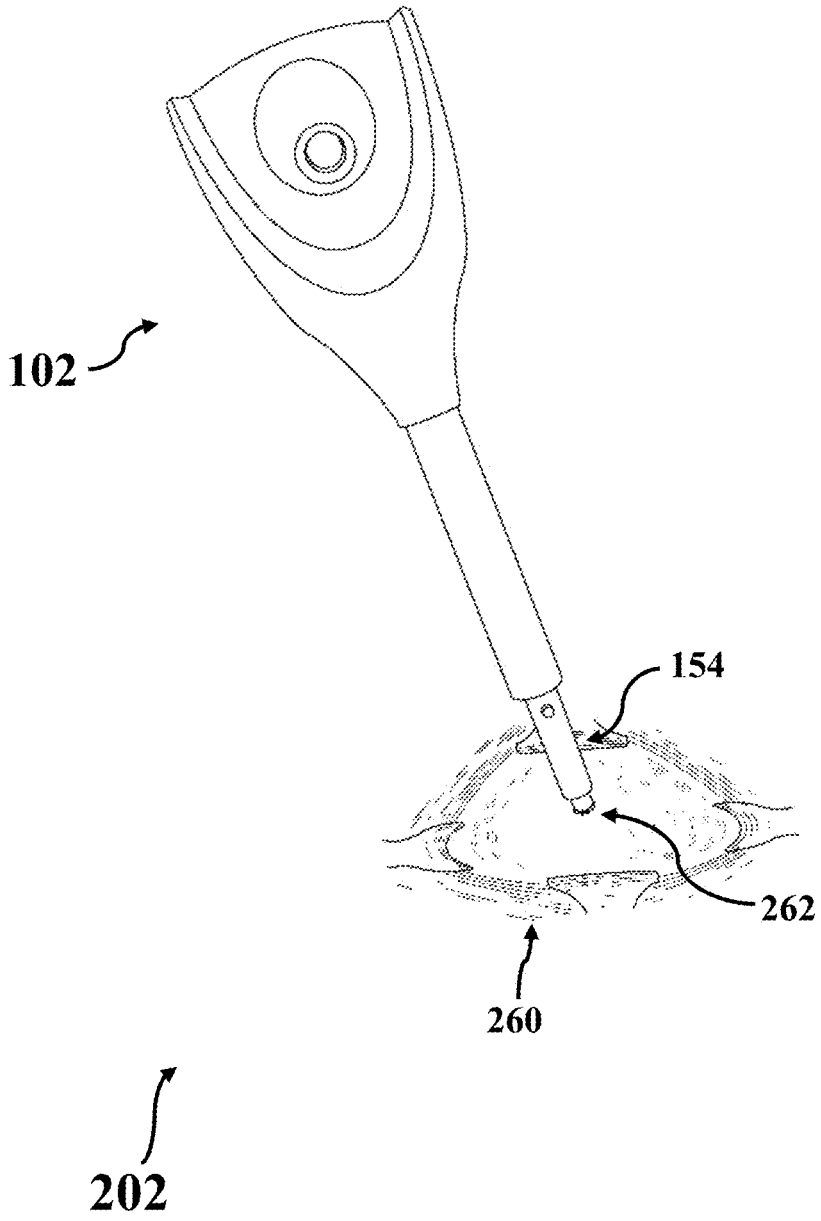

FIG. 2C

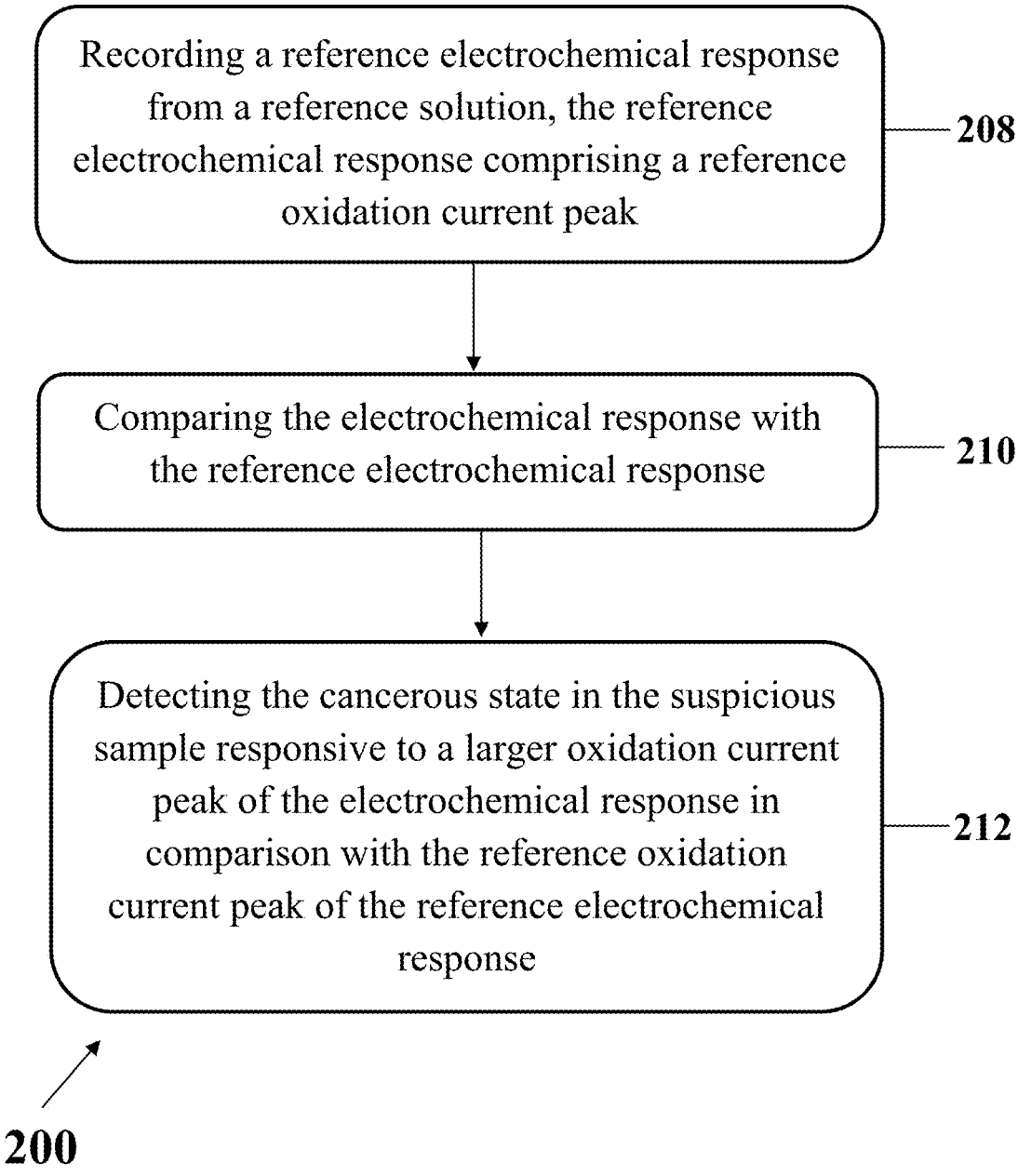
Recording a reference electrochemical response from a reference solution, the reference electrochemical response comprising a reference oxidation current peak
208
Comparing the electrochemical response with the reference electrochemical response
210
Detecting the cancerous state in the suspicious sample responsive to a larger oxidation current peak of the electrochemical response in comparison with the reference oxidation current peak of the reference electrochemical response
212
200

FIG. 2D

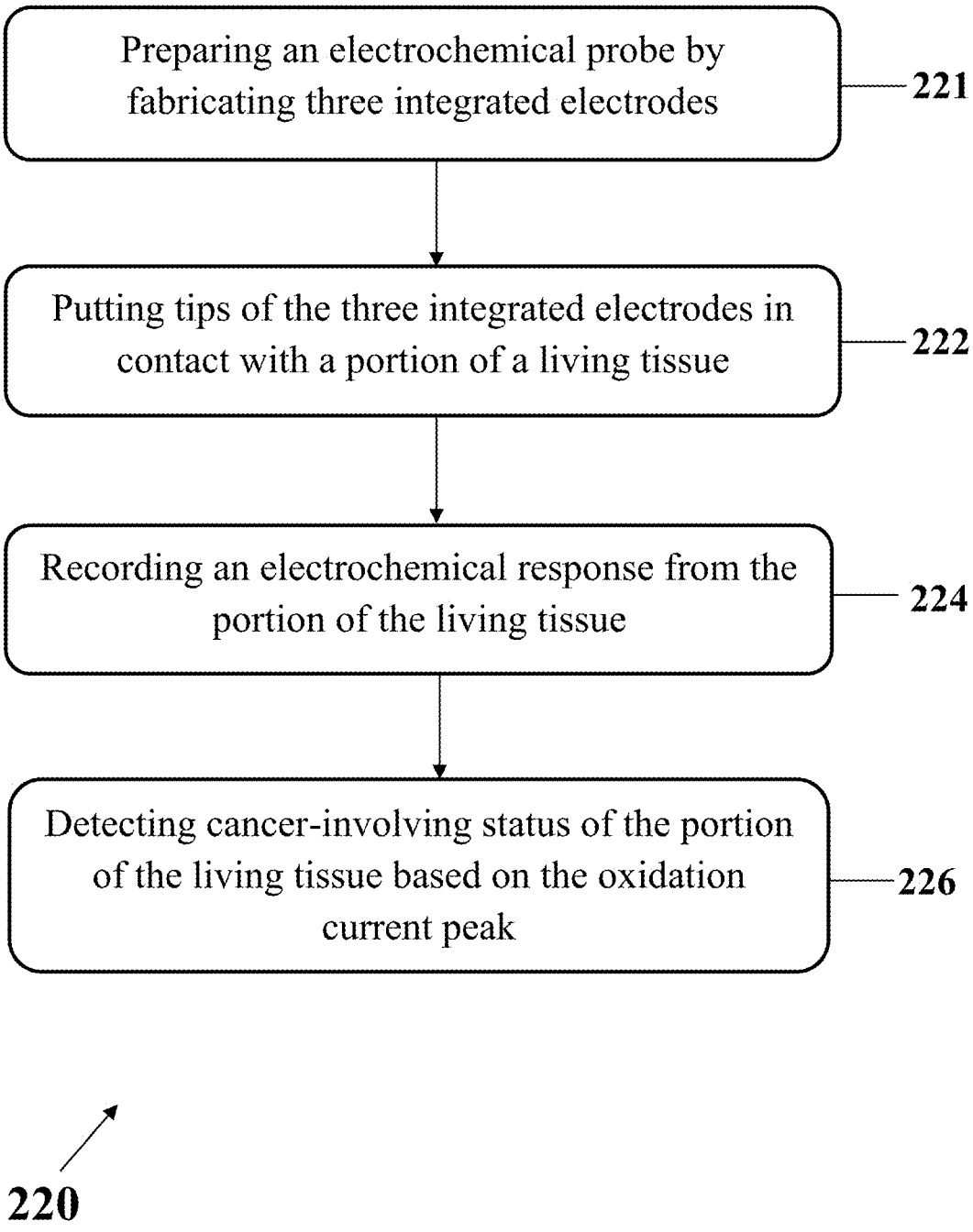
Preparing an electrochemical probe by fabricating three integrated electrodes
221
Putting tips of the three integrated electrodes in contact with a portion of a living tissue
222
Recording an electrochemical response from the portion of the living tissue
224
Detecting cancer-involving status of the portion of the living tissue based on the oxidation current peak
226
220

FIG. 2E

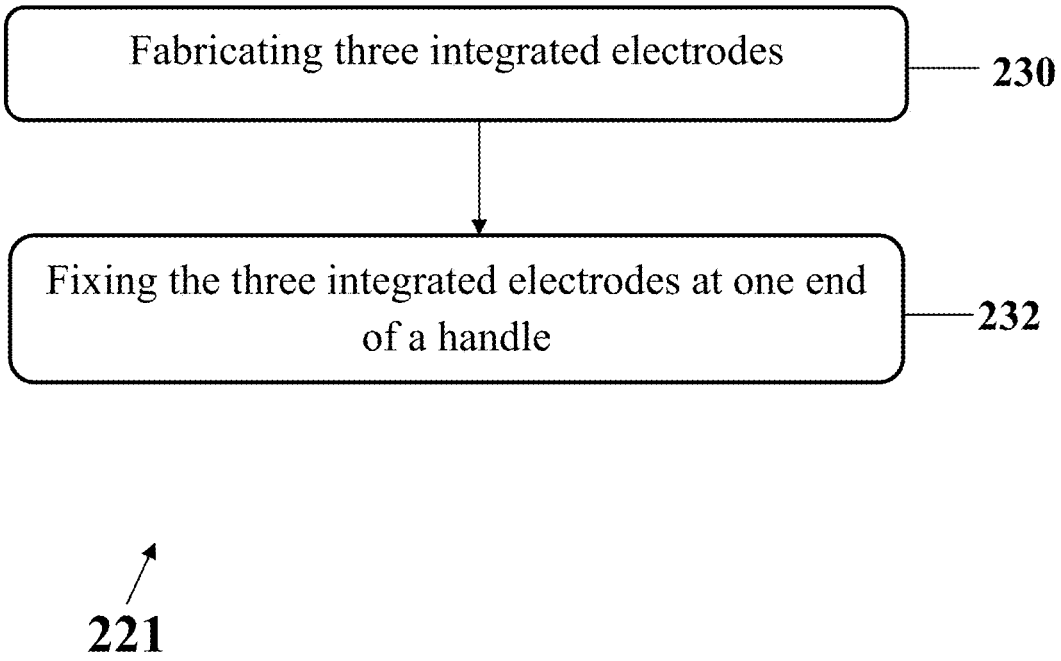
Fabricating three integrated electrodes
230
Fixing the three integrated electrodes at one end of a handle
232
221

FIG. 2F

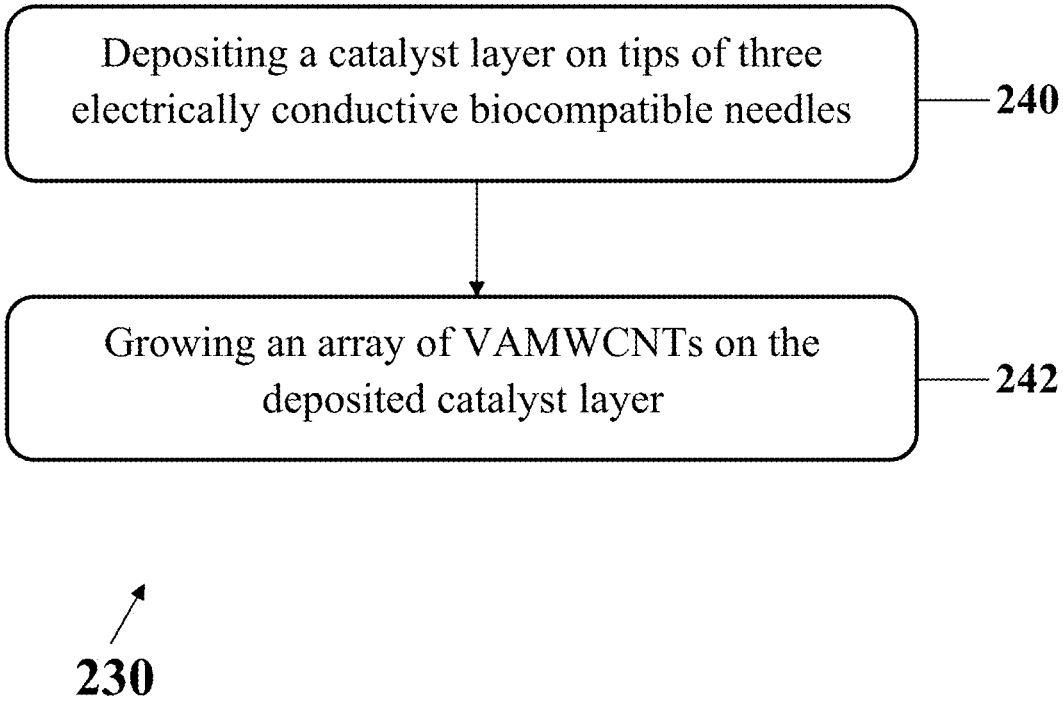
Depositing a catalyst layer on tips of three electrically conductive biocompatible needles
240
Growing an array of VAMWCNTs on the deposited catalyst layer
242
230

FIG. 2G

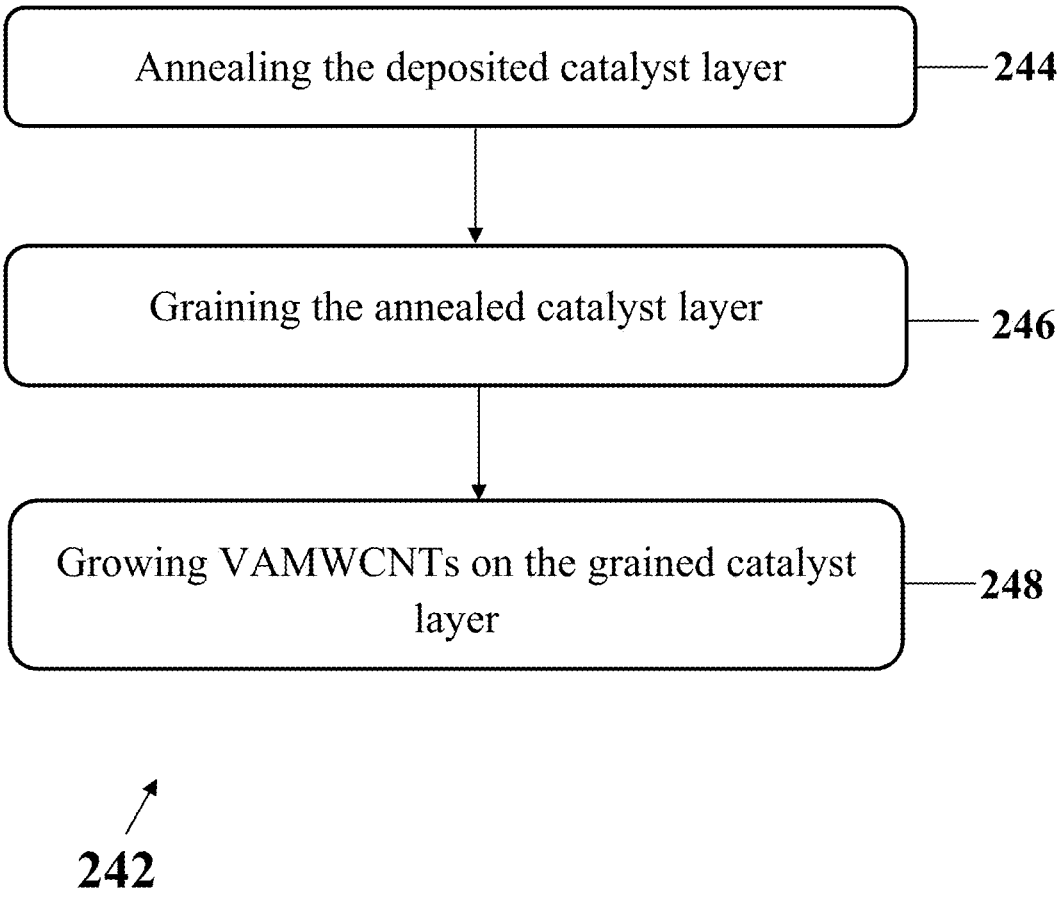
Annealing the deposited catalyst layer
244
Graining the annealed catalyst layer
246
Growing VAMWCNTs on the grained catalyst layer
248
242

FIG. 2H

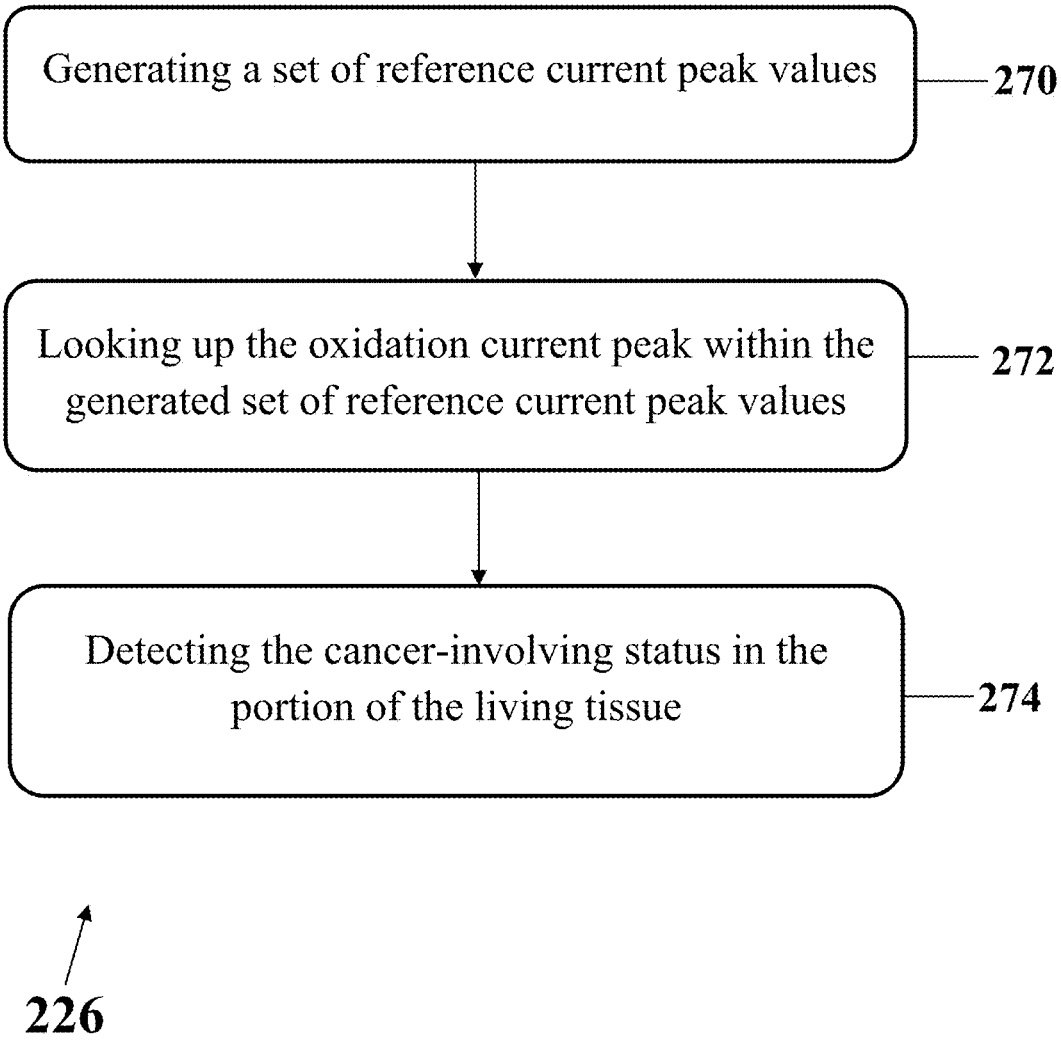
Generating a set of reference current peak values
270
Looking up the oxidation current peak within the generated set of reference current peak values
272
Detecting the cancer-involving status in the portion of the living tissue
274
226

FIG. 2I

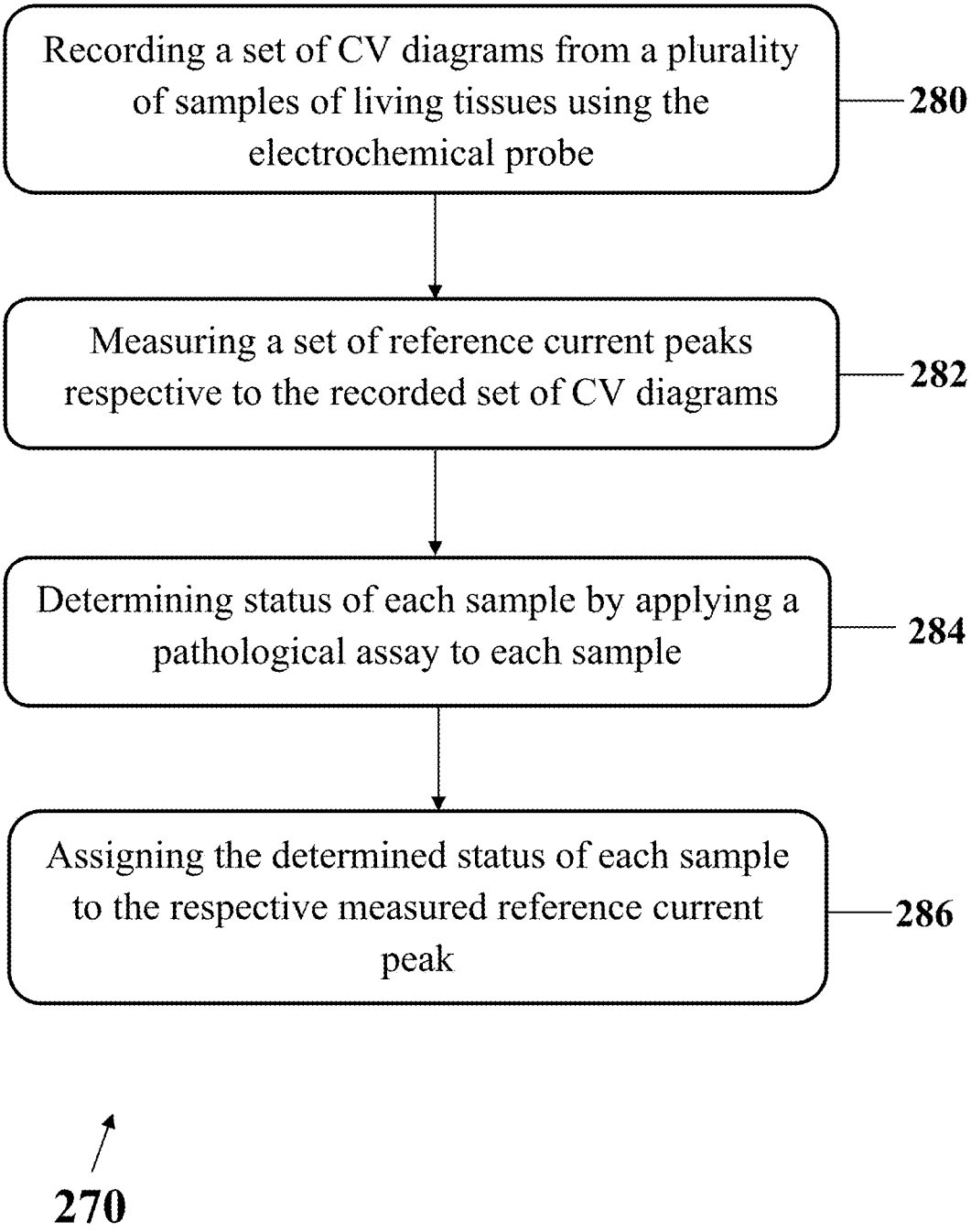
Recording a set of CV diagrams from a plurality of samples of living tissues using the electrochemical probe
280
Measuring a set of reference current peaks respective to the recorded set of CV diagrams
282
Determining status of each sample by applying a pathological assay to each sample
284
Assigning the determined status of each sample to the respective measured reference current peak
286
270

FIG. 2J

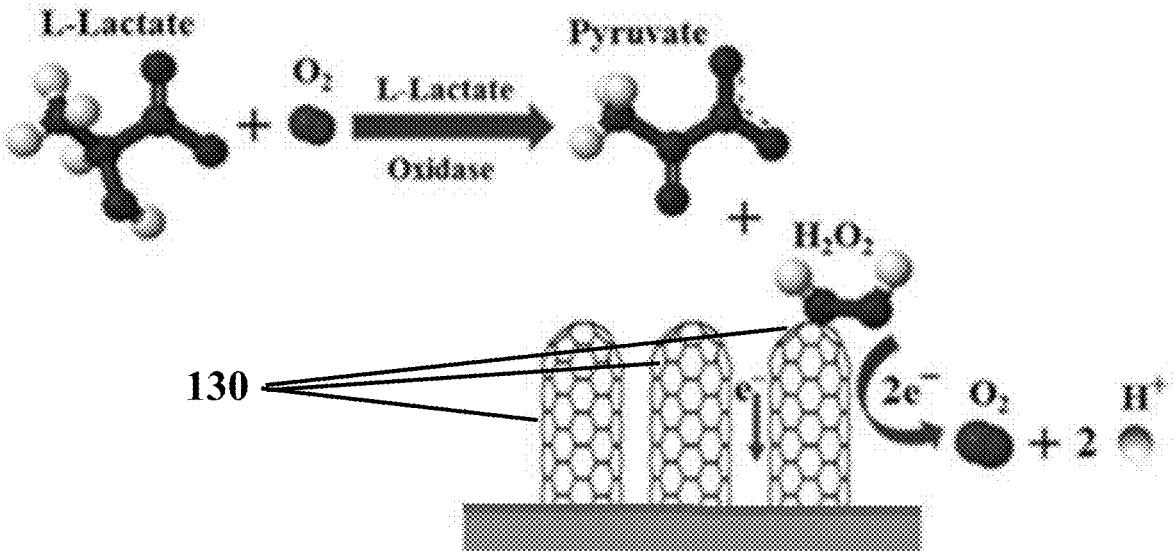

FIG. 3A

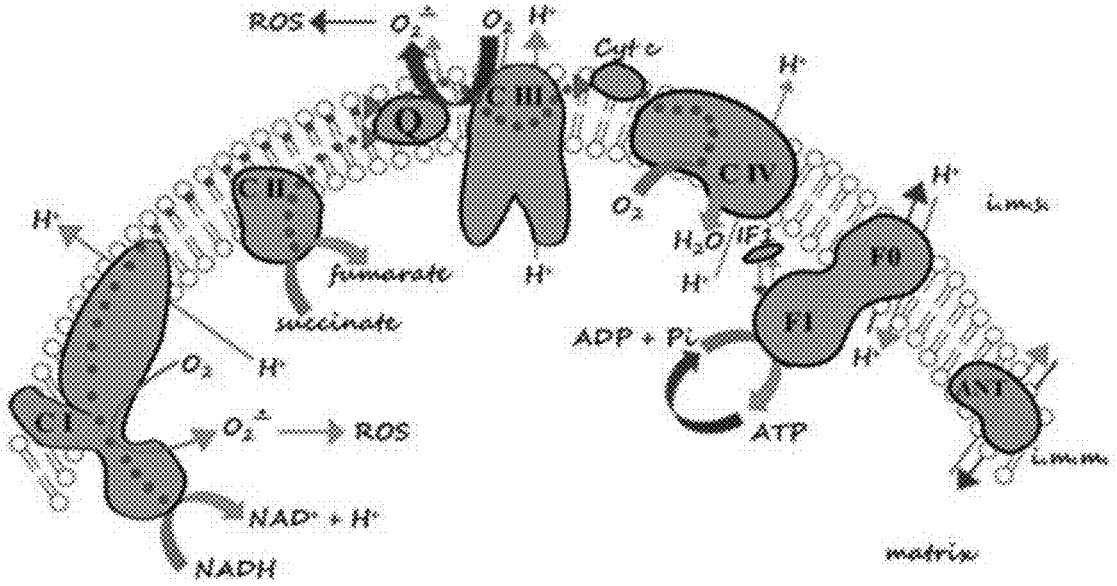
ROS
$O_2^{\cdot-}$
O_2
H^+
Cyt c
Q
C III
C IV
C II
C I
H^+
O_2
H_2O
IF1
F0
F1
ANT
fumarate
succinate
ADP + Pi
ATP
$O_2^{\cdot-}$ → ROS
$NAD^+ + H^+$
NADH
matrix

FIG. 3B

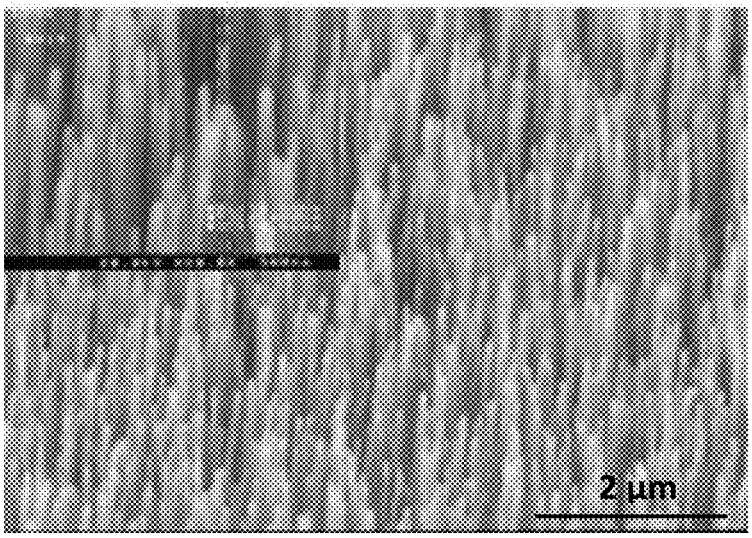

FIG. 4

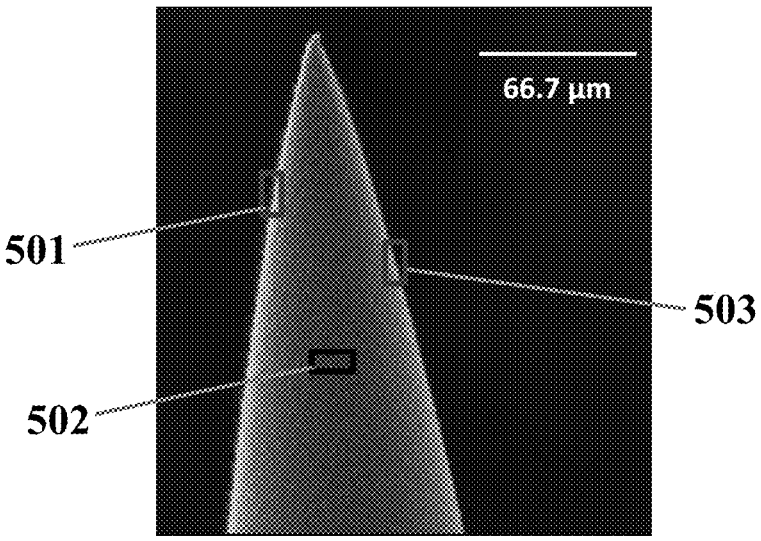

FIG. 5A

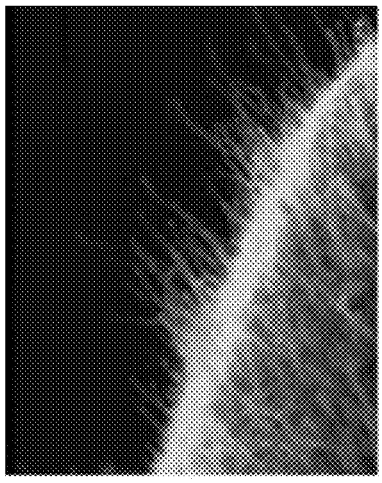

FIG. 5B

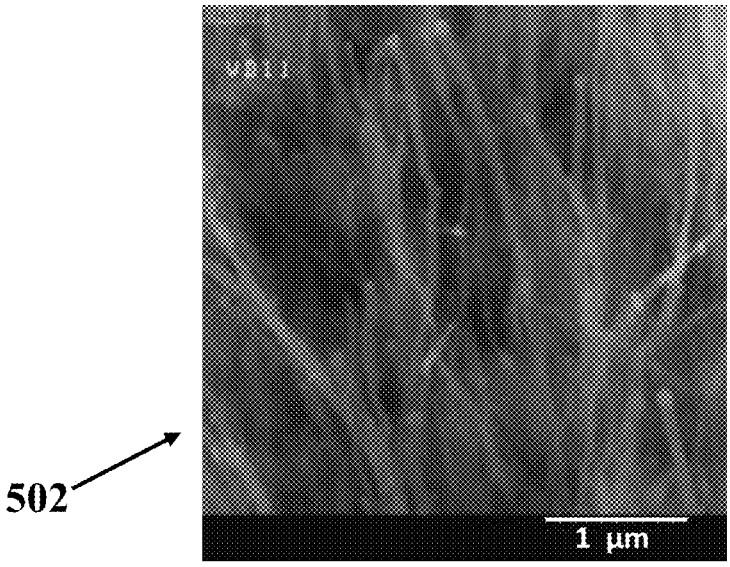

FIG. 5C

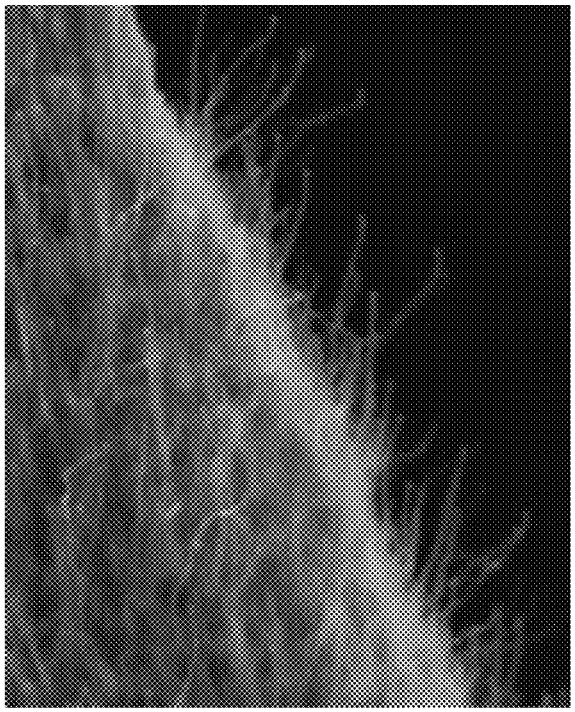

FIG. 5D

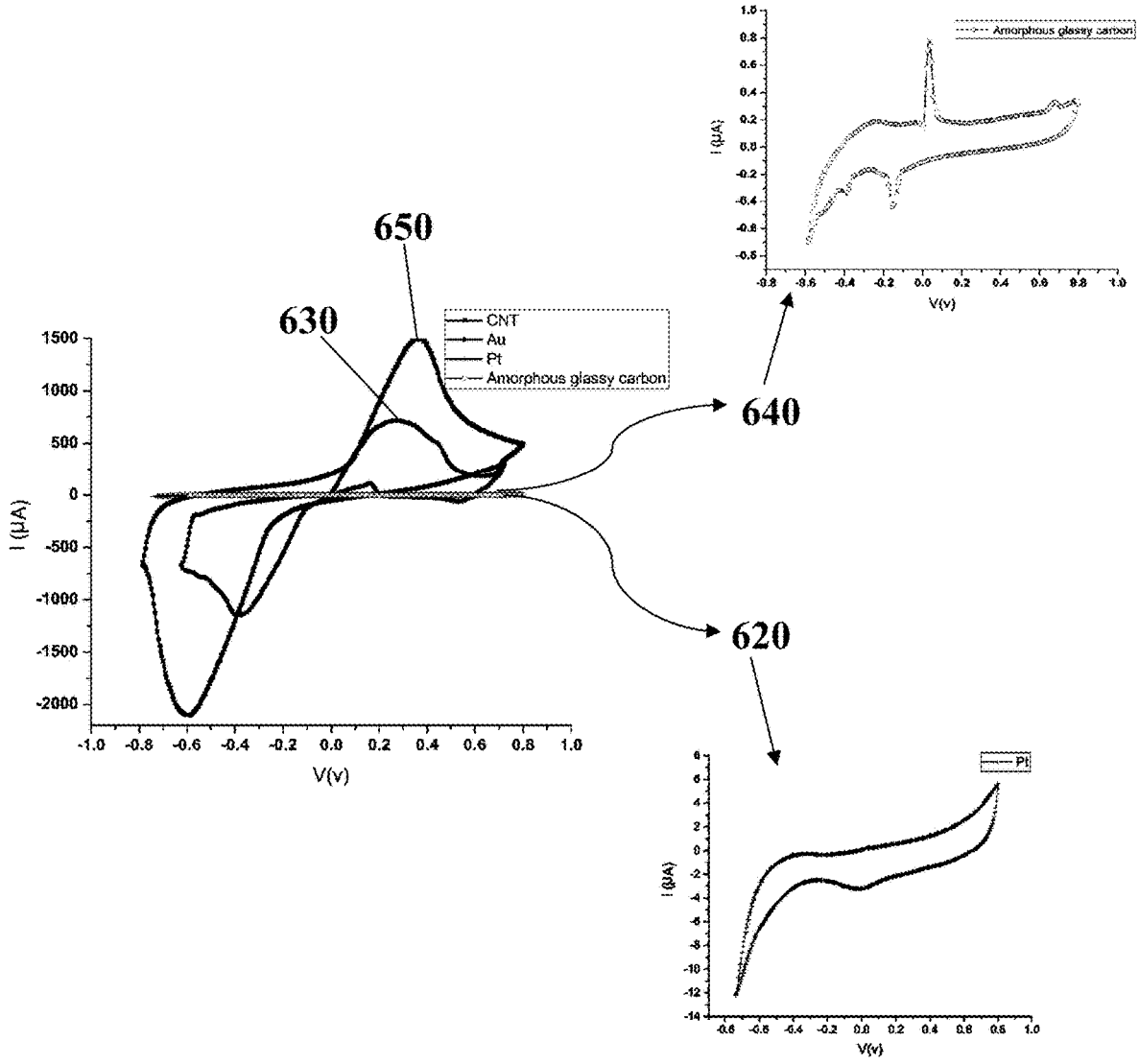
650
630
640
620
CNT
Au
Pt
Amorphous glassy carbon
I (μA)
V(v)
Amorphous glassy carbon
Pt

FIG. 6A

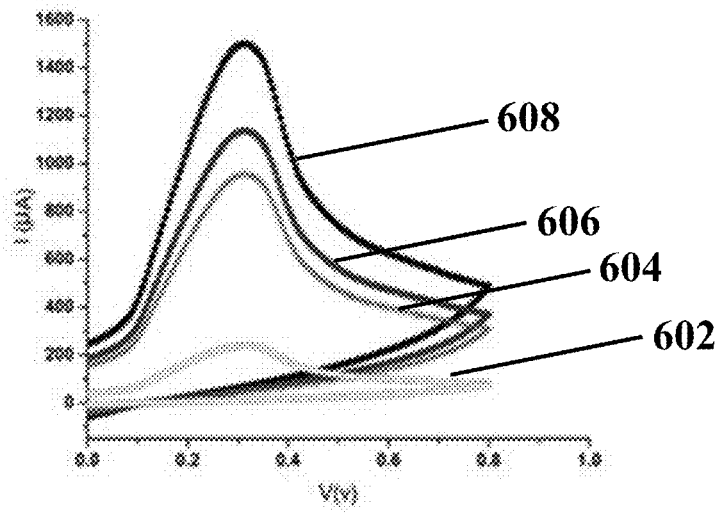

FIG. 6B

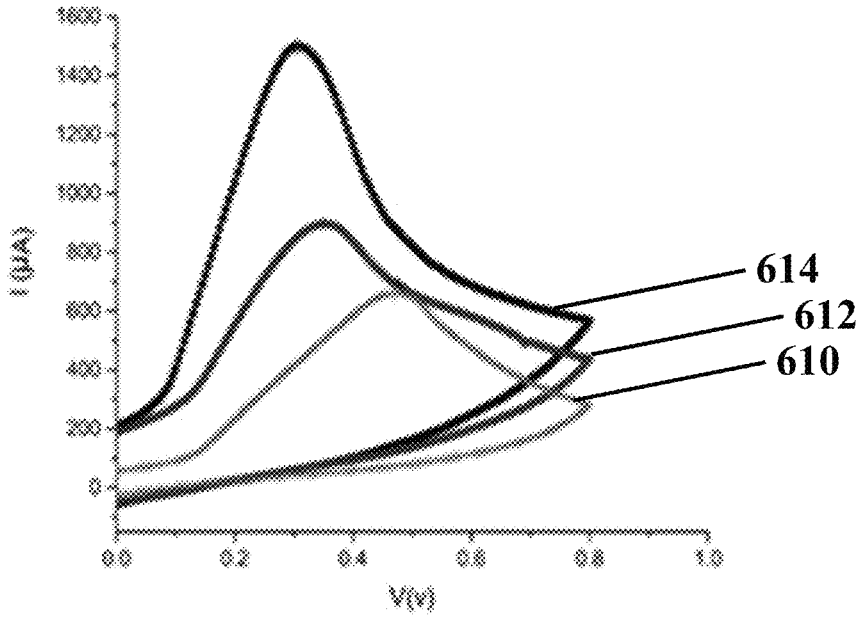
I (μA)
1600
1400
1200
1000
800
600
400
200
0
0.0
0.2
0.4
0.6
0.8
1.0
V(v)
614
612
610

FIG. 6C

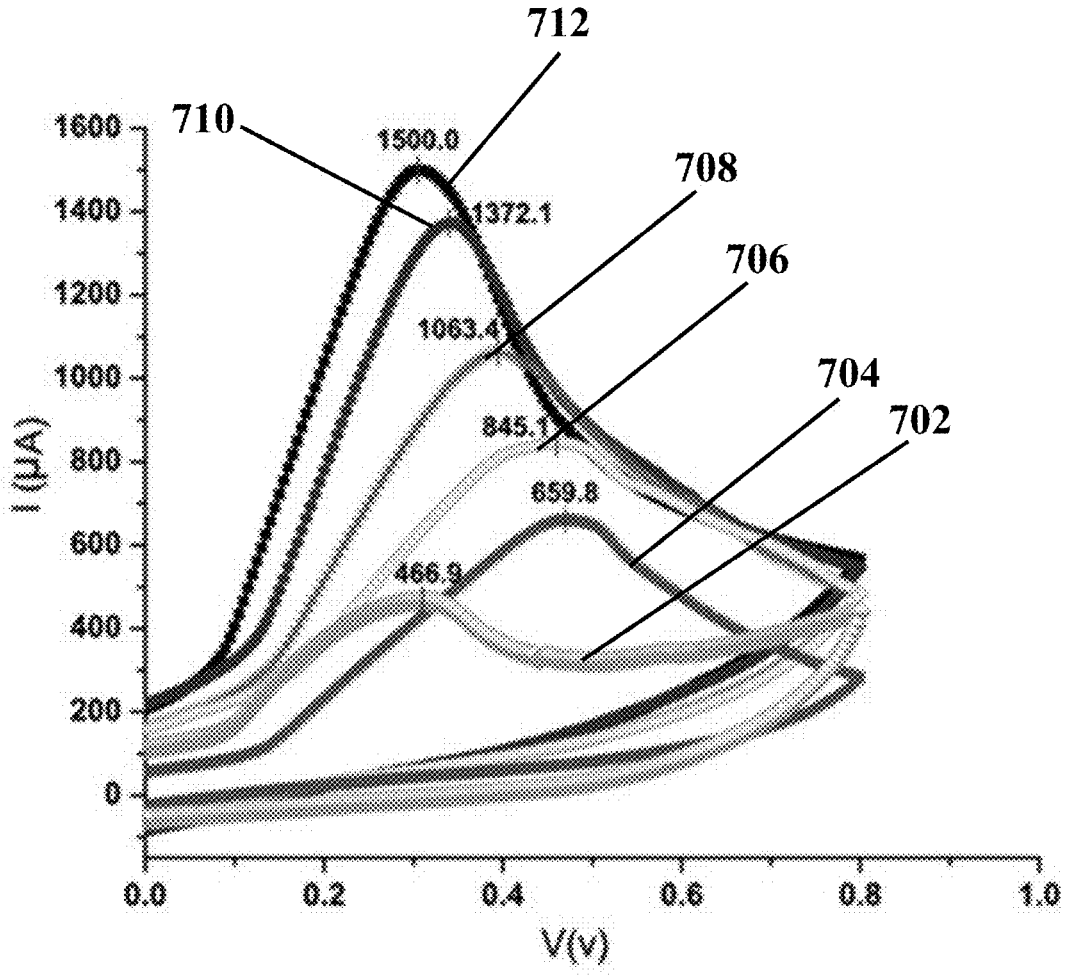
712
710
708
706
704
702
1500.0
1372.1
1063.4
845.1
659.8
466.9
I (μA)
V(v)
1600
1400
1200
1000
800
600
400
200
0
0.0
0.2
0.4
0.6
0.8
1.0

FIG. 7

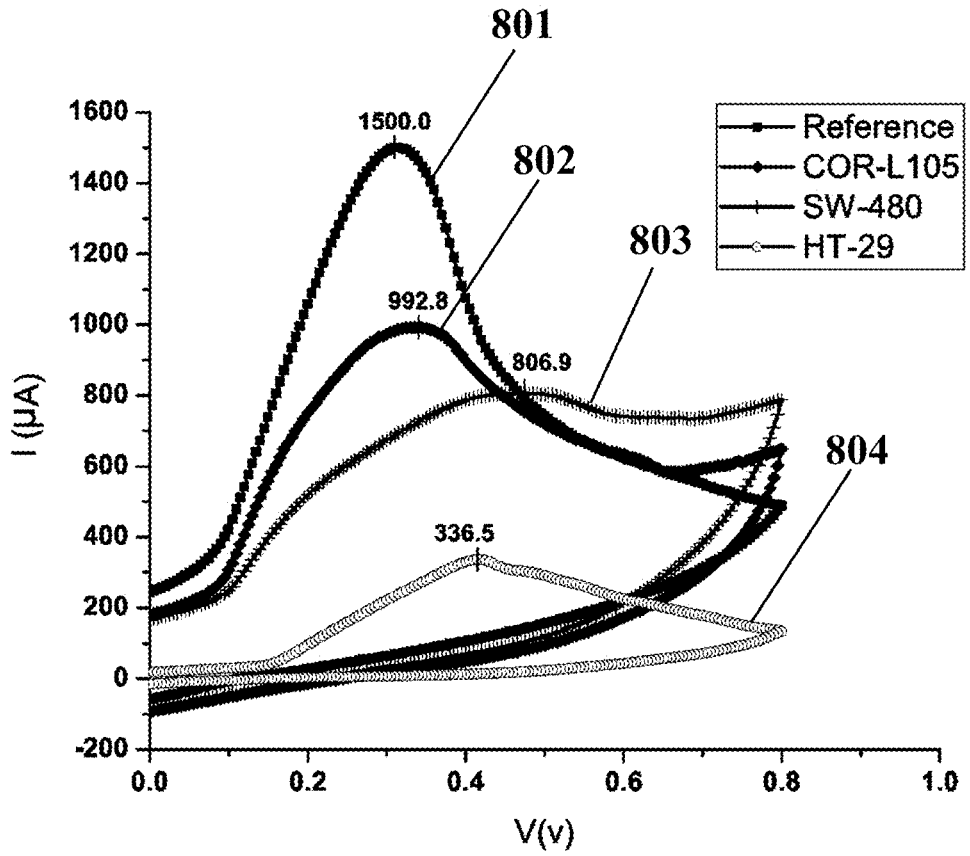
801
802
803
804
1500.0
992.8
806.9
336.5
Reference
COR-L105
SW-480
HT-29
I (μA)
V(v)
1600
1400
1200
1000
800
600
400
200
0
-200
0.0
0.2
0.4
0.6
0.8
1.0

FIG. 8A

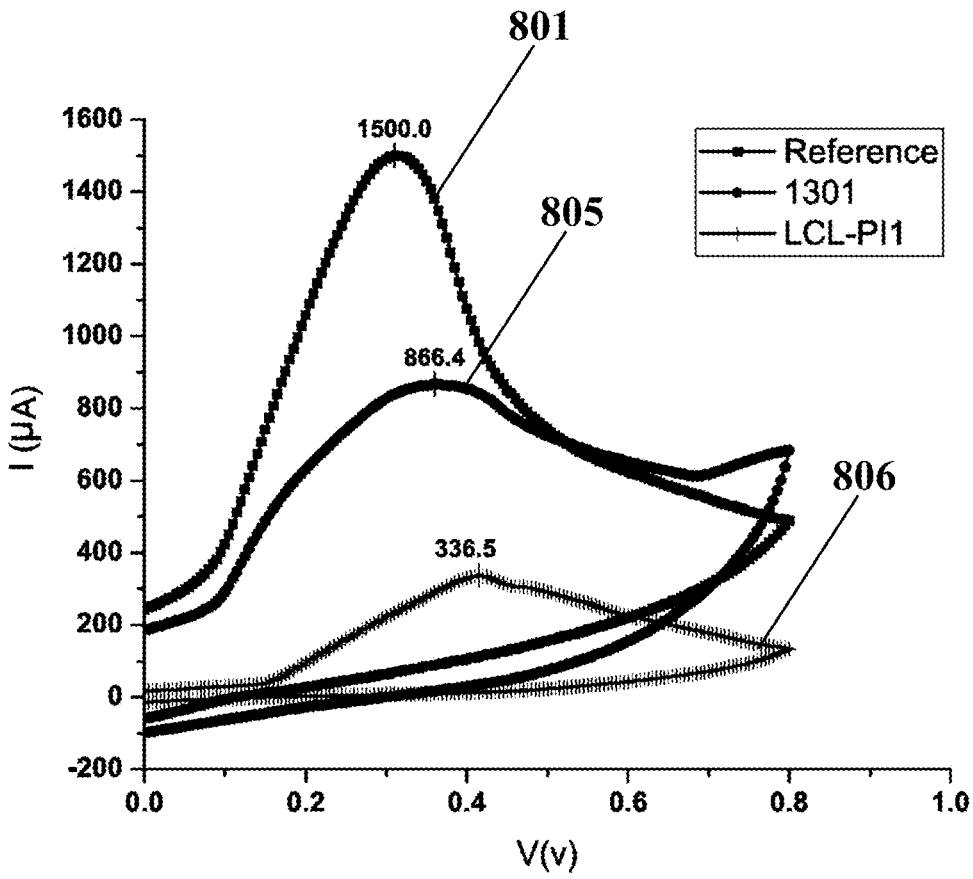
801
805
806
1500.0
866.4
336.5
Reference
1301
LCL-PI1
I (μA)
V(v)
1600
1400
1200
1000
800
600
400
200
0
-200
0.0
0.2
0.4
0.6
0.8
1.0

FIG. 8B

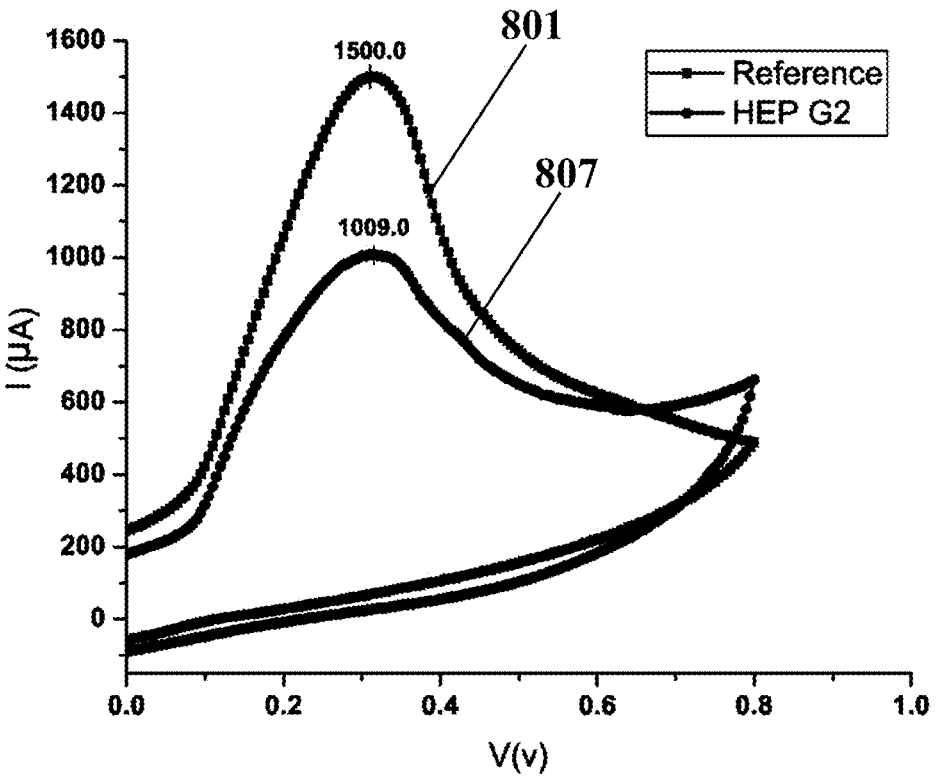
801
807
1500.0
1009.0
Reference
HEP G2
I (μA)
V(v)
1600
1400
1200
1000
800
600
400
200
0
0.0
0.2
0.4
0.6
0.8
1.0

FIG. 8C

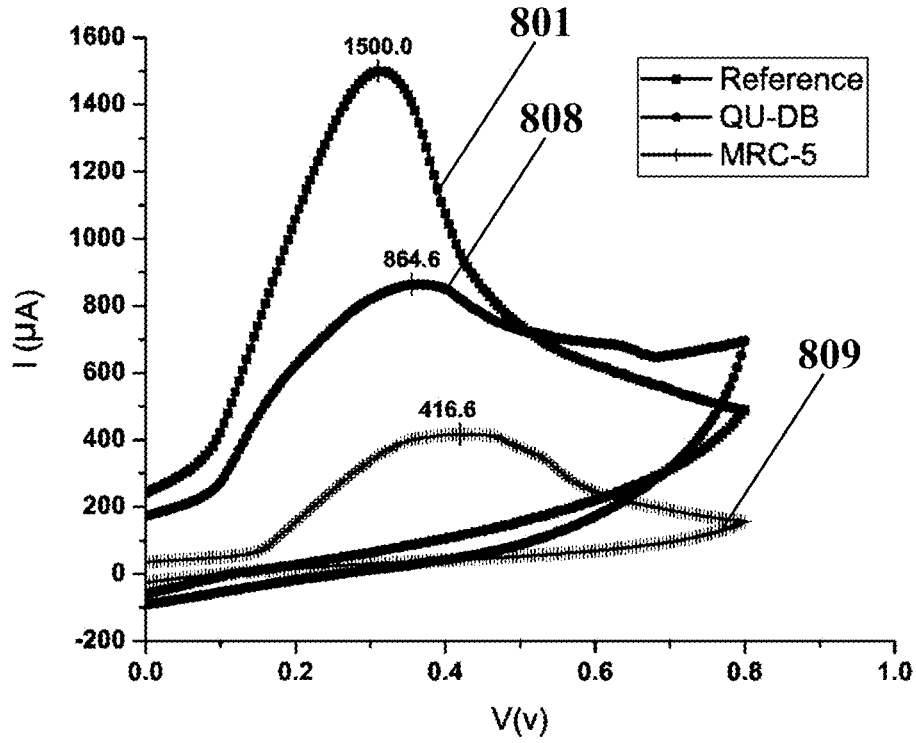
801
808
809
1500.0
864.6
416.6
Reference
QU-DB
MRC-5
I (μA)
V(v)
1600
1400
1200
1000
800
600
400
200
0
-200
0.0
0.2
0.4
0.6
0.8
1.0

FIG. 8D

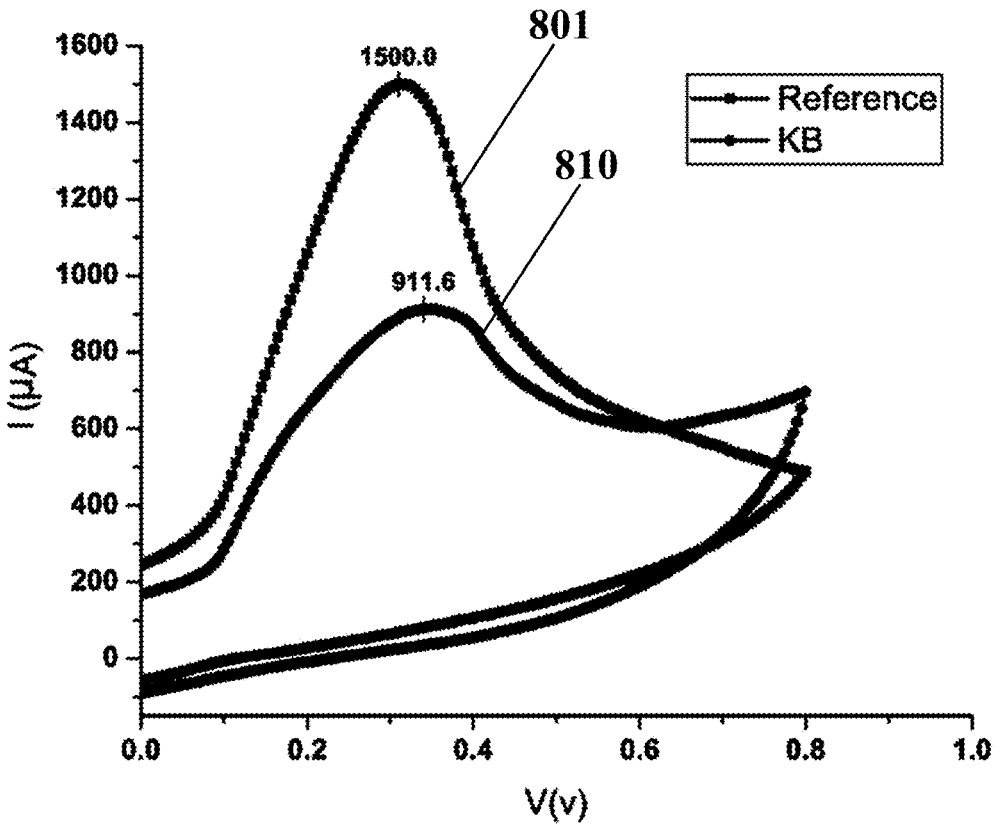
801
1500.0
810
911.6
Reference
KB
I (μA)
V(v)
1600
1400
1200
1000
800
600
400
200
0
0.0
0.2
0.4
0.6
0.8
1.0

FIG. 8E

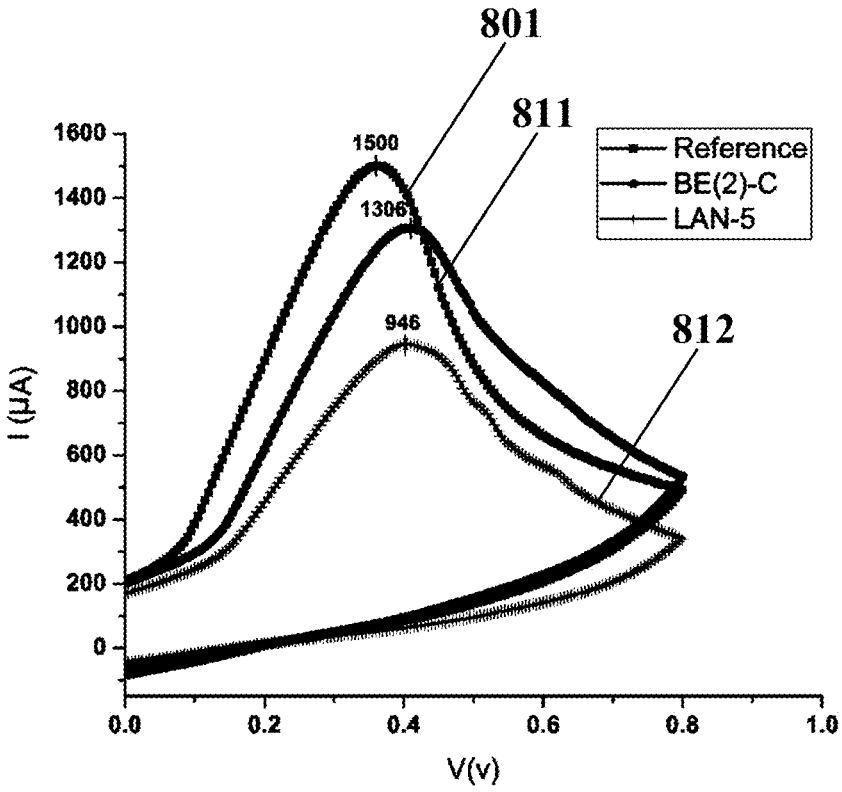
801
811
812
Reference
BE(2)-C
LAN-5
1500
1306
946
I (μA)
V(v)
1600
1400
1200
1000
800
600
400
200
0
0.0
0.2
0.4
0.6
0.8
1.0

FIG. 8F

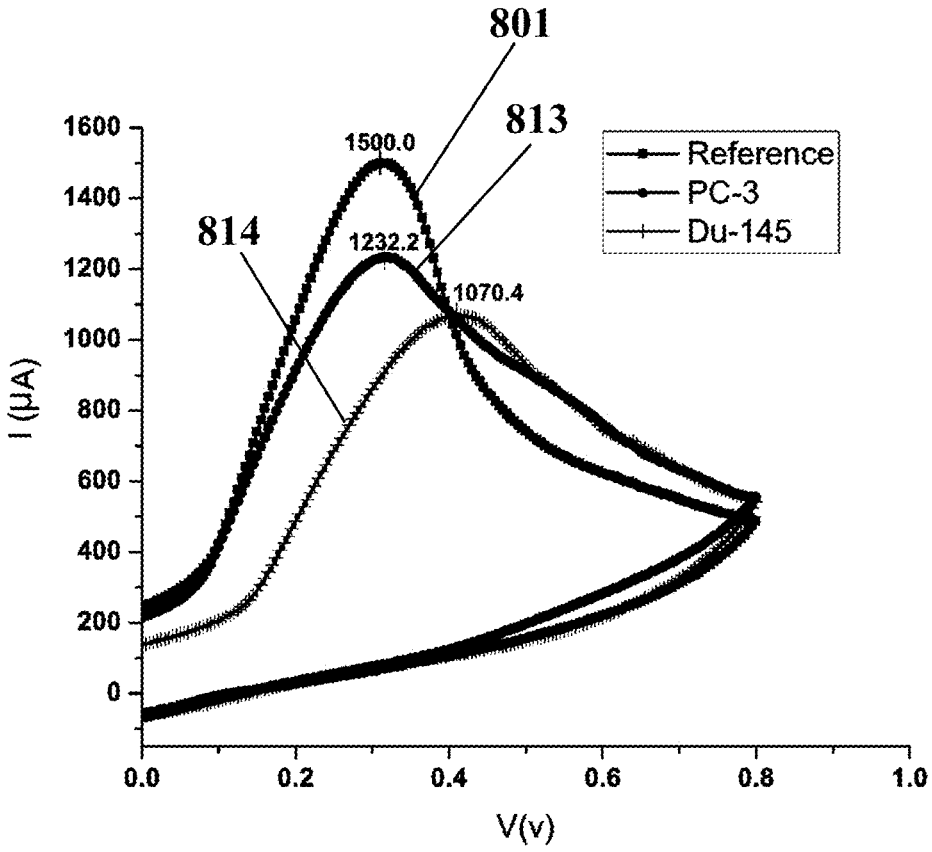
801
813
814
1500.0
1232.2
1070.4
Reference
PC-3
Du-145
I (μA)
V(v)
1600
1400
1200
1000
800
600
400
200
0
0.0
0.2
0.4
0.6
0.8
1.0

FIG. 8G

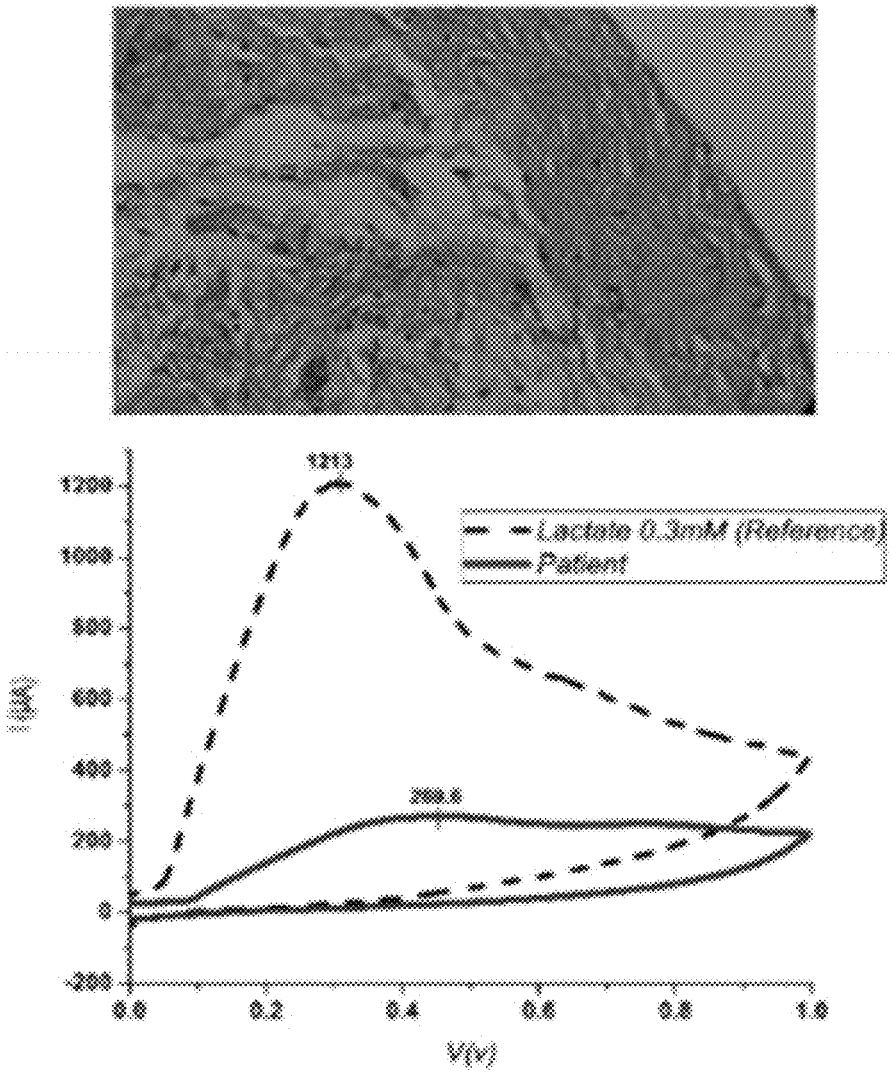
1213
Lactate 0.3mM (Reference)
Patient
1200
1000
800
600
400
200
0
-200
0.0
0.2
0.4
0.6
0.8
1.0
V(v)

FIG. 9A

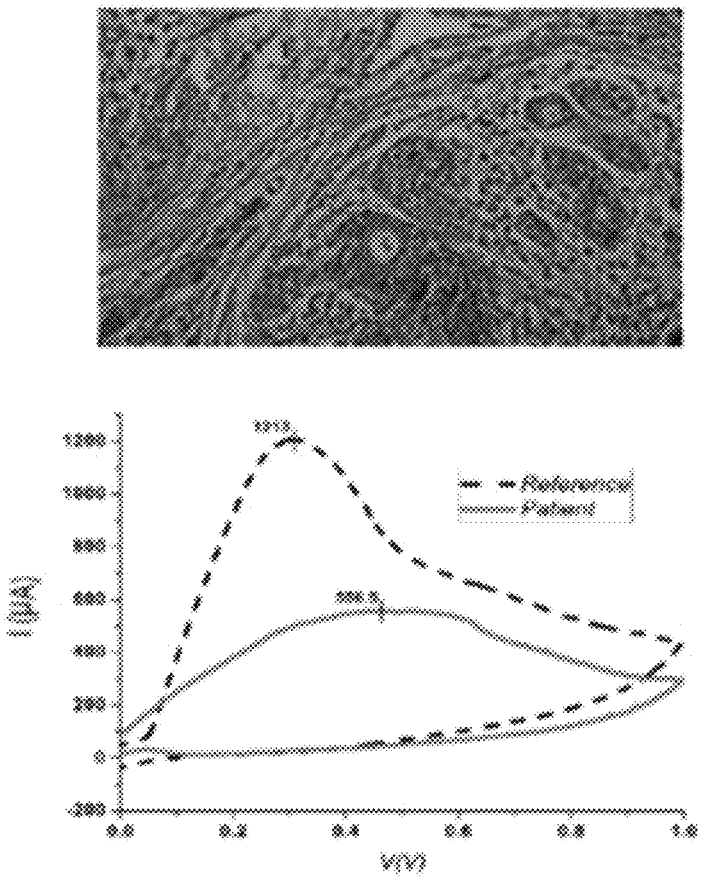

FIG. 9B

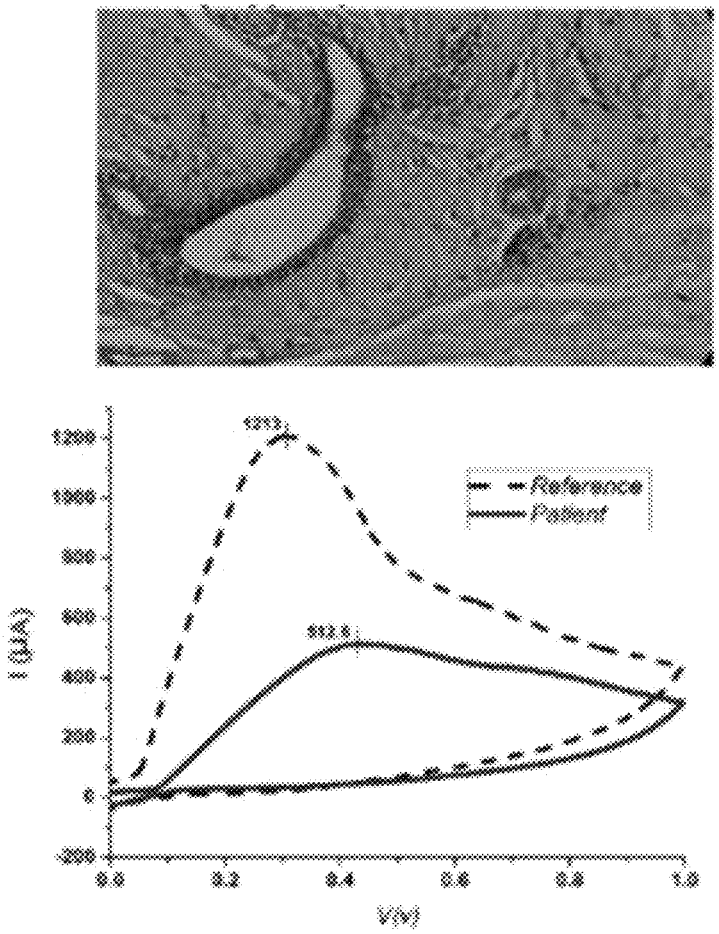

FIG. 9C

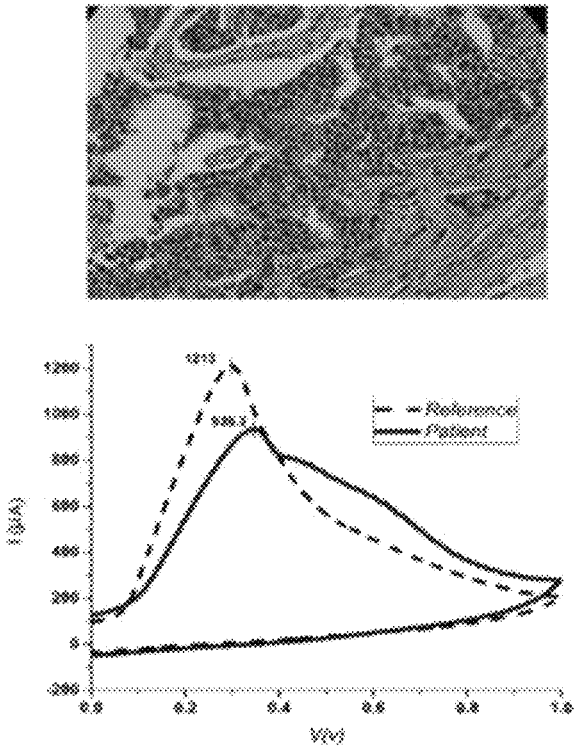

FIG. 9D

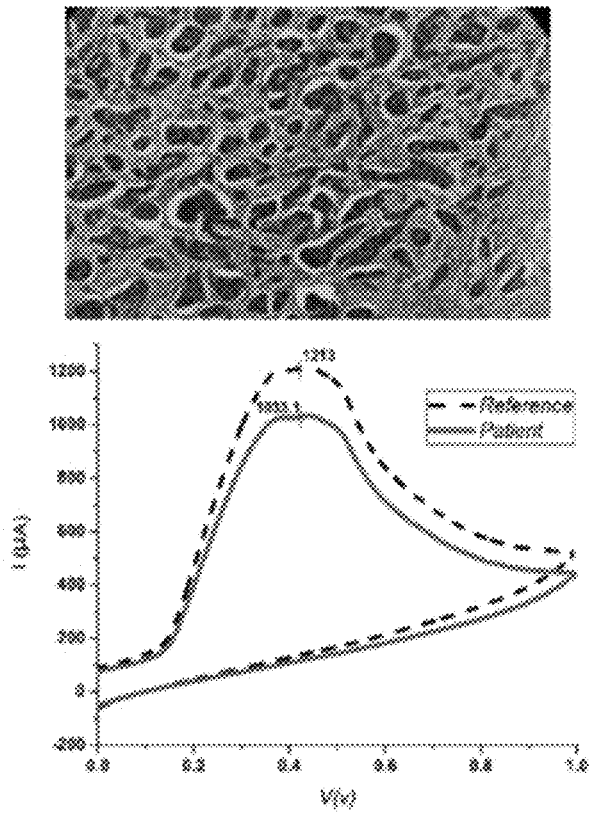

FIG. 9E

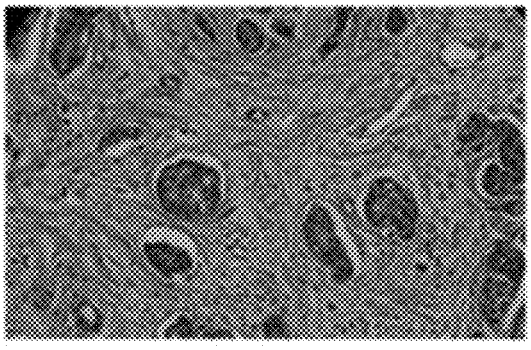

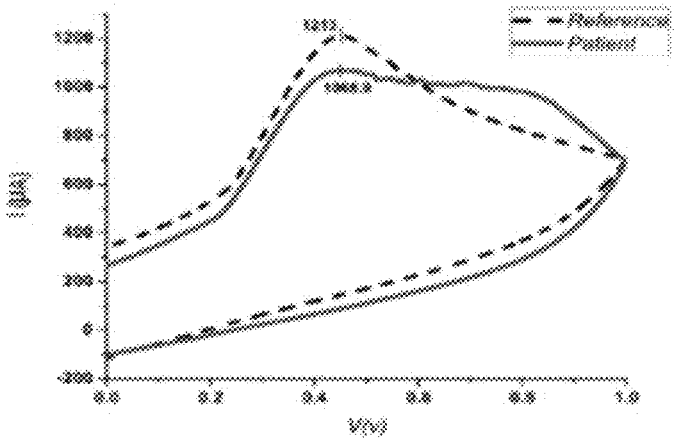

FIG. 9F

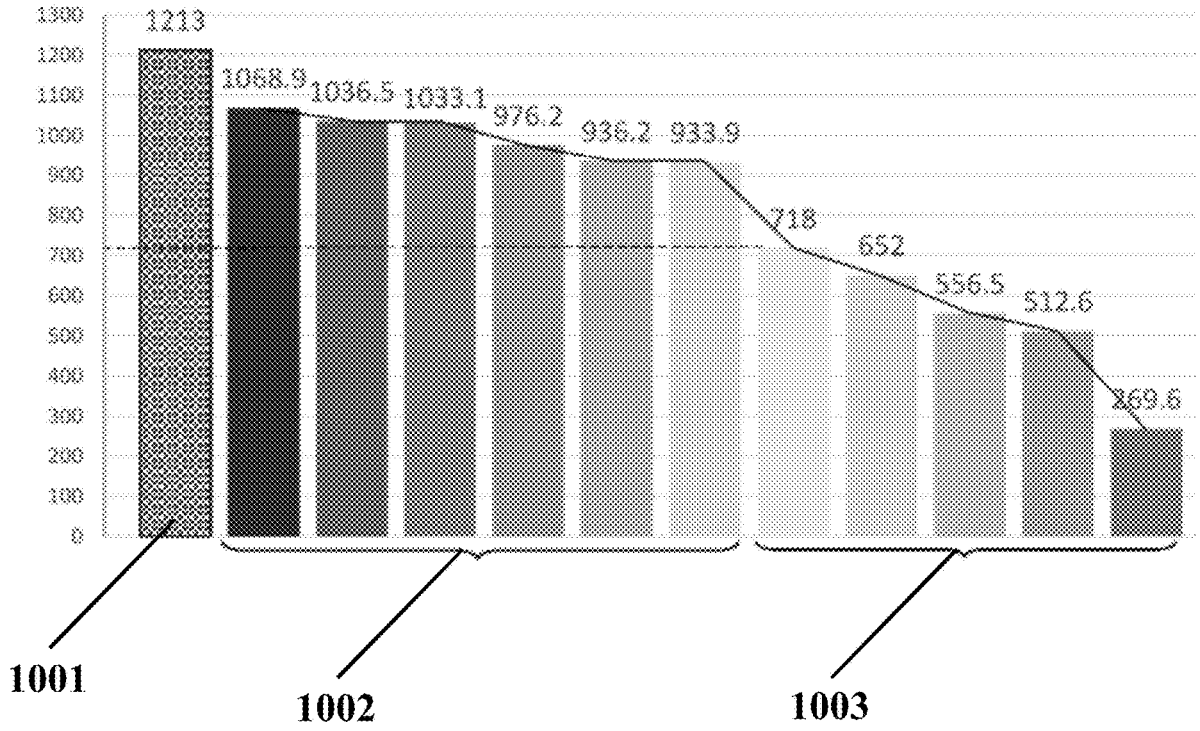
1300
1200
1100
1000
900
800
700
600
500
400
300
200
100
0
1213
1068.9
1036.5
1033.1
976.2
936.2
933.9
718
652
556.5
512.6
369.6
1001
1002
1003

FIG. 10

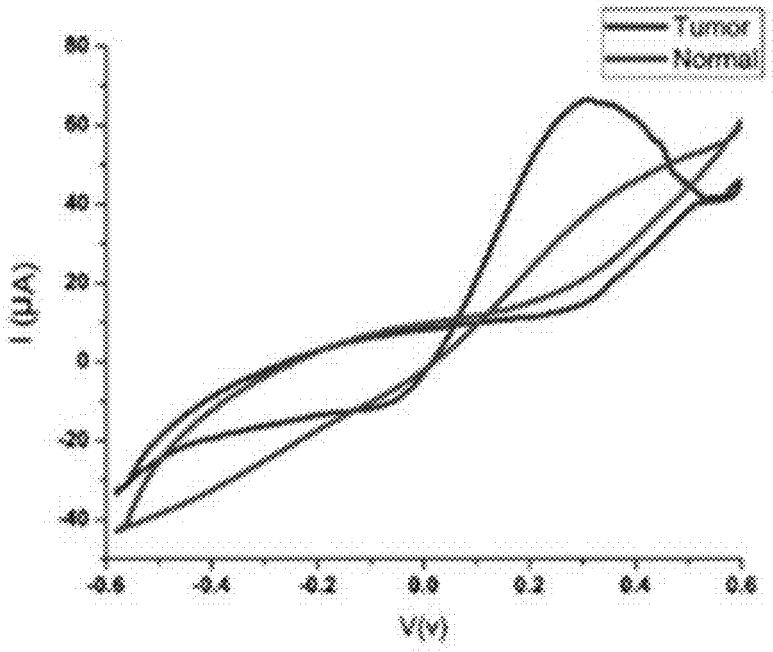

FIG. 11A

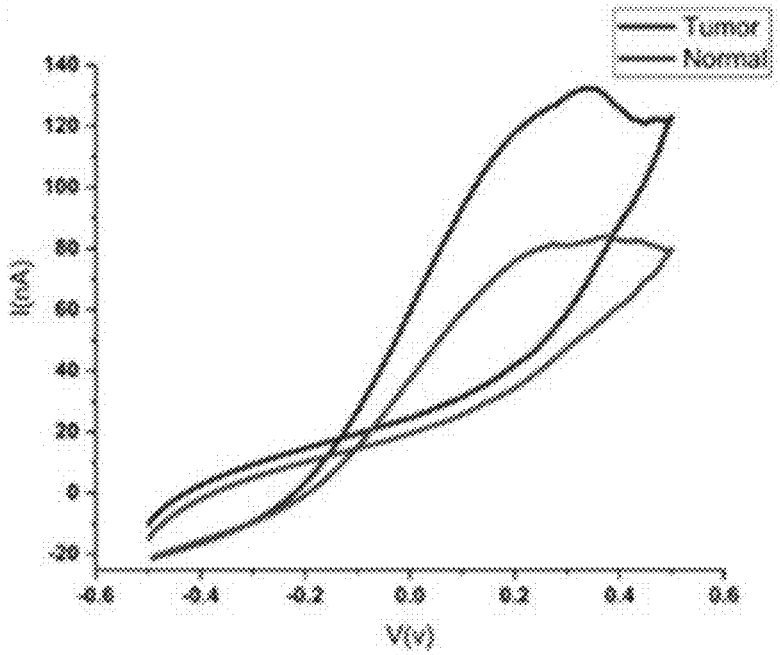

FIG. 11B

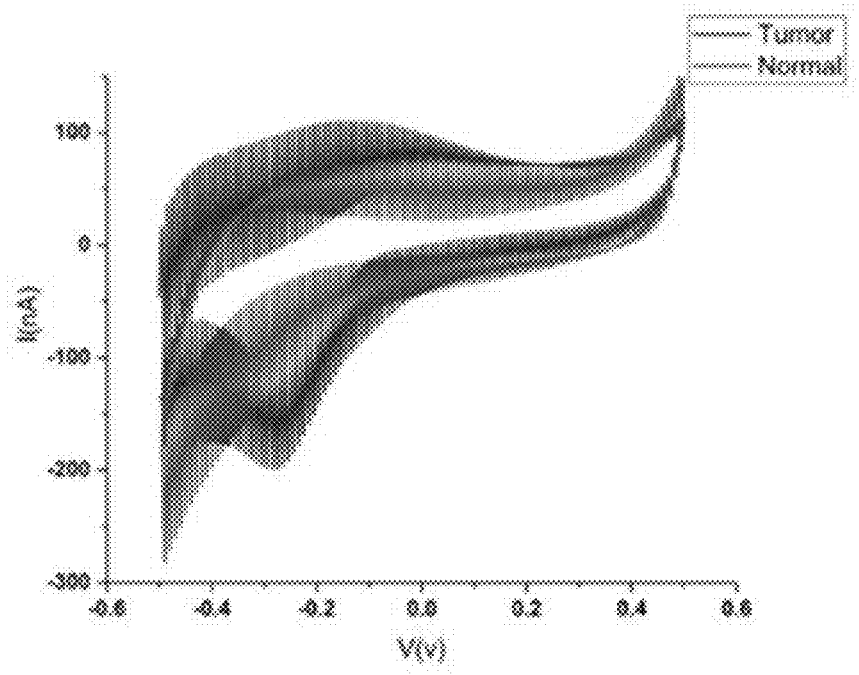

FIG. 11C

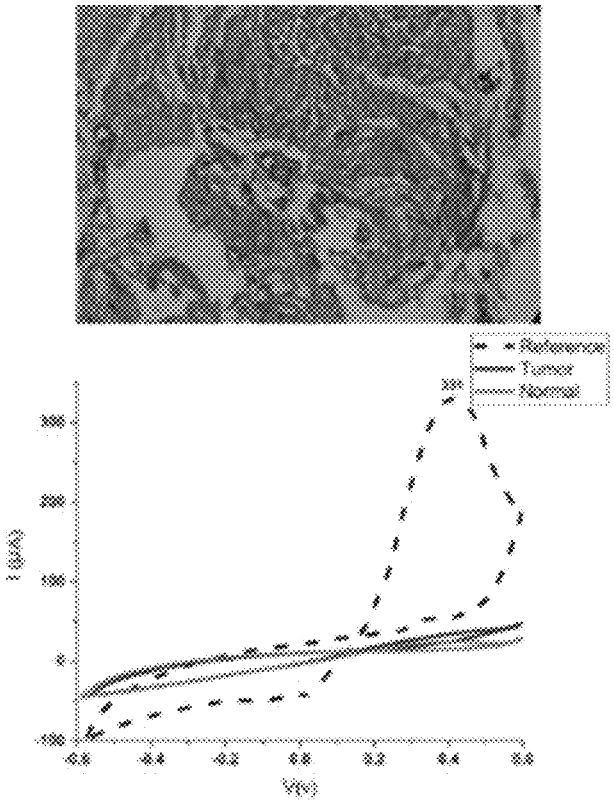

FIG. 12A

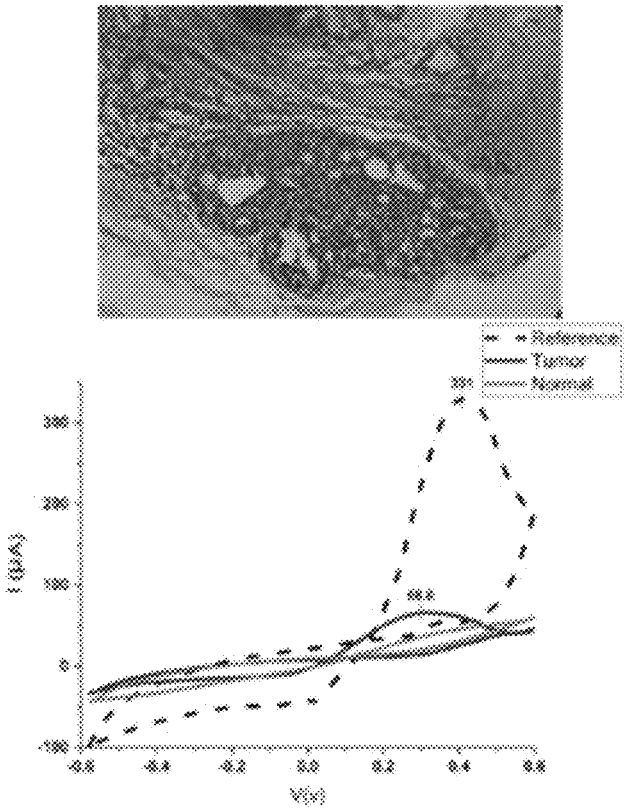

FIG. 12B

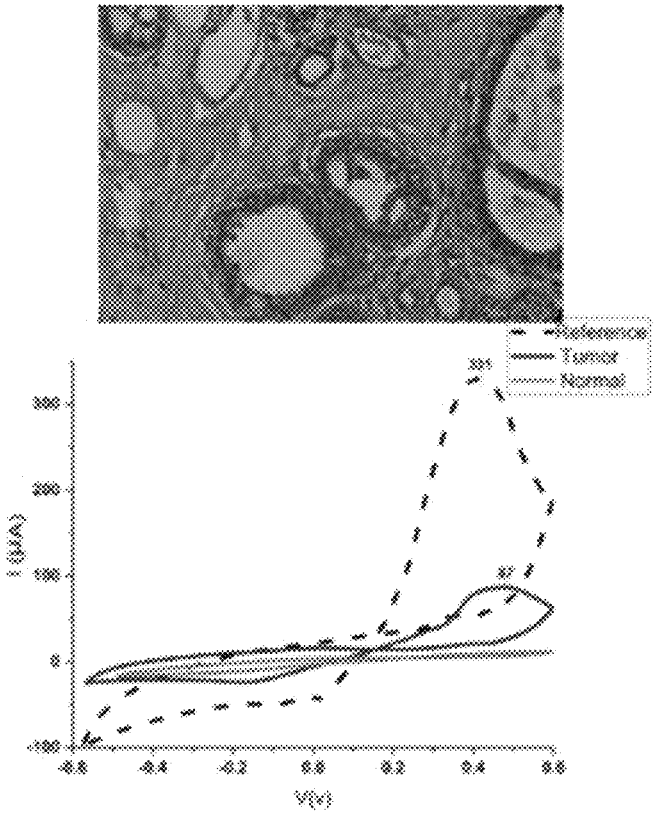

FIG. 12C

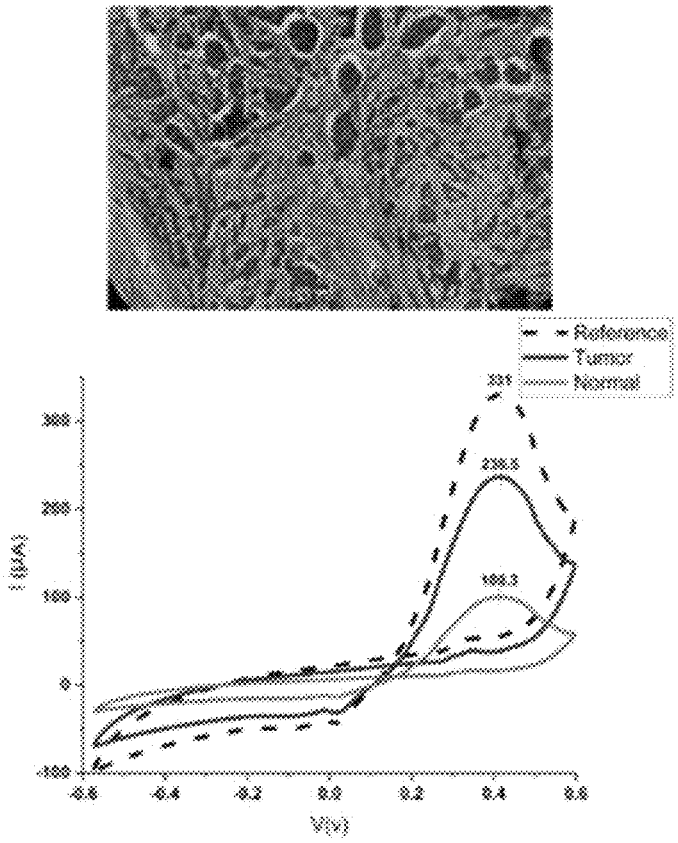

FIG. 12D

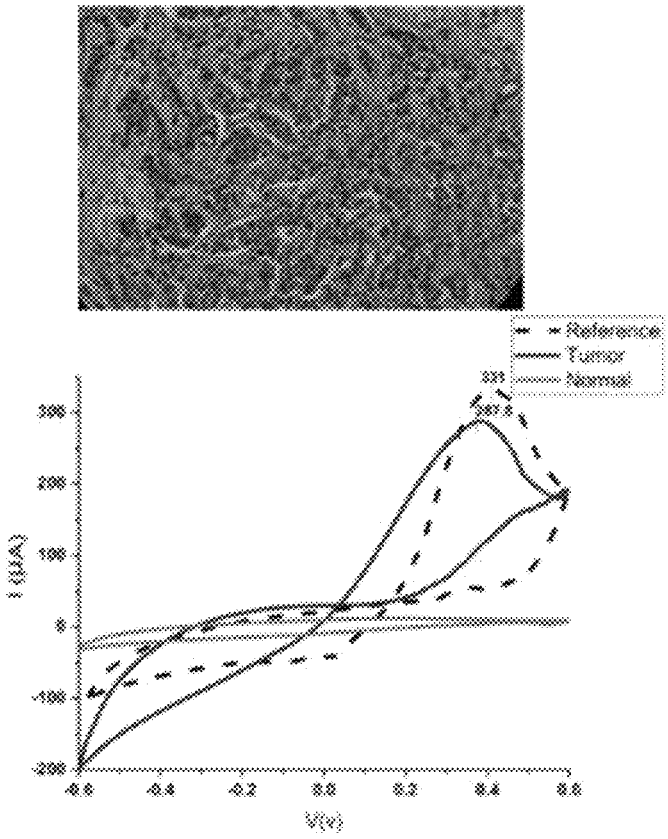

FIG. 12E

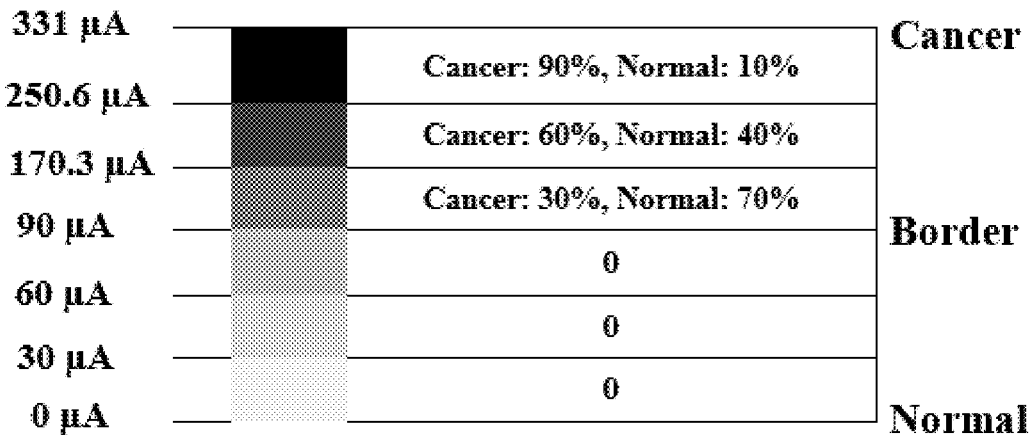
331 µA
250.6 µA
170.3 µA
90 µA
60 µA
30 µA
0 µA
Cancer: 90%, Normal: 10%
Cancer: 60%, Normal: 40%
Cancer: 30%, Normal: 70%
0
0
0
Cancer
Border
Normal

FIG. 13

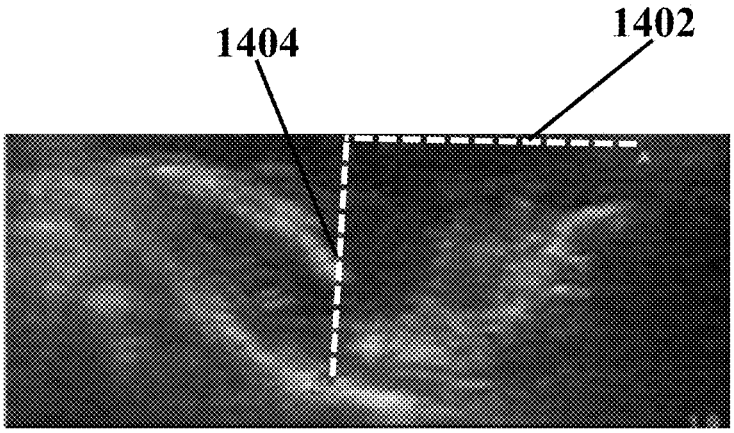

FIG. 14A

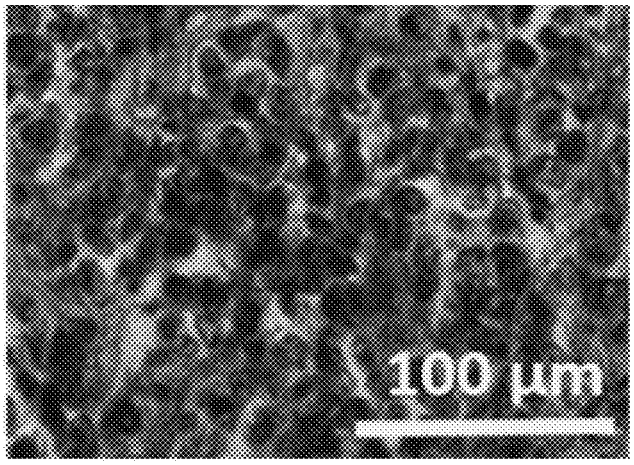

FIG. 14B

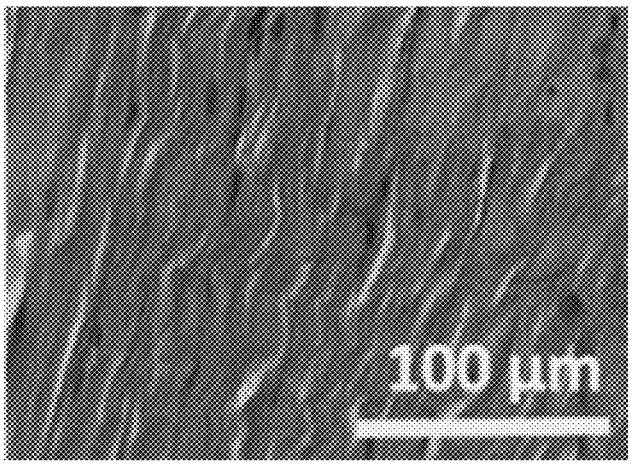

FIG. 14C

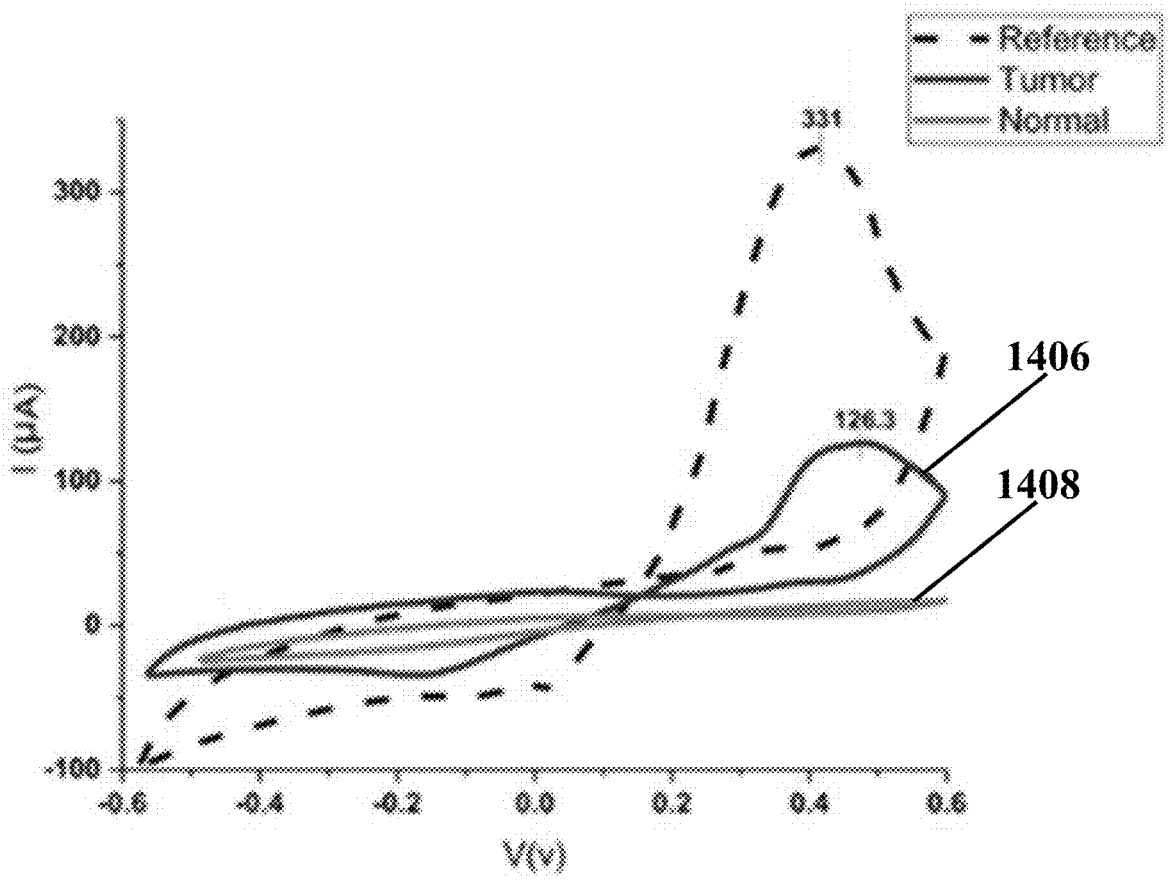
Reference
Tumor
Normal
331
126.3
1406
1408
300
200
100
0
-100
I (μA)
-0.6
-0.4
-0.2
0.0
0.2
0.4
0.6
V(v)

FIG. 14D

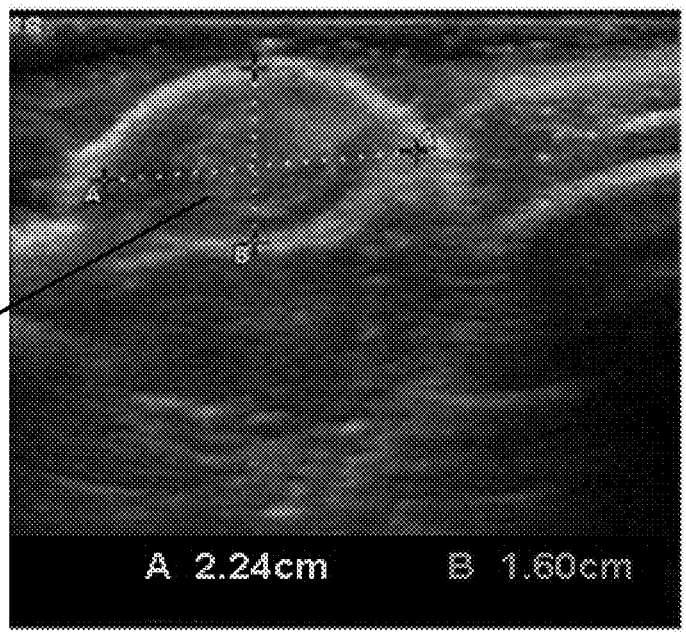

FIG. 15A

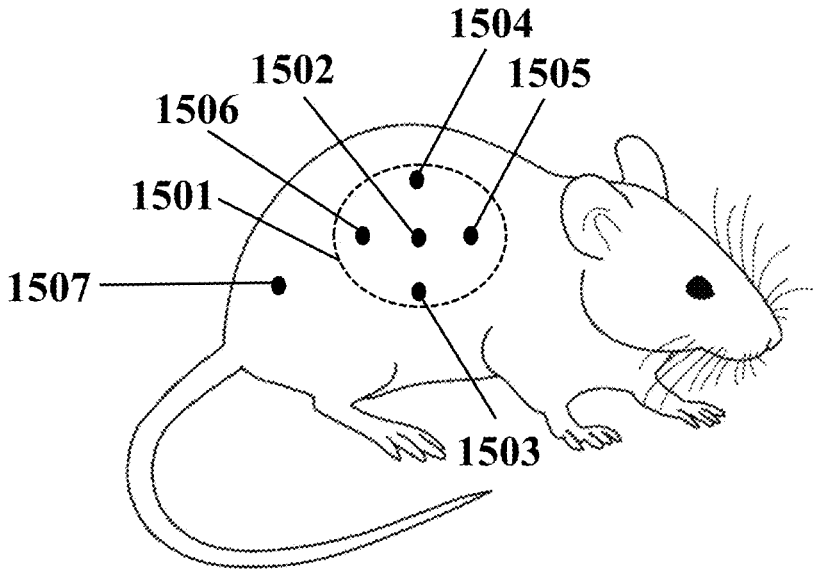

FIG. 15B

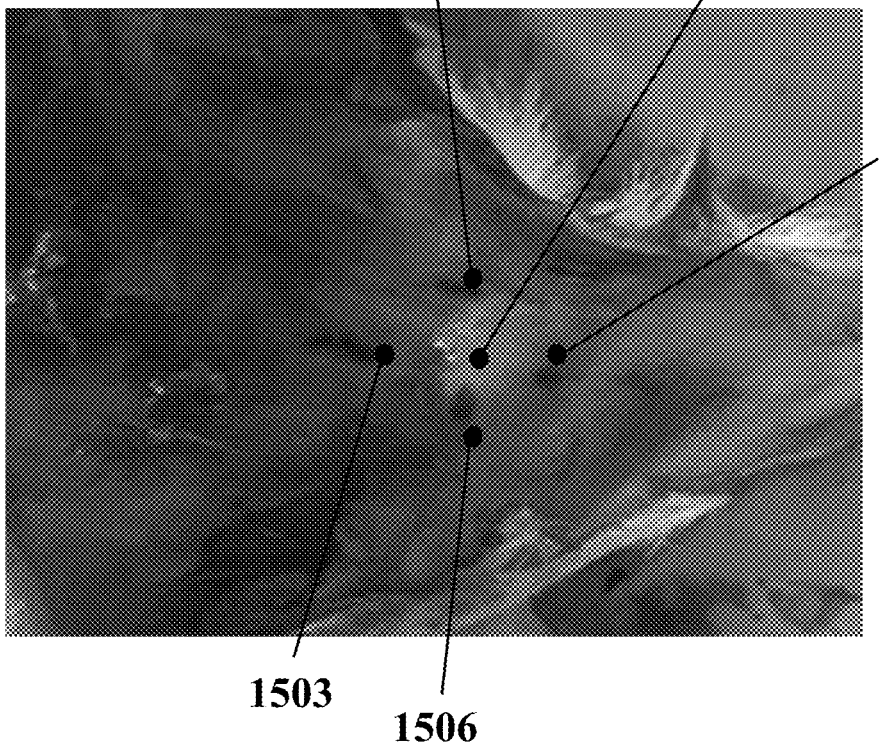

FIG. 15C

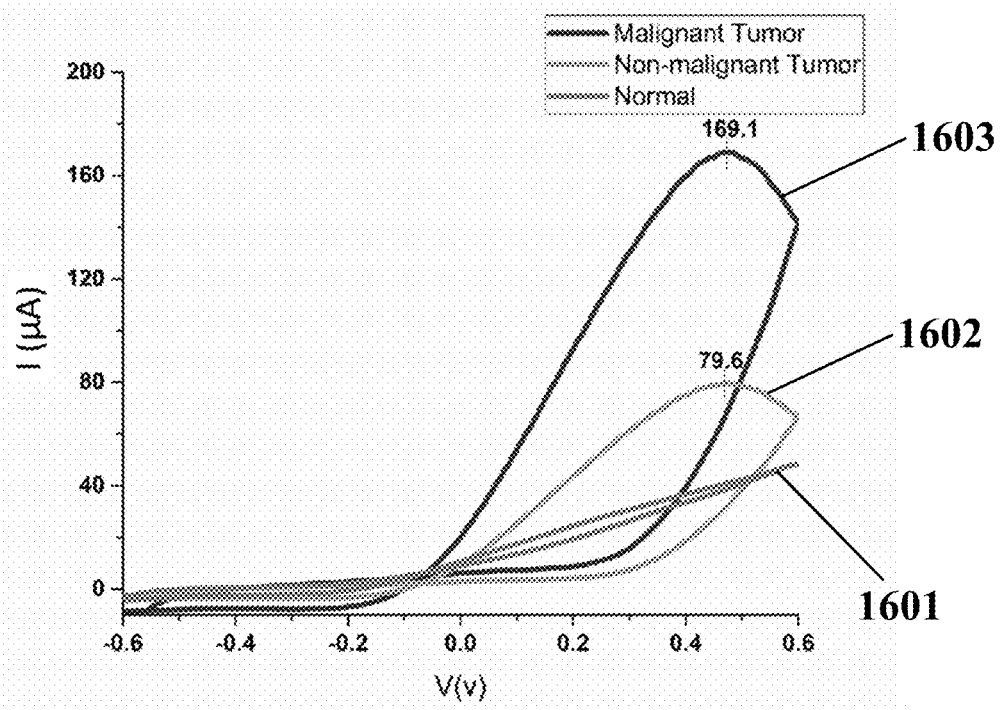
Malignant Tumor
Non-malignant Tumor
Normal
169.1
79.6
1603
1602
1601
200
160
120
80
40
0
I (μA)
-0.6
-0.4
-0.2
0.0
0.2
0.4
0.6
V(v)

FIG. 16

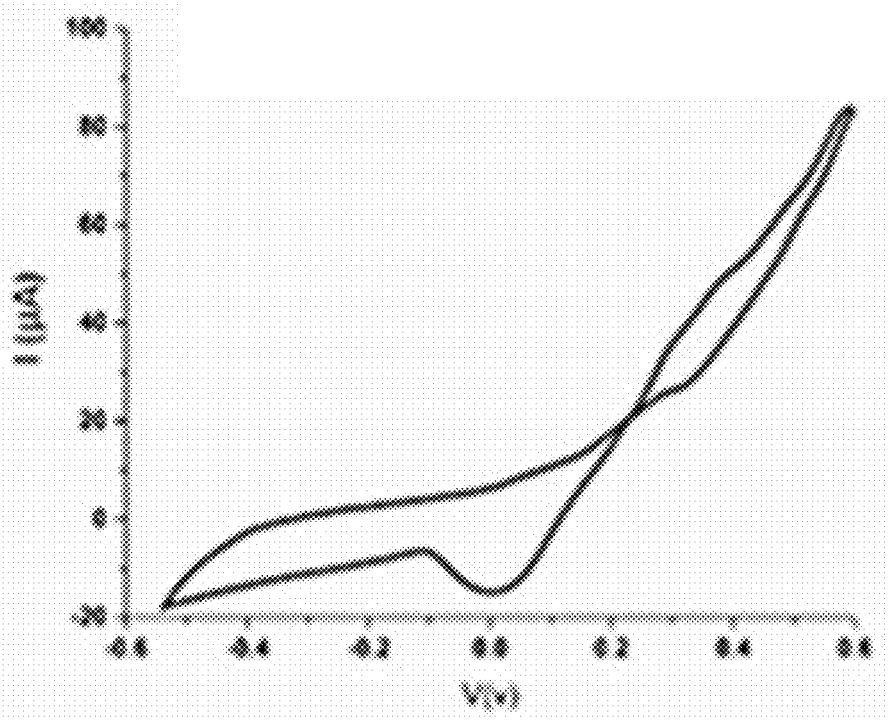

FIG. 17A

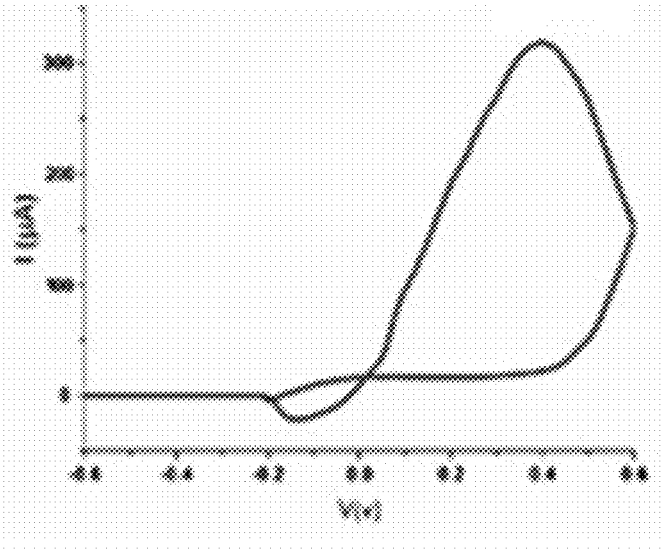

FIG. 17B

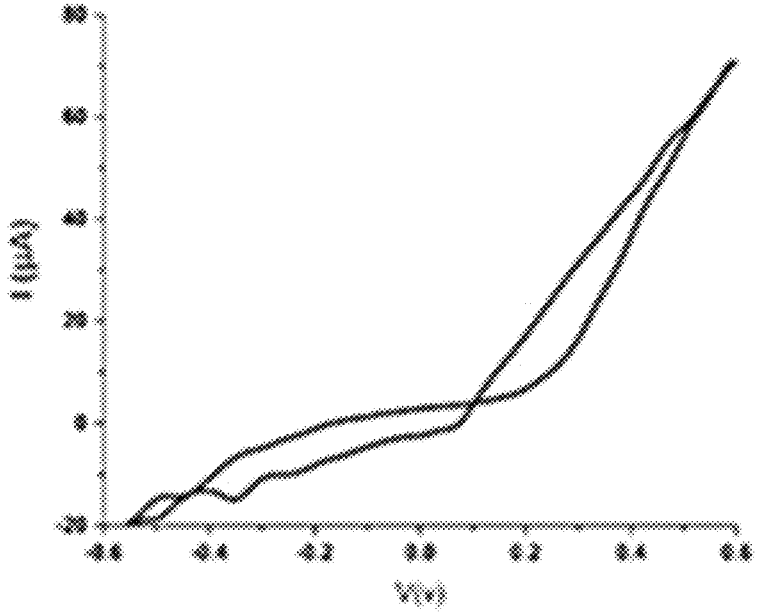

FIG. 17C

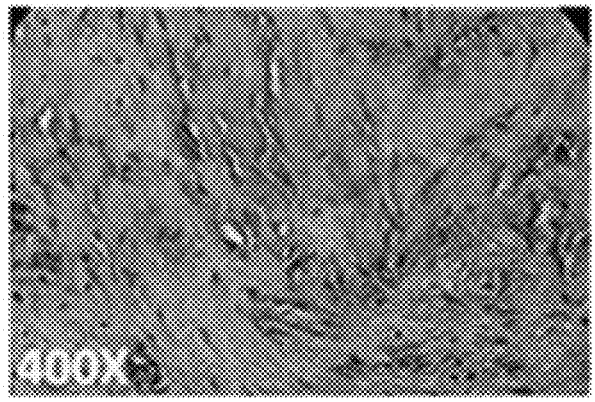

FIG. 17D

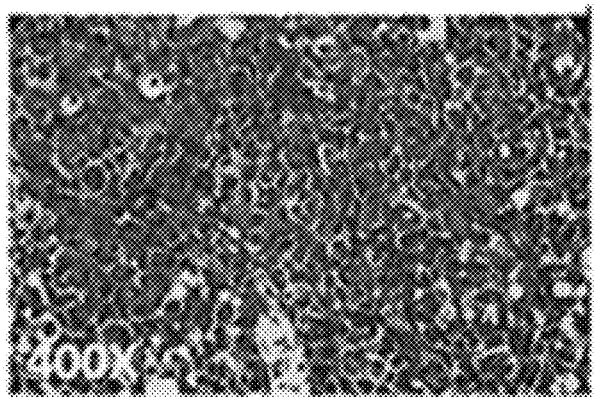

FIG. 17E

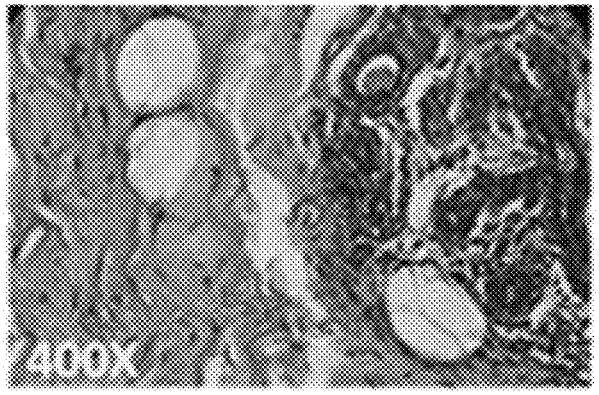

FIG. 17F

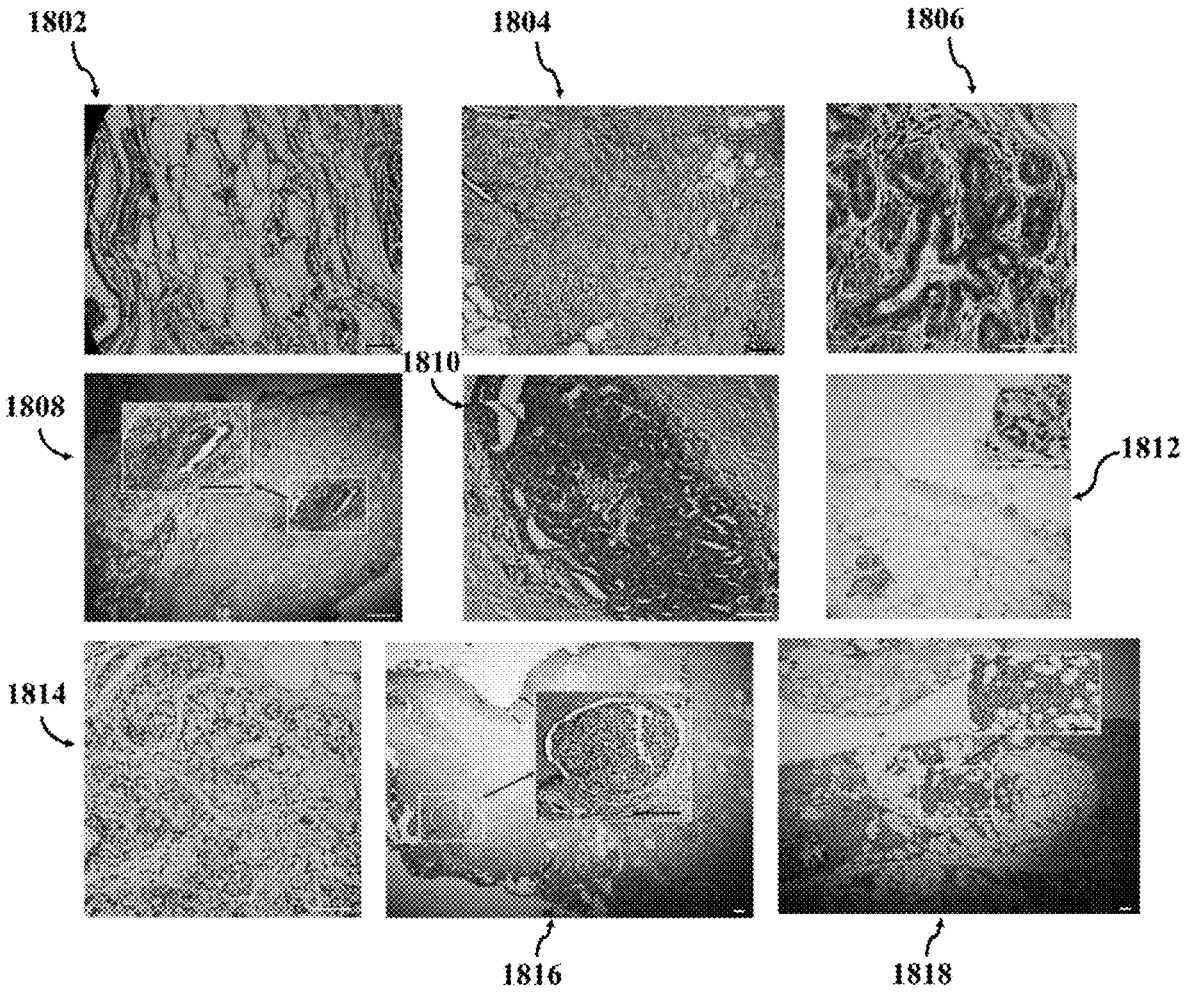

FIG. 18

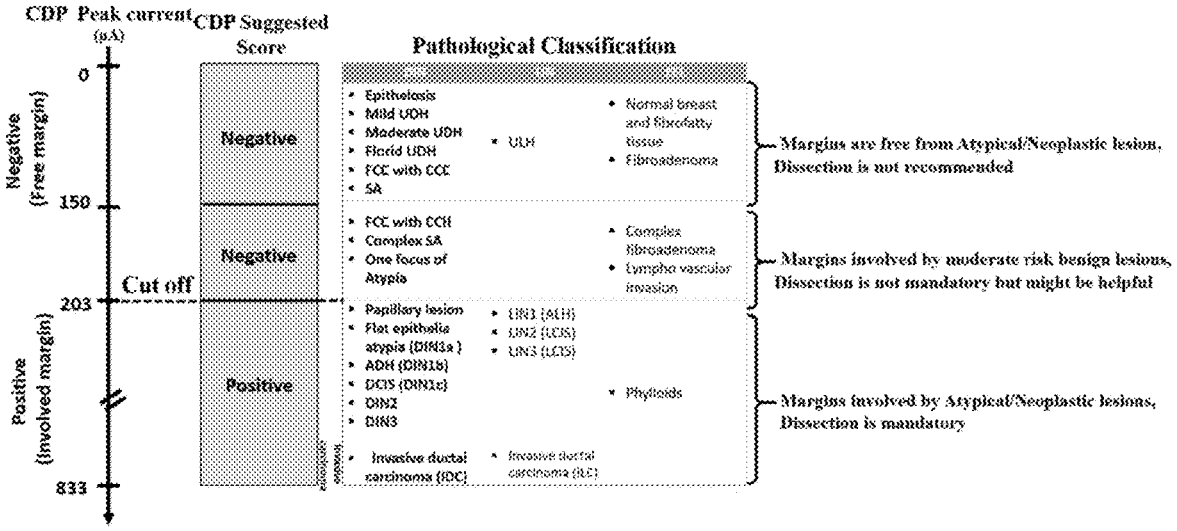

DIN: Ductal Intraepithelial Neoplasia, **LIN**: Lobular Intraepithelial Neoplasia, **FEL**: Fibroepithelial lesion

FIG. 19

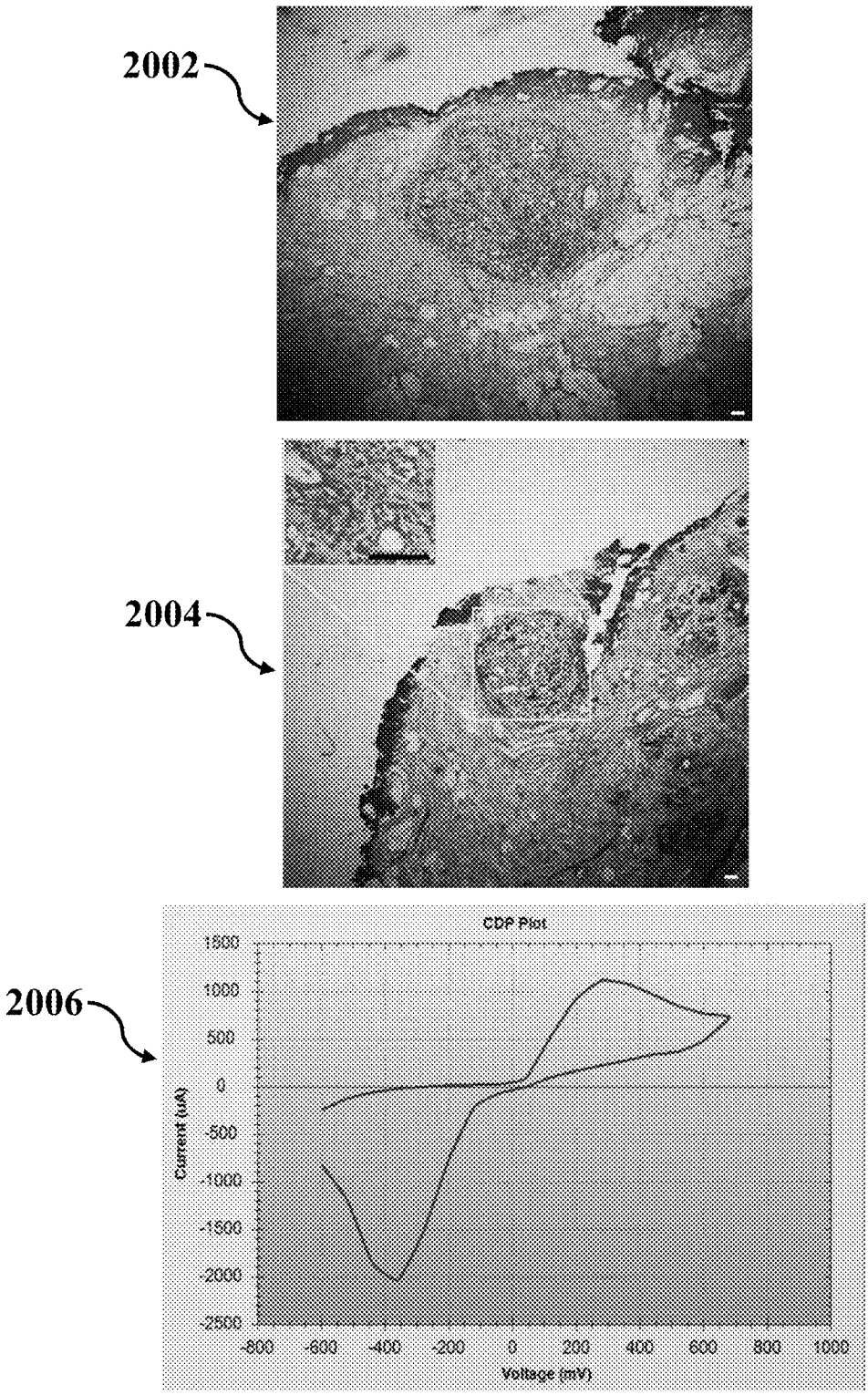
2002
2004
2006
CDP Plot
1500
1000
500
0
-500
-1000
-1500
-2000
-2500
Current (uA)
-800
-600
-400
-200
0
200
400
600
800
1000
Voltage (mV)

FIG. 20A

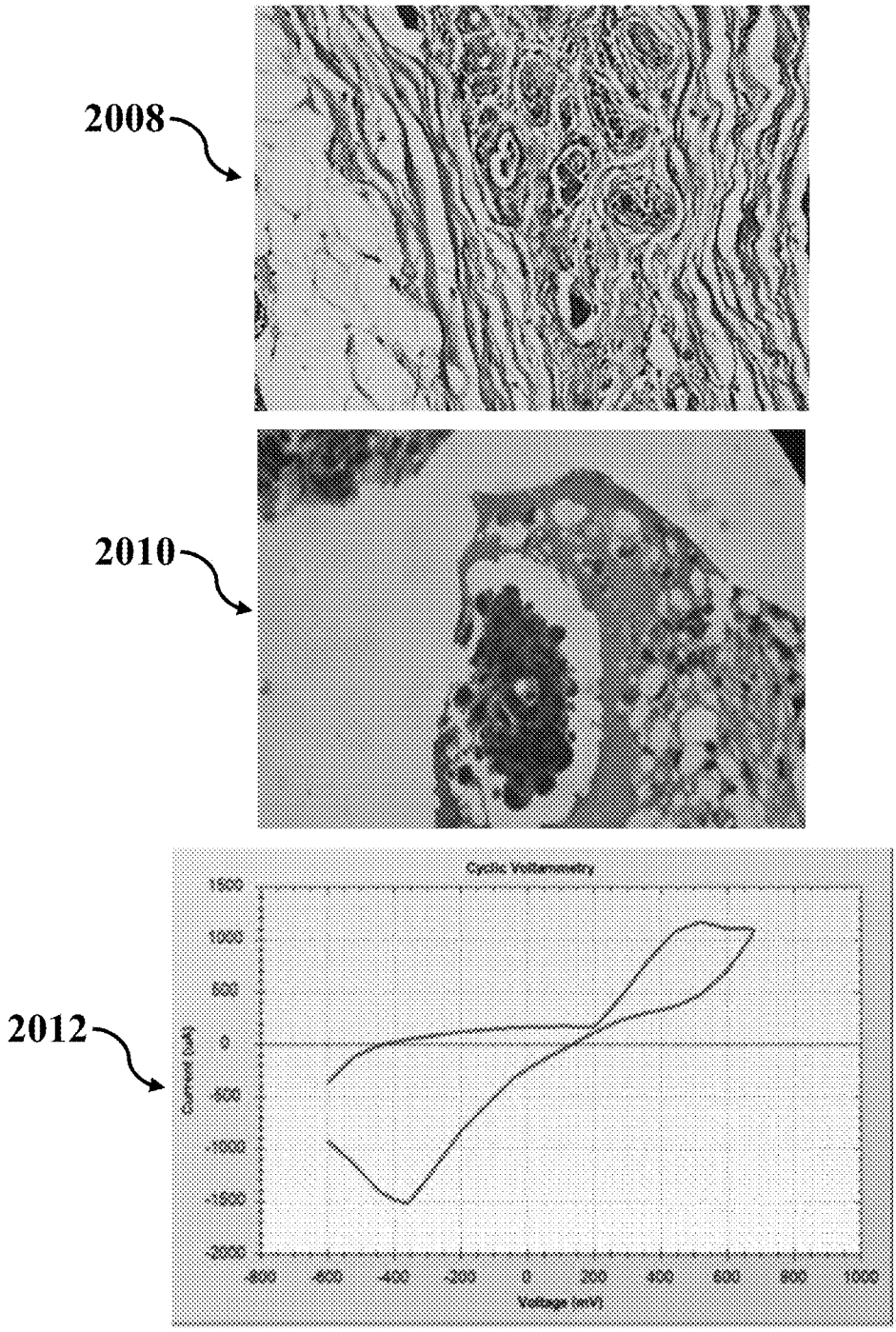

FIG. 20B

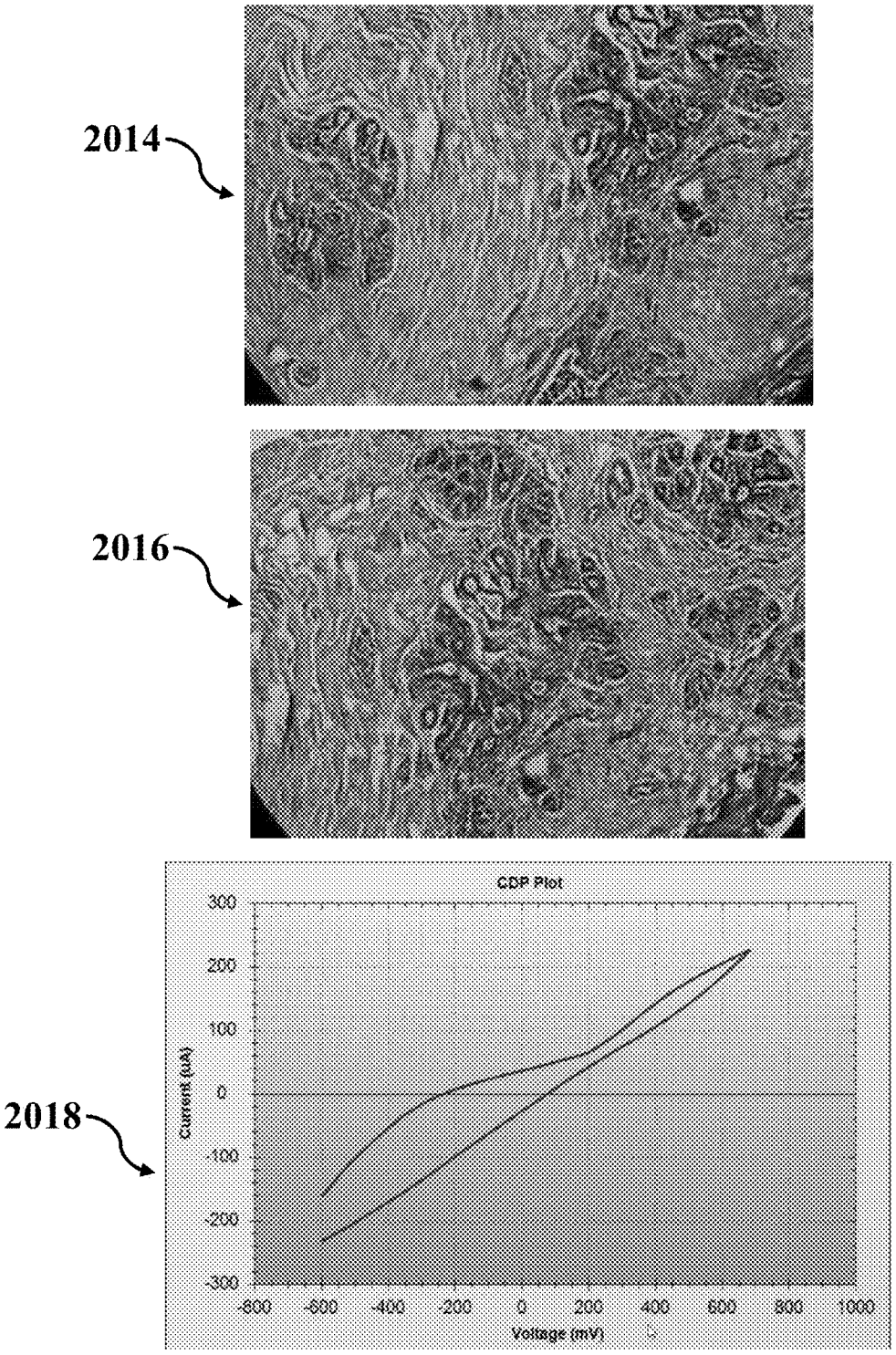
2014
2016
2018
CDP Plot
Current (uA)
Voltage (mV)
300
200
100
0
-100
-200
-300
-800
-600
-400
-200
0
200
400
600
800
1000

FIG. 20C

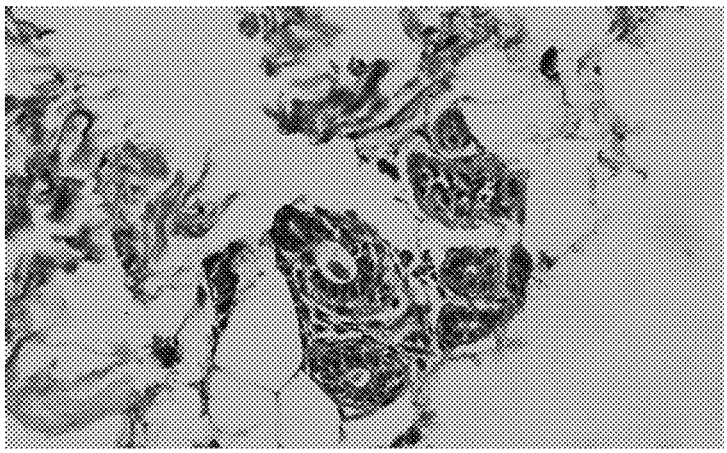
2020

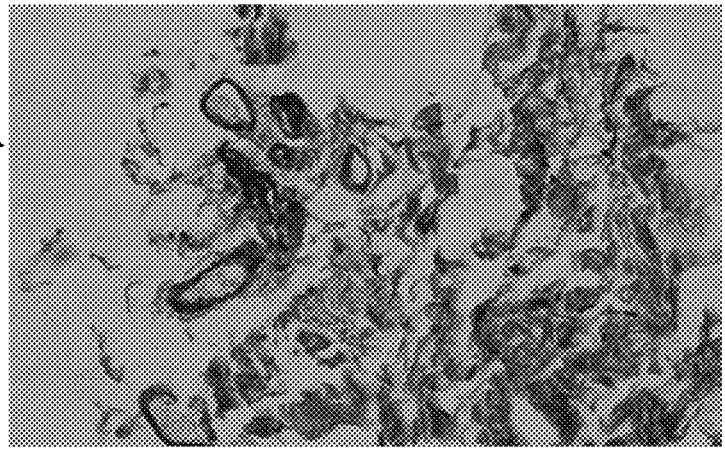
2022

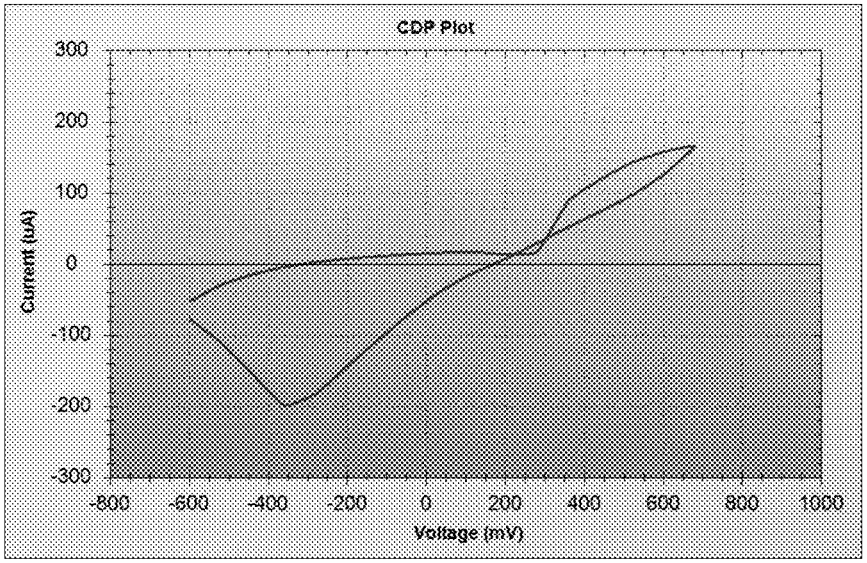
2024
CDP Plot
300
200
100
0
-100
-200
-300
Current (uA)
-800
-600
-400
-200
0
200
400
600
800
1000
Voltage (mV)

FIG. 20D

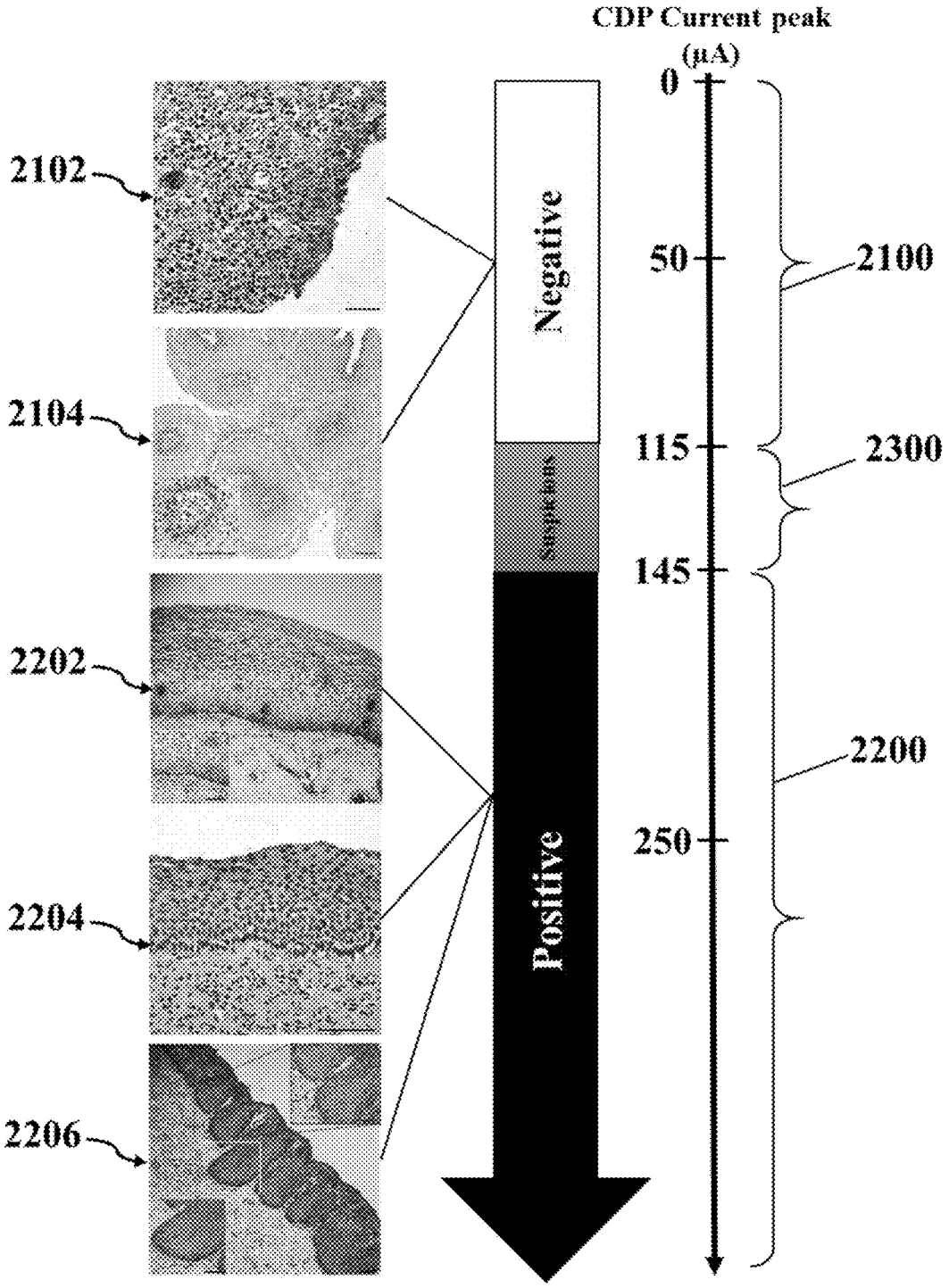
CDP Current peak
(μA)
0
50
115
145
250
2100
2300
2200
Negative
Suspicious
Positive
2102
2104
2202
2204
2206

FIG. 21

ELECTROCHEMICAL PROBE FOR CANCER DIAGNOSIS

CROSS-REFERENCE TO RELATED APPLICATION

This application is a continuation of patent application Ser. No. 16/857,428, filed Apr. 24, 2020, and entitled "REAL-TIME AND LABEL FREE ANALYZER FOR IN-VITRO AND IN-VIVO DETECTION OF CANCER", which is a continuation-in-part of U.S. patent application Ser. No. 16/010,510, filed Jun. 17, 2018, and entitled "REAL-TIME AND LABEL FREE ANALYZER FOR IN-VITRO AND IN-VIVO DETECTING OF CANCER", which takes priority from U.S. Provisional Patent Application Ser. No. 62/522,115 filed on Jun. 20, 2017, and entitled "DIAGNOSIS OF CANCER TUMORS IN BIOPSY BREAST TISSUES" and U.S. Provisional Patent Application Ser. No. 62/563,673 filed on Sep. 27, 2017, and entitled "CANCER DIAGNOSTIC PROBE", which are all incorporated herein by reference in their entirety.

SPONSORSHIP STATEMENT

This application has been sponsored by Iran Patent Office, which does not have any rights in this application.

TECHNICAL FIELD

The present disclosure generally relates to cancer diagnosis, and particularly, to a system, sensor, and method for diagnosing cancerous regions before and during surgery via a real-time and label free approach.

BACKGROUND

Glycolysis is the intracellular biochemical conversion of one molecule of glucose into two molecules of pyruvate, which can be used to attain cellular energy. With the assistance of sufficient oxygen, pyruvate could be converted by pyruvate dehydrogenase (PDH) into acetylCoA which is crucial in a metabolizing process to produce ATP in an oxidative way. A physiological concentration of pyruvate in human normal epithelial tissue has been reported to 0.7 mmol/g. Also the lactate-to-pyruvate ratio (L/P ratio) as a reflection of cell's redox state, illustrates the balance between NAD+ and NADH+H+, depending on the interconversion of lactate and pyruvate via lactate dehydrogenase (LDH). The L/P ratio in normal epithelial tissues is less than 20:1. Markers and assays have been developed to trace the LADH, P, or L/P in the patients' specimen as diagnostic or prognostic factors which reveal the interests on lactate based cancer research. Moreover some methods have been developed to trace pyruvate by electrochemical methods with the assistance of chemically labelled working electrodes. However, there is still no substitutive label free methods and/or devices to replace expensive, complicated, and late-responsive clinical methods and devices such as pathology assays.

Hence, there is a need for cost-effective, label free and real-time methods and devices, especially sensors and method to use thereof to detect cancer in suspicious regions especially during cancer surgery like mastectomy to remove involved regions with precise margins to reduce resection of normal sites.

SUMMARY

This summary is intended to provide an overview of the subject matter of the present disclosure, and is not intended to identify essential elements or key elements of the subject matter, nor is it intended to be used to determine the scope of the claimed implementations. The proper scope of the present disclosure may be ascertained from the claims set forth below in view of the detailed description below and the drawings.

In one general aspect, the present disclosure describes an exemplary method for in-vivo cancer diagnosis within a living tissue. The method may include preparing an electrochemical probe by fabricating three integrated electrodes via coating a layer of vertically aligned multi-walled carbon nanotubes (VAMWCNTs) on tips of three electrically conductive biocompatible needles, putting the tips of the three integrated electrodes in contact with a portion of the living tissue by inserting the tips of the three integrated electrodes into the portion of the living tissue, recording an electrochemical response from the portion of the living tissue, where the electrochemical response may include a cyclic voltammetry (CV) diagram with an oxidation current peak of hypoxic glycolysis chemical reaction in biological cells within the portion of the living tissue, and detecting cancer-involving status of the portion of the living tissue based on the oxidation current peak. In an exemplary embodiment, the electrochemical response may include a cyclic voltammetry (CV) diagram of H_2O_2 related oxidation/reduction chemical reaction in biological cells within the portion of the living tissue. The concentration of H_2O_2 may be in correlation with the hypoxia glycolysis occurred in tumor cells.

In an exemplary implementation, detecting the cancer-involving status of the portion of the living tissue based on the oxidation current peak may include detecting a healthy state at the portion of the living tissue responsive to a value of the oxidation current peak being smaller than a first threshold value, detecting a cancerous state at the portion of the living tissue responsive to the value of the oxidation current peak being larger than a second threshold value, and detecting a moderately cancer-involved state at the portion of the living tissue responsive to the value of the oxidation current peak being between the first threshold value and the second threshold value.

In an exemplary implementation, detecting the cancer-involving status of the portion of the living tissue based on the oxidation current peak may include generating a set of reference current peak values, looking up the oxidation current peak within the generated set of reference current peak values, and detecting the cancer-involving status in the portion of the living tissue. In an exemplary implementation, generating the set of reference current peak values may include recording a set of CV diagrams from a plurality of samples of living tissues using the electrochemical probe, measuring a set of reference current peaks respective to the recorded set of CV diagrams for each sample of the plurality of samples of living tissues, determining status of each sample by applying a pathological assay to each sample, and assigning the determined status of each sample to the respective measured reference current peak. The determined status may include one of a healthy state, a cancerous state, and a moderately cancer-involved state, based on result of the applied pathological assay. In an exemplary implementation, detecting the cancer-involving status in the portion of the living tissue may include detecting the healthy state for the portion of the living tissue responsive to the oxidation current peak being in a first range of the generated set of reference current peak values assigned as being of the healthy state, detecting the cancerous state for the portion of the living tissue responsive to the oxidation current peak being in a second range of the generated set of reference

current peak values assigned as being of the cancerous state, and detecting the moderately cancer-involved state for the portion of the living tissue responsive to the oxidation current peak being in a third range of the generated set of reference current peak values assigned as being of the moderately cancer-involved state.

In an exemplary implementation, preparing the electrochemical probe may include fabricating the three integrated electrodes by coating the layer of vertically aligned multi-walled carbon nanotubes (VAMWCNTs) on the tips of the three electrically conductive biocompatible needles, and fixing the three integrated electrodes at one end of a handle. In an exemplary implementation, fabricating the three integrated electrodes may include depositing a catalyst layer on the tips of the three electrically conductive biocompatible needles, and growing an array of VAMWCNTs on the deposited catalyst layer.

In an exemplary implementation, depositing the catalyst layer on the tips of the three electrically conductive biocompatible needles may include depositing a layer of Nickel (Ni) with a thickness of less than 10 nm using an E-beam evaporation system at a temperature of 120° C. with a depositing rate of 0.1 Angstroms/s. In an exemplary implementation, growing the array of VAMWCNTs on the deposited catalyst layer may include annealing the deposited catalyst layer at a temperature of 680° C. in an H_2 environment with a flow rate of 20-35 standard cubic centimeters per minute (sccm) for about 30 minutes, graining the annealed catalyst layer by plasma hydrogenation of surface of the catalyst layer for 5 minutes with an intensity of 5.5 $W \cdot cm^{-2}$, and growing VAMWCNTs on the grained catalyst layer in a chamber by introducing a plasma comprising a mixture of C_2H_2 with flow rate of 5 sccm and H_2 with flow rate of 35 sccm to the chamber for 15 minutes.

In an exemplary implementation, detecting the cancerous state in the portion of the living tissue may include recording a reference electrochemical response from a reference solution, the reference electrochemical response comprising a reference oxidation current peak, comparing the electrochemical response with the reference electrochemical response, and detecting the cancerous state in the portion of the living tissue responsive to a larger oxidation current peak of the electrochemical response in comparison with the reference oxidation current peak of the reference electrochemical response. In an exemplary embodiment, the reference solution may include a lactate solution with a lactate concentration of 0.05 mM or more.

In an exemplary embodiment, the portion of the living tissue may include at least one of a liquid suspicious sample, a solid suspicious sample, and combinations thereof. In an exemplary embodiment, the portion of the living tissue may include a suspicious mass to be cancerous that may include at least one of a biopsied sample from a human or animal body, a removed sample from a human or animal body by surgery, a portion of a living tissue in a human or animal body, a portion of a living tissue in a human or animal body during tumor removal surgery, and combinations thereof.

In an exemplary implementation, recording the electrochemical response from the portion of the living tissue may include connecting the electrochemical probe to an electrochemical stimulator-analyzer, applying a set of electrical potentials to the electrochemical probe using the electrochemical stimulator-analyzer, and recording a set of electrical currents respective to the applied set of electrical potentials from the portion of the living tissue using the electrochemical stimulator-analyzer. In an exemplary embodiment, the electrochemical stimulator-analyzer may include a potentiostat.

In an exemplary implementation, applying the set of electrical potentials to the probe may include applying a sweeping range of electrical potentials between −1 V and 1 V to the working electrode.

In an exemplary implementation, each tip of the tips of the three electrically conductive biocompatible needles may include a respective sensing tip with a diameter between 100 μm and 200 μm, and a length between 0.1 cm and 1 cm.

In an exemplary implementation, the electrochemical probe may include a sensing part and the handle. In an exemplary embodiment, the sensing part may include a working electrode including a first biocompatible conductive needle of the three electrically conductive biocompatible needles, a counter electrode including a second biocompatible conductive needle of the three electrically conductive biocompatible needles, and a reference electrode including a third biocompatible conductive needle of the three electrically conductive biocompatible needles.

In an exemplary embodiment, the handle may include an insertion part and a releasing button. In an exemplary implementation, the insertion part may be configured to insert the electrochemical probe into the living tissue. In an exemplary implementation, the releasing button may be configured to release the sensing part for replacing the sensing part with a fresh one. Where, the sensing part may be attached to the insertion part.

In an exemplary embodiment, the working electrode, the counter electrode, and the reference electrode may be attached to the insertion part at one end of the handle apart from each other with a distance between 1 mm and 5 mm.

In an exemplary embodiment, the sensing part may further include an electrode holder encompassing the working electrode, the counter electrode, and the reference electrode. In an exemplary embodiment, the handle may further include a handle head and a switch located on the handle head. In an exemplary implementation, the switch may be configured to connect the electrochemical probe to an electrochemical stimulator-analyzer device, and disconnect the electrochemical probe from the electrochemical stimulator-analyzer device.

In an exemplary embodiment, the VAMWCNTs may include VAMWCNTs with a length of between 0.5 μm and 10 μm. In an exemplary embodiment, the VAMWCNTs may include VAMWCNTs with a diameter of between 20 nm and 100 nm.

In one general aspect, the present disclosure describes an electrochemical probe for in-vivo measurement of H_2O_2 oxidation within a living tissue. The electrochemical probe may include a sensing part and a handle. In an exemplary embodiment, the sensing part may include a working electrode including a first biocompatible conductive needle, a counter electrode including a second biocompatible conductive needle, and a reference electrode including a third biocompatible conductive needle. The working electrode, the counter electrode, and the reference electrode may be configured to put in contact with the living tissue by inserting the sensing part into the living tissue. In an exemplary embodiment, the handle may include an insertion part that may be configured to insert the sensing part into the living tissue. The sensing part may be attached to the insertion part.

In an exemplary embodiment, each of the first biocompatible conductive needle, the second biocompatible conductive needle, and the third biocompatible conductive needle may include a respective sensing tip. In an exemplary

embodiment, each sensing tip may include a catalyst layer that may be deposited on the sensing tip and an array of vertically aligned multi-walled carbon nanotubes (VAMWCNTs) that may be grown on the catalyst layer.

In an exemplary embodiment, the catalyst layer may include a layer of Nickel (Ni) with a thickness of less than 10 nm. In an exemplary embodiment, the VAMWCNTs may include VAMWCNTs with a length of between 0.5 μm and 10 μm. In an exemplary embodiment, the VAMWCNTs may include VAMWCNTs with a diameter of between 20 nm and 100 nm.

In an exemplary embodiment, the respective sensing tip of each of the working electrode, the counter electrode, and the reference electrode may include may have a diameter between 100 μm and 200 μm, and a length between 0.1 cm and 1 cm. In an exemplary embodiment, the working electrode, the counter electrode, and the reference electrode may be attached to the insertion part at one end of the handle apart from each other with a distance between 1 mm and 5 mm.

In an exemplary embodiment, the sensing part may further include an electrode holder that may encompass the working electrode, the counter electrode, and the reference electrode. In an exemplary embodiment, the handle may further include a releasing button configured to release the sensing part for replacing the sensing part. In an exemplary embodiment, the handle may further include a handle head and a switch located on the handle head. In an exemplary implementation, the switch may be configured to connect the electrochemical probe to an electrochemical stimulator-analyzer device, and disconnect the electrochemical probe from the electrochemical stimulator-analyzer device.

BRIEF DESCRIPTION OF THE DRAWINGS

The drawing figures depict one or more implementations in accord with the present teachings, by way of example only, not by way of limitation. In the figures, like reference numerals refer to the same or similar elements.

FIG. **1**A illustrates a schematic view of an exemplary electrochemical system for cancer diagnosis, consistent with one or more exemplary embodiments of the present disclosure.

FIG. **1**B illustrates a schematic view of an exemplary CNT based electrochemical chip, consistent with one or more exemplary embodiments of the present disclosure.

FIG. **1**C illustrates a schematic view of an exemplary sensing well, consistent with one or more exemplary embodiments of the present disclosure.

FIG. **1**D illustrates a schematic view of an exemplary magnified portion of exemplary working electrode within exemplary sensing well of FIG. **1**C, consistent with one or more exemplary embodiments of the present disclosure.

FIG. **1**E illustrates a schematic view of an exemplary cancer diagnosis probe (CDP), consistent with one or more exemplary embodiments of the present disclosure.

FIG. **1**F illustrates a schematic view of an exemplary needle electrode of exemplary CDP corresponding to the working electrode, consistent with one or more exemplary embodiments of the present disclosure.

FIG. **1**G illustrates a schematic view of an exemplary magnified portion of a tip of exemplary needle electrode of FIG. **1**C, consistent with one or more exemplary embodiments of the present disclosure.

FIG. **1**H illustrates a schematic view of another implementation of an exemplary cancer diagnosis probe (CDP) for in-vivo measurement of H_2O_2 oxidation in a living tissue, consistent with one or more exemplary embodiments of the present disclosure.

FIG. **1**I illustrates a schematic view of an exemplary scenario in which an exemplary sensing part has been separated from an exemplary handle of an exemplary CDP, consistent with one or more exemplary embodiments of the present disclosure.

FIG. **1**J illustrates a schematic view of an exemplary working electrode, consistent with one or more exemplary embodiments of the present disclosure.

FIG. **2**A illustrates an exemplary implementation of a method for cancer diagnosis, consistent with one or more exemplary embodiments of the present disclosure.

FIG. **2**B illustrates a schematic implementation of putting the array of vertically aligned multi-walled carbon nanotubes (VAMWCNTs) grown on tip of each needle electrode of three needles electrodes of exemplary CDP in contact with exemplary suspicious sample, consistent with one or more exemplary embodiments of the present disclosure.

FIG. **2**C illustrates a schematic view of another exemplary implementation of putting exemplary electrodes of exemplary CDP in contact with an exemplary portion of a living tissue, consistent with one or more exemplary embodiments of the present disclosure.

FIG. **2**D illustrates an implementation of detecting the cancerous state in the suspicious sample, consistent with one or more exemplary embodiments of the present disclosure.

FIG. **2**E illustrates an exemplary implementation of an exemplary method for in-vivo cancer diagnosis within a living tissue, consistent with one or more exemplary embodiments of the present disclosure.

FIG. **2**F illustrates an exemplary implementation of preparing an exemplary electrochemical probe similar to the exemplary CDP, consistent with one or more exemplary embodiments of the present disclosure.

FIG. **2**G illustrates an exemplary implementation of fabricating three integrated electrodes by coating a layer of vertically aligned multi-walled carbon nanotubes (VAMWCNTs) on tips of three electrically conductive biocompatible needles, consistent with one or more exemplary embodiments of the present disclosure.

FIG. **2**H illustrates an exemplary implementation of growing an array of VAMWCNTs on exemplary deposited catalyst layer, consistent with one or more exemplary embodiments of the present disclosure.

FIG. **2**I shows an exemplary implementation of detecting the cancer-involving status of the exemplary portion of the exemplary living tissue based on the oxidation current peak, consistent with one or more exemplary embodiments of the present disclosure.

FIG. **2**J shows an exemplary implementation of generating a set of reference current peak values, consistent with one or more exemplary embodiments of the present disclosure.

FIG. **3**A illustrates a schematic view of exemplary electrochemical reactions involved on sensor including exemplary VAMWCNTs as shown in FIGS. **1**D and **1**G, consistent with one or more exemplary embodiments of the present disclosure.

FIG. **3**B illustrates a schematic overview of mitochondrial electron and proton fluxes in hypoxia, consistent with one or more exemplary embodiments of the present disclosure.

FIG. **4** illustrates a field emission scanning electron microscopy (FESEM) image of the VAMWCNTs array on a portion of an exemplary fabricated CNT based electro-

chemical chip, consistent with one or more exemplary embodiments of the present disclosure.

FIG. **5**A illustrates a FESEM image of a tip of a needle electrode of an exemplary fabricated cancer diagnostic probe (CDP) coated with an array of VAMWCNTs on the tip, consistent with one or more exemplary embodiments of the present disclosure.

FIG. **5**B illustrates a FESEM image of a first portion of an exemplary VAMWCNTs array grown on the tip of the needle electrode of exemplary fabricated CDP, consistent with one or more exemplary embodiments of the present disclosure.

FIG. **5**C illustrates a FESEM image of a second portion of an exemplary VAMWCNTs array grown on the tip of the needle electrode of exemplary fabricated CDP, consistent with one or more exemplary embodiments of the present disclosure.

FIG. **5**D illustrates a FESEM image of a third portion of an exemplary VAMWCNTs array grown on the tip of the needle electrode of exemplary fabricated CDP, consistent with one or more exemplary embodiments of the present disclosure.

FIG. **6**A illustrates the CV diagrams of L-lactic acid solution individually recorded by electrochemical sensors fabricated from platinum (Pt), Gold (Au), amorphous glassy carbon (GC) and carbon nanotube (CNT) working electrodes (WEs), consistent with one or more exemplary embodiments of the present disclosure.

FIG. **6**B illustrates the CV diagrams of solutions with various concentrations of Hydrogen Peroxide (H_2O_2) resulted from the lactate turn to H_2O_2 and pyruvate recorded by electrochemical sensors with CNT arrays working electrode, consistent with one or more exemplary embodiments of the present disclosure.

FIG. **6**C illustrates the CV diagrams of H_2O_2 contained lactate solution in comparison with two cell culture solutions recorded by electrochemical sensors with CNT arrays working electrode, consistent with one or more exemplary embodiments of the present disclosure.

FIG. **7** illustrates the CV diagrams of hypoxic glycolysis in MCF 10A, MCF-7, MBA-MB-231, and MDA-MB-468 cell lines in comparison with H_2O_2 contained lactate solution and RPMI measured and recorded by exemplary CNT based electrochemical chip, consistent with one or more exemplary embodiments of the present disclosure.

FIG. **8**A illustrates the CV responses of the solution media of different normal and cancerous cell lines in various phenotypes for Colon (COR-L 105, SW-480, HT-29) cell lines in comparison with Reference diagram for solution H_2O_2 contained solution with a lactate concentration of about 0.3 mM, consistent with one or more exemplary embodiments of the present disclosure.

FIG. **8**B illustrates the CV responses of the solution media of different normal and cancerous cell lines in various phenotypes for Hematopoietic (1301, LCL-PI 1) cell lines in comparison with Reference diagram for H_2O_2 contained solution with a lactate concentration of about 0.3 mM, consistent with one or more exemplary embodiments of the present disclosure.

FIG. **8**C illustrates the CV responses of the solution media of different normal and cancerous cell lines in various phenotypes for Liver (HEP G2) cell lines in comparison with Reference diagram for H_2O_2 contained lactate solution with a lactate concentration of about 0.3 mM, consistent with one or more exemplary embodiments of the present disclosure.

FIG. **8**D illustrates the CV responses of the solution media of different normal and cancerous cell lines in various phenotypes for Lung (QU-DB, MRC-5) cell lines in comparison with Reference diagram for H_2O_2 contained lactate solution with a lactate concentration of about 0.3 mM, consistent with one or more exemplary embodiments of the present disclosure.

FIG. **8**E illustrates the CV responses of the solution media of different normal and cancerous cell lines in various phenotypes for Mouth (KB) cell lines in comparison with Reference diagram for H_2O_2 contained lactate solution with a lactate concentration of about 0.3 mM, consistent with one or more exemplary embodiments of the present disclosure.

FIG. **8**F illustrates the CV responses of the solution media of different normal and cancerous cell lines in various phenotypes for Neuron (BE(2)-C, LAN-5) cell lines in comparison with Reference diagram for H_2O_2 contained lactate solution with a lactate concentration of about 0.3 mM, consistent with one or more exemplary embodiments of the present disclosure.

FIG. **8**G illustrates the CV responses of the solution media of different normal and cancerous cell lines in various phenotypes for Prostate (PC-3, Du-145) cell lines in comparison with Reference diagram for H_2O_2 contained lactate solution with a lactate concentration of about 0.3 mM, consistent with one or more exemplary embodiments of the present disclosure.

FIGS. **9**A-**9**F illustrate the cytopathological results (top side) and electrochemical responses (bottom side) of the breast tissues removed by biopsy or surgery from 6 suspicious patients to cancer, consistent with one or more exemplary embodiments of the present disclosure.

FIG. **10** illustrates a columnar diagram of electrochemical responses of the breast tissues removed by biopsy or surgery from 11 suspicious patients to cancer, consistent with one or more exemplary embodiments of the present disclosure.

FIG. **11**A illustrates CV response of exemplary CDP with all three needles covered by VAMWCNTs immediately after connection to the tissues, consistent with one or more exemplary embodiments of the present disclosure.

FIG. **11**B illustrates CV response of exemplary CDP with only working electrode covered by VAMWCNTs immediately after connection to the tissues, consistent with one or more exemplary embodiments of the present disclosure.

FIG. **11**C illustrates CV response of exemplary CDP with non-CNT covered by needles immediately after connection to the tissues, consistent with one or more exemplary embodiments of the present disclosure.

FIGS. **12**A-**12**E illustrate CV responses recorded by exemplary CDP (needle based electrochemical sensor) from the resected tissues from five patients among 50 individual patients suspicious to breast cancer (bottom side) in comparison with images obtained by conventional pathological methods (H&E) (top side), consistent with one or more exemplary embodiments of the present disclosure.

FIG. **13** illustrates a summary of categorized regimes of CV responses recorded by exemplary CDP from the resected tissues from five patients among 50 individual patients suspicious to breast cancer representing CV regimes along a spectrum from a completely non-cancerous state to cancerous state, consistent with one or more exemplary embodiments of the present disclosure.

FIG. **14**A illustrates a sonography image from a tumor side taken from an exemplary mouse tumorized by 4T1 breast cancer cell lines, consistent with one or more exemplary embodiments of the present disclosure.

FIG. **14**B illustrates H&E image from the tumor side taken from exemplary tumorized mouse by 4T1 breast

cancer cell lines, consistent with one or more exemplary embodiments of the present disclosure.

FIG. **14**C illustrates H&E image from a normal/healthy side taken from exemplary tumorized mouse by 4T1 breast cancer cell lines, consistent with one or more exemplary embodiments of the present disclosure.

FIG. **14**D illustrates CV diagrams of normal and tumor regions/sides of exemplary tumorized mouse by 4T1 breast cancer cell lines calibrated by a Reference CV diagram from H_2O_2 contained lactate solution with a lactate concentration of about 0.3 mM obtained using exemplary CDP, consistent with one or more exemplary embodiments of the present disclosure.

FIG. **15**A illustrates a sonography image from a tumor taken from an exemplary mouse tumorized by 4T1 breast cancer cell lines, consistent with one or more exemplary embodiments of the present disclosure.

FIG. **15**B illustrates exemplary six analyzed regions of an exemplary tumorized mouse among the exemplary five tumorized mice before surgery, consistent with one or more exemplary embodiments of the present disclosure.

FIG. **15**C illustrates exemplary six analyzed regions of an exemplary tumorized mouse among the exemplary five tumorized mice during surgery, consistent with one or more exemplary embodiments of the present disclosure.

FIG. **16** illustrates comparative diagram of CDP responses in interaction with normal, nonmalignant tumor, and malignant tumor recorded from individual mice, consistent with one or more exemplary embodiments of the present disclosure.

FIG. **17**A illustrates CV response diagram obtained by applying exemplary CDP in detection of suspicious margins during breast cancer surgery for a known normal region, consistent with one or more exemplary embodiments of the present disclosure.

FIG. **17**B illustrates CV response diagram obtained by applying exemplary CDP in detection of suspicious margins during breast cancer surgery for a suspicious region, consistent with one or more exemplary embodiments of the present disclosure.

FIG. **17**C illustrates CV response diagram obtained by applying exemplary CDP in detection of suspicious margins during breast cancer surgery for another suspicious region, consistent with one or more exemplary embodiments of the present disclosure.

FIG. **17**D illustrates an H&E resulted image after the surgery for a known normal region, consistent with one or more exemplary embodiments of the present disclosure.

FIG. **17**E illustrates an H&E resulted image after the surgery for a suspicious region, consistent with one or more exemplary embodiments of the present disclosure.

FIG. **17**F illustrates an H&E resulted image after the surgery for another suspicious region, consistent with one or more exemplary embodiments of the present disclosure.

FIG. **18** illustrates H&E images from nine exemplary samples, consistent with one or more exemplary embodiments of the present disclosure.

FIG. **19** illustrates classification of current peaks recorded by exemplary CDP after examining more than 250 samples in consistence with pathological diagnosis, consistent with one or more exemplary embodiments of the present disclosure.

FIG. **20**A illustrates an image resulted from frozen H&E (top-side image), an image resulted from permanent H&E (middle-side image), and a CV response recorded by exemplary CDP (bottom-side image) for the anterior IM of a patient (ID 18), consistent with one or more exemplary embodiments of the present disclosure.

FIG. **20**B illustrates an image resulted from frozen H&E (top-side image), an image resulted from permanent H&E (middle-side image), and a CV response recorded by exemplary CDP (bottom-side image) for a suspicious margin inside the body of the patient (anterior margin of patient ID 46), consistent with one or more exemplary embodiments of the present disclosure.

FIG. **20**C illustrates an image resulted from frozen H&E (top-side image), an image resulted from permanent H&E (middle-side image), and a CV response recorded by exemplary CDP (bottom-side image) for a suspicious margin inside the body of the patient (posterior IM of patient ID 46), consistent with one or more exemplary embodiments of the present disclosure.

FIG. **20**D illustrates an image resulted from frozen H&E (top-side image), an image resulted from permanent H&E (middle-side image), and a CV response recorded by exemplary CDP (bottom-side image) for Sentinel Lymph Node (SLN) of patient ID 18, consistent with one or more exemplary embodiments of the present disclosure.

FIG. **21** illustrates a visually summarized comparison between current peak values of recorded CV responses utilizing the exemplary CDP via exemplary methods for in-vivo cancer diagnosis within a living tissue, and CIN pathological classification, consistent with one or more exemplary embodiments of the present disclosure.

DETAILED DESCRIPTION

In the following detailed description, numerous specific details are set forth by way of examples in order to provide a thorough understanding of the relevant teachings. However, it should be apparent that the present teachings may be practiced without such details. In other instances, well known methods, procedures, components, and/or circuitry have been described at a relatively high-level, without detail, in order to avoid unnecessarily obscuring aspects of the present teachings. The following detailed description is presented to enable a person skilled in the art to make and use the methods and devices disclosed in exemplary embodiments of the present disclosure. For purposes of explanation, specific nomenclature is set forth to provide a thorough understanding of the present disclosure. However, it will be apparent to one skilled in the art that these specific details are not required to practice the disclosed exemplary embodiments. Descriptions of specific exemplary embodiments are provided only as representative examples. Various modifications to the exemplary implementations will be readily apparent to one skilled in the art, and the general principles defined herein may be applied to other implementations and applications without departing from the scope of the present disclosure. The present disclosure is not intended to be limited to the implementations shown, but is to be accorded the widest possible scope consistent with the principles and features disclosed herein.

A number of current methods utilize lactate and/or pyruvate as cancer markers. However, herein the oxidation of Hydrogen Peroxide (H_2O_2) molecules measured by carbon nanotubes (CNTs) based electrodes is utilized to detect cancer and especially distinguish cancerous regions from healthy regions in a suspicious tissue. The main consequence of pyruvate formation from lactate is release of H_2O_2 molecules as the main byproduct of hypoxia glycolysis. An abnormal redox state appears in cancer cells based on modulation of hypoxia with increased pyruvate concentra-

tion and lactate-to-pyruvate ratio (L/P ratio) which results in increasing the concentration of H_2O_2 in interstitial fluid (stroma). So, determination of H_2O_2 molecules would be an indication for the presence of cancer cells in a tissue. As H_2O_2 is an active and non-stable molecule it would turn to O_2, H^+ and release electrons which are great target charges for electrochemical sensation.

Herein, an electrochemical approach based on multi-walled carbon nanotubes (MWCNTs) electrodes is disclosed for fast tracking of hypoxia glycolysis in the interstitial fluid of biopsied tissues suspicious to cancer, such as breast tissues. Electrochemical reduction of H_2O_2 molecules, produced in lactate to pyruvate transformation, on the electrodes of disclosed system may present a significant quantitate response signal in correlation with the presence of cancer cells in a suspicious sample. Here, a cancer diagnostic probe (CDP) based on vertically aligned multi-walled carbon nanotubes (VAMWCNTs) arrays as sensing electrode with direct and selective electron transfer abilities in interaction with H_2O_2 may be utilized.

Disclosed herein may include a label free method for diagnosis of the presence of cancer in suspicious regions based on determination of the hypoxia glycolysis in a quantitative manner. The method may be based on measuring the oxidative currents released during glycolysis from the tissue. A matched diagram between an electrochemical response measured from a suspicious sample and cancerous state curves may be utilized for a final diagnostic result. Over expression of glycolysis assisted mRNAs in cancerous samples may be observed as an indicator of a presence of cancer in a sample. Exemplary method may be applied as an alternative for frozen pathology during the surgery with faster and more precise efficiency. Furthermore, a label free system including an electrochemical sensor with integrated three CNT based electrodes is disclosed for tracking hypoxia glycolysis via detecting electrochemical reduction of H_2O_2 molecules, which may be produced in Lactate to pyruvate transformation in cancer cells. Exemplary simple and label free electrochemical assay may also be used for measuring the drug resistance of the tumors as a pre therapeutic prediction (as a new prognostic factor) to increase the survival rate in future.

In some implementations, exemplary electrochemical sensor may include an integrated sensor on the needles, named herein as a cancer diagnostic probe (CDP). Exemplary CDP may be fabricated and utilized in real-time on the suspicious regions to cancer before and during surgery in patients (In vivo). The domain of suspicious regions with a resolution of about 3 mm may be detected using exemplary method and CDP. The significant specification of CDP rather than recently reported real-time diagnostic methods, such as mass-spec, may allow the CDP to track the cancer involved regions before surgery by squeezing exemplary CDP to suspicious regions through the skin with the tracking resolution of 3 mm. In conventional diagnostic protocols, to precisely remove the cancer regions during surgery, a frozen sample from each suspicious region may need to be sent for pathologists. The pathology results may be available after about 15 minutes with the false negative response ratio of about 10%. Whereas, a cancer region may be distinguished in-situ utilizing exemplary CDP in less than about 10 seconds or even instantaneously before or during surgery and without any need for resecting and freezing a sample from a patient. The diagnostic information obtained by exemplary CDP may be used to detect cancer in marginally suspicious regions with rare distributions of cancer cells filtrated between normal stroma in less than about 20 seconds during the surgery or biopsy of live animal or human models without any requirement of tissue resection and preparation for frozen pathology. Exemplary CDP may be also utilized to detect an accurate location of cancer involved regions before surgery in superficial tumors.

Moreover, exemplary sensor may include a CNT based electrochemical chip for in vitro cancer diagnosis in suspicious samples. Exemplary CNT based electrochemical chip may include an array of electrodes of VAMWCNTs used in electrochemical assays. Both liquid and solid suspicious samples may be analyzed using exemplary CNT based electrochemical chip to detect a cancer presence within the suspicious samples.

FIG. **1**A shows a schematic view of an electrochemical system **100** for cancer diagnosis, consistent with one or more exemplary embodiments of the present disclosure. Exemplary electrochemical system **100** may include an exemplary sensor **102**, an electrochemical stimulator-analyzer **104**, and an array of electrically conductive connectors **106**. Exemplary sensor **102** may be configured to put in contact with a suspicious sample for cancer. Exemplary sensor **102** may include an integrated three-electrodes array, which may include the working electrode **108**, the counter electrode **110**, and the reference electrode **112**. Each of the working electrode **108**, the counter electrode **110** and the reference electrode **112** may include an array of vertically aligned multi-walled carbon nanotubes (VAMWCNTs). The electrochemical stimulator-analyzer **104** may be configured to measure electrochemical responses from the working electrode **108** and sensor **102** may be connected to the electrochemical stimulator-analyzer **104** via the array of electrically conductive connectors **106**.

In an exemplary implementation, exemplary electrochemical system **100** may be configured to detect a cancerous state via measuring H_2O_2 during hypoxia glycolysis in the suspicious sample for cancer. Exemplary electrochemical system **100** may be utilized by an exemplary method for cancer diagnosis described herein below.

In an exemplary embodiment, electrochemical stimulator-analyzer **104** may include a device that may be capable of measuring cyclic voltammetry (CV) based diagrams. In an exemplary embodiment, electrochemical stimulator-analyzer **104** may include a potentiostat.

In an exemplary implementation, electrochemical system **100** may further include a processor **114** that may be utilized for recording and analyzing electrochemical measurements that may be measured by electrochemical stimulator-analyzer **104**. Processor **114** may also be used for controlling electrochemical stimulations that may be carried out by electrochemical stimulator-analyzer **104**. In an exemplary embodiment, processor **114** may include an EVIUM readout system.

In an exemplary implementation, sensor **102** may include a CNT based electrochemical chip that may be configured to conduct in vitro cancer diagnosis assays. FIG. **1**B shows a schematic view of exemplary CNT based electrochemical chip **102**, consistent with one or more exemplary embodiments of the present disclosure. Exemplary CNT based electrochemical chip **102** may include at least one sensing well **120** and one array of electrically conductive connectors **106**. FIG. **1**C shows a schematic view of exemplary sensing well **120**, consistent with one or more exemplary embodiments of the present disclosure. Each sensing well **120** may include a substrate **122**, a passivation layer **124** that may be grown on substrate **122**, a catalyst layer **126** that may be coated or deposited and subsequently patterned on the passivation layer **124**, and three arrays of VAMWCNTs that

may be grown on the catalyst layer **126**. Three arrays of VAMWCNTs may include the working electrode **108**, the counter electrode **110**, and the reference electrode **112**.

In an exemplary embodiment, substrate **122** may include a silicon chip or wafer. Passivation layer **124** may include a layer of SiO_2 with a thickness of less than about 500 nm that may be grown by wet oxidation furnace on the surface of on substrate **122**. Catalyst layer **126** may include a layer of Nickel (Ni) with a thickness of less than about 10 nm that may be coated on passivation layer **124** by an E-beam evaporation system at a temperature of about 120° C. with depositing rate of about 0.1 Angstroms/s. Three arrays of VAMWCNTs (the working electrode **108**, the counter electrode **110**, and the reference electrode **112**) may be grown on catalyst layer **126** using a direct current plasma enhanced chemical vapor deposition (DC-PECVD) system. The growth process of VAMWCNTs may include three steps of firstly, annealing at a temperature of about 680° C. in an H_2 environment with a flow rate of about 35 standard cubic centimeters per minute (sccm) for about 30 minutes; secondly, graining, including plasma hydrogenation of surface for about 5 minutes with the intensity of about 5.5 $W \cdot cm^{-2}$ that may result in the catalyst layer **126** graining and formation of Ni nano-sized islands, and finally, growth of VAMWCNTs by introducing a plasma of C_2H_2 and H_2 mixture with flow rates of about 5 sccm and about 35 sccm to the chamber for about 15 minutes. Each of the VAMWCNTs may have a length between about 0.5 μm and about 5 μm and a diameter between about 20 nm and about 100 nm. The working electrode **108** may be grown on an area of about 1 cm×1 cm, the counter electrode **110** may be grown on an area of about 1 cm×1 cm, and the reference electrode **112** may be grown on an area of about 0.5 cm×0.5 cm.

FIG. **1**D shows a schematic view of an exemplary magnified portion **128** of exemplary working electrode **108** within exemplary sensing well **120** of FIG. **1**C, consistent with one or more exemplary embodiments of the present disclosure. Exemplary VAMWCNTs **130** of an array of VAMWCNTs of working electrode **108** may be grown vertically on catalyst layer **126**. Catalyst layer **126** may be coated or deposited and subsequently patterned on the passivation layer **124**, where passivation layer **124** may be grown on substrate **122**.

In an exemplary implementation, sensor **102** may include a cancer diagnosis probe (CDP) that may be configured to conduct in vivo cancer diagnosis assays. FIG. **1**E shows a schematic view of exemplary cancer diagnosis probe (CDP) **102**, consistent with one or more exemplary embodiments of the present disclosure. Exemplary cancer diagnosis probe (CDP) may include three needle electrodes **132**, **134**, and **136** as exemplary implementations of the working electrode **108**, the counter electrode **110**, and the reference electrode **112**, respectively. Moreover, CDP **102** may include a holding member **138** that may be configured to hold three needle electrodes **132**, **134**, and **136**. Three needle electrodes **132**, **134**, and **136** may be fixed on one end **140** of the holding member **138**.

FIG. **1**F shows a schematic view of an exemplary needle electrode **132** corresponding to the working electrode **108**, consistent with one or more exemplary embodiments of the present disclosure. Referring to FIG. **1**F, each needle electrode of three needles electrodes **132**, **134**, and **138** may include a tip **142**. Each needle electrode of the three needles electrodes **132**, **134**, and **136** may include a catalyst layer **144** that may be deposited on tips **142** of three needles electrodes **132**, **134**, and **136** and an array of VAMWCNTs **146** that may be grown on catalyst layer **144** on tip **142** of each needle electrode of three needles electrodes **132**, **134**, and **138**.

In an exemplary embodiment, each needle electrode of three needles electrodes **132**, **134**, and **138** may include a steel needle with a diameter between about 100 μm and about 200 μm, and a length between about 0.1 cm and about 1 cm. Three needle electrodes **132**, **134**, and **138** may be fixed on the end **140** of the holding member **138** apart from each other with a distance (interspace) between each other in a range of about 1 mm to about 5 mm.

In an exemplary embodiment, catalyst layer **144** may include a layer of Nickel (Ni) with a thickness of less than about 10 nm that may be coated on tip **142** of each needle electrode by an E-beam evaporation system at a temperature of about 120° C. with a depositing rate of about 0.1 Angstroms/s. Three arrays of VAMWCNTs (the working electrode **108**, the counter electrode **110**, and the reference electrode **112**) may be grown on catalyst layer **144** using a direct current plasma enhanced chemical vapor deposition (DC-PECVD) system as described herein above.

FIG. **1**G shows a schematic view of an exemplary magnified portion **148** of tip **142** of exemplary needle electrode **132** shown in FIG. **1**F, consistent with one or more exemplary embodiments of the present disclosure. Exemplary VAMWCNTs **130** of an array of VAMWCNTs **146** may be grown vertically on catalyst layer **144**. Catalyst layer **144** may be coated or deposited on a surface of tip **142**.

Exemplary cancer diagnosis probe (CDP) **102** may have various implementations. Exemplary cancer diagnosis probe (CDP) **102** may include an electrochemical probe with three integrated needle-shaped electrodes for in-vivo electrochemical measurements and diagnosis operations, such as cancer diagnostic techniques or methods. FIG. **111** shows a schematic view of another implementation of exemplary cancer diagnosis probe (CDP) **102** for in-vivo measurement of H_2O_2 oxidation in a living tissue, consistent with one or more exemplary embodiments of the present disclosure. Exemplary CDP **102** may be utilized for in-vivo measurement of H_2O_2 oxidation in a living tissue; thereby, allowing for detecting a cancerous state within the living tissue. Exemplary CDP **102** may include a handle **152** and a sensing part **154**, where sensing part **154** may be attached to a first end **156** of handle **152**. Exemplary sensing part **154** may include an exemplary working electrode **158**, an exemplary counter electrode **160**, and an exemplary reference electrode **162**. Exemplary sensing part **154** may further include an electrode holder **164**. In an exemplary embodiment, each of exemplary working electrode **158**, counter electrode **160**, and reference electrode **162** may be attached to electrode holder **164**.

In an exemplary embodiment, handle **152** may include a handle head **166**, an insertion part **168**, a switch **170**, and a releasing button **172**. Exemplary insertion part **168** may allow for inserting CDP **102** into a biological sample, for example, an exemplary living tissue in a patient's body, a tumor in a patient's body, or a biopsied sample from a patient who may involve with cancer. Exemplary switch **170** may be located on head **166** and switch **170** may be configured to connect CDP **102** to an electrochemical stimulator-analyzer device and/or disconnect CDP **102** from the electrochemical stimulator-analyzer device. In an exemplary embodiment, the electrochemical stimulator-analyzer device may include a potentiostat device or an electrochemical workstation.

In an exemplary embodiment, CDP **102** may be connected to an electrochemical stimulator-analyzer device through an

electrical connector, for example, an electrical wire, that may be connected to a second end **174** of handle **152**. In another exemplary embodiment, CDP **102** may be connected to the electrochemical stimulator-analyzer device utilizing a wireless connection between CDP **102** and the electrochemical stimulator-analyzer device without any needs to connecting wires. For example, CDP **102** may be connected to the electrochemical stimulator-analyzer device via Bluetooth devices or Bluetooth modules that may be embedded in CDP **102** and the electrochemical stimulator-analyzer device. The wireless connection may allow for simplifying utilizing CDP **102** in a surgery room by a surgeon, removing redundant wires that may require to sanitize iteratively, etc.

In an exemplary embodiment, sensing part **154** may be replaceable by releasing from handle **152** using releasing button **172**. Although electrochemical measurements that may be carried out utilizing CDP **102** may be repeatable, sensing part **154** may be replaced by another sensing part **154** (a fresh/new sensing part **154**) for each insertion into each part of the biological sample, which may be an obligation regarding medical ethics. Such obligations may be mandatory to avoid transferring cancer cells from one part of the biological sample to another part of the biological sample; i.e., from one part of a patient's body to another part of a patient's body. In an exemplary embodiment, sensing part **154** may be attached to insertion part **168** at the first end **156** of handle **152**. Furthermore, releasing button **172** may be located on insertion part **168** in proximity to the first end **156** of handle **152**. Exemplary sensing part **154** may be separated from handle **152** by pressing releasing button **172**. FIG. **1**I shows a schematic view of an exemplary scenario in which sensing part **154** has been separated from handle **152** of exemplary CDP **102**, consistent with one or more exemplary embodiments of the present disclosure.

Referring to FIG. **111**, exemplary CDP **102** may include three exemplary electrodes including working electrode **158**, counter electrode **160**, and reference electrode **162**. In an exemplary embodiment, working electrode **158** may comprise of a first needle coated with a layer of VAMWCNTs (an array of VAMWCNTs). VAMWCNTs may be great sensitive agents for sensing and measuring H_2O_2 as well as high electrically conductive agents for accurate electrochemical measurements. Exemplary counter electrode **160** may comprise of a second needle, and exemplary reference electrode **162** may comprise of a third needle. In an exemplary embodiment, the second needle may be coated with a layer of VAMWCNTs (an array of VAMWCNTs). In another exemplary embodiment, the third needle may be coated with a layer of VAMWCNTs (an array of VAMWCNTs).

In an exemplary embodiment, working electrode **158**, counter electrode **160**, and reference electrode **162** may be located apart from each other with a distance between each two respective electrodes of between about 1 mm and about 5 mm. In an exemplary embodiment, the distance between each two respective electrodes may be more than about 5 mm. It should be noted that the distance between each two respective electrodes may be selected depending on size of a sample, in which exemplary CDP **102** may be inserted. The distance between each two respective electrodes may be selected less than about 5 mm in order to obtain high-accurate electrochemical responses (i.e., CV diagrams) from the sample. In addition, the distance between each two respective electrodes should not be selected may be selected more than about 1 mm in order to avoid electrical noise in electrochemical measurements.

In an exemplary embodiment, each of the first needle, the second needle, and the third needle may include a biocompatible conductive needle with a diameter between about 100 μm and about 200 μm, and a length between about 0.1 cm and about 1 cm. In one embodiment, each of the first needle, the second needle, and the third needle may include a biocompatible metallic needle, for example, a steel needle. In one example, each of the first needle, the second needle, and the third needle may include an acupuncture needle.

In an exemplary embodiment, each of the first needle, the second needle, and the third needle may comprise a biocompatible conductive needle with a sensing tip. The sensing tip may have a diameter between about 100 μm and about 200 μm, and a length between about 0.1 cm and about 1 cm. In an exemplary embodiment, a layer (an array) of CNTs, for example, VAMWCNTs may be coated on each sensing tip of the first needle, the second needle, and the third needle.

FIG. **1**J shows a schematic view of exemplary working electrode **158**, consistent with one or more exemplary embodiments of the present disclosure. Each of the exemplary counter electrode **160** and exemplary reference electrode **162** may be similar to exemplary working electrode **158** shown in FIG. **1**J. Exemplary working electrode **158** may include exemplary first needle **180** with sensing tip **182**. In an exemplary embodiment, sensing tip **182** may be coated with an array of VAMWCNTs **184**.

In an exemplary embodiment, a catalyst layer may be deposited on sensing tip **182**. The catalyst layer may include a layer of Nickel (Ni) with a thickness of less than about 10 nm that may be coated on sensing tip **182** by an E-beam evaporation system at a temperature of about 120° C. with a depositing rate of about 0.1 Angstroms/s. Exemplary array of VAMWCNTs **184** may be grown on the catalyst layer using a direct current plasma enhanced chemical vapor deposition (DC-PECVD) system as described herein above.

In another aspect of the present disclosure, a method for cancer diagnosis is disclosed. FIG. **2**A shows an exemplary implementation of method **200** for cancer diagnosis, consistent with one or more exemplary embodiments of the present disclosure. Method **200** may include putting an array of vertically aligned multi-walled carbon nanotubes (VAMWCNTs) of a sensor in contact with a suspicious sample (step **202**), recording an electrochemical response from the suspicious sample, where the electrochemical response may include an oxidation current peak (step **204**), and detecting a cancerous state in the suspicious sample responsive to a larger amount of the oxidation current peak than a threshold value (step **206**). The sensor may be similar to exemplary sensor **102** described hereinabove.

Step **202** may include putting the array of vertically aligned multi-walled carbon nanotubes (VAMWCNTs) of the sensor in contact with the suspicious sample. In an exemplary implementation, putting the array of VAMWCNTs of the sensor in contact with the suspicious sample may include one of dropping the suspicious sample onto the sensor, placing the suspicious sample onto the sensor, squeezing the sensor into the suspicious sample, inserting the sensor into the suspicious sample, and combinations thereof.

In an exemplary embodiment, the suspicious sample may include one of a liquid suspicious sample, a solid suspicious sample, and combinations thereof. In an exemplary embodiment, the suspicious sample may include one of a plurality of cell lines, a biopsied sample from a human or animal body, a removed sample from a human or animal body by surgery, a portion of a living tissue in a human or animal body, and a portion of a living tissue in a human or animal body during surgery.

In an exemplary implementation, the sensor may be similar to sensor **102** and may include a substrate, a catalyst layer, and three arrays of vertically aligned multi-walled carbon nanotubes (VAMWCNTs) grown on the catalyst layer. Three arrays of VAMWCNTs may include a working electrode that may include a first array of VAMWCNTs, a reference electrode that may include a second array of VAMWCNTs, and a counter electrode that may include a third array of VAMWCNTs. In an exemplary implementation, the sensor may further include a passivation layer between the substrate and the catalyst layer.

In an exemplary implementation, the sensor may include one of a CNT based electrochemical chip similar to exemplary CNT based electrochemical chip **102** shown in FIG. **1**B, and a cancer diagnosis probe (CDP) similar to exemplary CDP **102** shown in FIG. **1**E. The substrate of the cancer CDP may include three needles, where each needle of the three needles may be coated by an array of VAMWCNTs of the three arrays of VAMWCNTs. In an exemplary implementation, the sensor may include exemplary sensor **102** as shown schematically in FIGS. **1**A, **1**B, and **1**E.

FIG. **2**B shows a schematic implementation of step **202** that may include putting the array of vertically aligned multi-walled carbon nanotubes (VAMWCNTs) grown on tip of each needle electrode of three needles electrodes **132**, **134**, and **138** of exemplary cancer diagnosis probe (CDP) **102** in contact with exemplary suspicious sample **250**, consistent with one or more exemplary embodiments of the present disclosure. Step **102** may include inserting or squeezing exemplary cancer diagnosis probe (CDP) **102** in exemplary suspicious sample **250**.

In an exemplary implementation, putting the array of VAMWCNTs of exemplary sensor **102** in contact with the suspicious sample may take place temporarily or over a time duration of less than 1 seconds for a real-time cancer diagnosis case. In an exemplary embodiment, putting the array of VAMWCNTs of exemplary sensor **102** in contact with the suspicious sample may take place temporarily or over a time duration of less than 1 seconds for in vivo or in vitro cancer diagnosis using exemplary sensor which may be an exemplary CDP or exemplary CNT based electrochemical chip. In an exemplary embodiment, putting the array of VAMWCNTs of exemplary sensor **102** in contact with the suspicious sample may be for a time duration of about 12 hours or more for in vitro cancer diagnosis cases with high levels of accuracy utilizing exemplary CNT based electrochemical chip **102**. In an exemplary embodiment, putting the array of VAMWCNTs of exemplary sensor **102** in contact with the suspicious sample may be carried out in a time duration of about 0.1 seconds to about 24 hours.

Step **204** may include recording the electrochemical response from the suspicious sample, where the electrochemical response may include an oxidation current peak. In an exemplary embodiment, the electrochemical response may include a cyclic voltammetry (CV) diagram of hypoxic glycolysis chemical reaction in biological cells within the suspicious sample. In an exemplary embodiment, the electrochemical response may include a cyclic voltammetry (CV) diagram of H_2O_2 related oxidation/reduction chemical reaction in biological cells within the suspicious sample. The concentration of H_2O_2 may be in correlation with the hypoxia glycolysis occurred in tumor cells. In an exemplary embodiment, the electrochemical response may include a cyclic voltammetry (CV) diagram of H_2O_2 oxidation that may be electrically sensed by VAMWCNTs in biological cells within the suspicious sample. In an exemplary embodiment, the electrochemical response may include an oxidation current peak of exemplary CV diagram of hypoxic glycolysis chemical reaction in biological cells within a suspicious sample.

In an exemplary implementation, recording the electrochemical response from the suspicious sample (step **204**) may include connecting the sensor to an electrochemical stimulator-analyzer, applying an electrical voltage on the sensor using the electrochemical stimulator-analyzer, and measuring the electrochemical response from the suspicious sample using the electrochemical stimulator-analyzer. In an exemplary embodiment, the electrochemical stimulator-analyzer may include a potentiostat.

Step **206** may include detecting the cancerous state in the suspicious sample responsive to a larger amount of the oxidation current peak than a threshold value. In an exemplary embodiment, the threshold value may include an oxidation current peak of about 700 μA or more when a time duration of putting the array of vertically aligned multi-walled carbon nanotubes (VAMWCNTs) of the sensor in contact with the suspicious sample (step **202**) may be more than about 12 hours. In an exemplary embodiment, the threshold value may include an oxidation current peak of about 80 μA or more when a time duration of putting the array of vertically aligned multi-walled carbon nanotubes (VAMWCNTs) of the sensor in contact with the suspicious sample (step **202**) may be about 5 seconds or less.

FIG. **2**C shows an implementation of detecting the cancerous state in the suspicious sample (step **206**), consistent with one or more exemplary embodiments of the present disclosure. Detecting the cancerous state in the suspicious sample (step **206**) may include recording a reference electrochemical response from a reference solution, where the reference electrochemical response may include a reference oxidation current peak (step **208**), comparing the electrochemical response with the reference electrochemical response (step **210**), and detecting the cancerous state in the suspicious sample responsive to a larger oxidation current peak of the electrochemical response in comparison with the reference oxidation current peak (step **212**). In an exemplary embodiment, the reference solution may include a lactate solution with a lactate concentration of about 0.05 mM or more.

Disclosed systems, methods and sensors herein may have various implementations, all based on measuring H_2O_2 oxidation current peak due to hypoxia glycolysis and reverse Warburg phenomena in cancer cells in order to for diagnosing cancerous tumors in real-time and with highly accuracy. Exemplary CDP **102** may be utilized via exemplary system **100** and/or utilizing exemplary method **200** for non-invasively diagnosing, in real-time, a presence of pre-neoplastic/neoplastic cells in either internal or external margins of a patient during tumor surgery, for example, breast cancer surgery. The exemplary systems, methods, and sensors may be capable of instantaneously determining an amount of H_2O_2 released from cancer or atypical cells, through reverse Warburg effect and hypoxia assisted glycolysis pathways, in a quantitative electrochemical manner. Reverse Warburg effect and hypoxia assisted glycolysis pathways may lead to high levels of H_2O_2 concentration in cancerous tumors in comparison with healthy tissues. Due to limited precision of conventional H&E pathology of biopsy samples and requirement to time-consuming preparation and consideration of many blocks and slides for complete evaluation of biopsy samples, exemplary systems, methods, and sensors of the present disclosure may be applied for cancer diagnosis, which may be based on live detecting the hypoxia glycolytic functions of high risk/premalignant cells based on the H_2O_2

released from cancer or atypical cells (through reverse Warburg effect **10** and hypoxia assisted glycolysis pathways). The exemplary systems, methods, and sensors may be utilized for diagnosing all cancerous tumors, in which hypoxia glycolysis may be the main differential mechanism between the phenotypes of healthy, precancerous and cancerous cells.

In an exemplary implementation, method **200** may further include fabrication of exemplary sensor **102** (not illustrated), for example, exemplary CDP **102**. In an exemplary implementation, method **200** may be utilized for in-vivo cancer diagnosis within a living tissue utilizing exemplary CDP **102**.

FIG. **2**E shows an exemplary implementation of exemplary method **220** for in-vivo cancer diagnosis within a living tissue, consistent with one or more exemplary embodiments of the present disclosure. Exemplary method **220** may be similar to method **200** shown in FIG. **2**A. Exemplary method **220** may include preparing an electrochemical probe by fabricating three integrated electrodes (step **221**), putting tips of the three integrated electrodes in contact with a portion of the living tissue by inserting the tips of the three integrated electrodes into the portion of the living tissue (step **222**), recording an electrochemical response from the portion of the living tissue, where the electrochemical response may include a cyclic voltammetry (CV) diagram with an oxidation current peak of hypoxic glycolysis chemical reaction in biological cells within the portion of the living tissue (step **224**), and detecting a cancer-involving status of the portion of the living tissue based on the oxidation current peak (step **226**).

In detail, step **221** may include preparing an electrochemical probe. In an exemplary embodiment, the electrochemical probe may be similar to exemplary CDP **102** that is shown in FIGS. **1**E, **1**H and **1**I. FIG. **2**F shows an exemplary implementation of preparing an exemplary electrochemical probe similar to CDP **102** (step **221**), consistent with one or more exemplary embodiments of the present disclosure. Step **221** may include fabricating three integrated electrodes by coating a layer of vertically aligned multi-walled carbon nanotubes (VAMWCNTs) on tips of three electrically conductive biocompatible needles (step **230**), and fixing the three integrated electrodes at one end of a handle (or a holding member) (step **232**).

FIG. **2**G shows an exemplary implementation of fabricating three integrated electrodes by coating a layer of vertically aligned multi-walled carbon nanotubes (VAMWCNTs) on tips of three electrically conductive biocompatible needles (step **230**), consistent with one or more exemplary embodiments of the present disclosure. Step **230** may include depositing a catalyst layer on the tips of the three electrically conductive biocompatible needles (step **240**), and growing an array of VAMWCNTs on the deposited catalyst layer (step **242**). In an exemplary implementation, step **230** may include fabricating three integrated electrodes by coating three respective layers of VAMWCNTs on tips of three electrically conductive biocompatible needles.

In detail, step **240** may include depositing a catalyst layer on tips of three electrically conductive biocompatible needles. In an exemplary implementation, step **240** may include depositing three catalyst layers on three respective tips of the three electrically conductive biocompatible needles. In an exemplary implementation, step **240** may include depositing a respective layer of Nickel (Ni) with a thickness of less than about 10 nm using an E-beam evaporation system at a temperature of about 120° C. with a depositing rate of about 0.1 Angstroms/s on each tip of the tips of the three electrically conductive biocompatible needles.

Furthermore, step **242** may include growing an array of VAMWCNTs on the deposited catalyst layer on each tip of the tips of the three electrically conductive biocompatible needles. FIG. **2**H shows an exemplary implementation of growing an array of VAMWCNTs on the deposited catalyst layer (step **242**), consistent with one or more exemplary embodiments of the present disclosure. Step **242** may include annealing the deposited catalyst layer at a temperature of about 680° C. in an H_2 environment with a flow rate of about 20 standard cubic centimeters per minute (sccm) to 35 sccm for about 30 minutes (step **244**), graining the annealed catalyst layer by plasma hydrogenation of surface of the catalyst layer for about 5 minutes with an intensity of about 5.5 $W \cdot cm^{-2}$ (step **246**), and growing VAMWCNTs on the grained catalyst layer in a chamber by introducing a plasma comprising a mixture of C_2H_2 with flow rate of about 5 sccm and H_2 with flow rate of about 35 sccm to the chamber for about 15 minutes (step **248**). In an exemplary implementation, graining the annealed catalyst layer by plasma hydrogenation of surface of the catalyst layer for about 5 minutes with an intensity of about 5.5 $W \cdot cm^{-2}$ (step **246**) may result in catalyst graining, and formation of nano-sized islands of the catalyst.

Referring to FIG. **2**E, step **222** may include putting tips of the three integrated electrodes in contact with a portion of the living tissue by inserting the tips of the three integrated electrodes into the portion of the living tissue. In an exemplary implementation, step **222** may include putting tips of exemplary three integrated electrodes of exemplary CDP **102** in contact with a portion of a living tissue by inserting the tips of the three integrated electrodes into the portion of the living tissue. As used herein, "the portion of the living tissue" may refer to an implementation of "the suspicious sample" described hereinabove, which may include a biological sample that may be suspicious to be cancerous. FIG. **2**C shows a schematic view of another exemplary implementation of putting electrodes **158**, **160**, and **162** of exemplary CDP **102** in contact with exemplary portion **262** of living tissue **260** (step **222**), consistent with one or more exemplary embodiments of the present disclosure. Putting electrodes **158**, **160**, and **162** of exemplary CDP **102** in contact with exemplary portion **262** of living tissue **260** may include inserting sensing part **154** into exemplary portion **262** of living tissue **260**.

In an exemplary implementation, putting electrodes **158**, **160**, and **162** of exemplary CDP **102** in contact with exemplary portion **262** of living tissue **260** may include at least one of putting electrodes **158**, **160**, and **162** inside portion **262** of living tissue **260**, inserting electrodes **158**, **160**, and **162** inside portion **262** of living tissue **260**, interacting a secretion of living tissue **260** with electrodes **158**, **160**, and **162**, squeezing electrodes **158**, **160**, and **162** inside portion **262** of living tissue **260**, and combinations thereof. In an exemplary embodiment, inserting electrodes **158**, **160**, and **162** inside portion **262** of living tissue **260** may include penetrating electrodes **158**, **160**, and **162** into portion **262** of living tissue **260**. In one implementation, putting electrodes **158**, **160**, and **162** of exemplary CDP **102** in contact with portion **262** of living tissue **260** (step **222**) may be done during at least one of a surgery operation, a mastectomy operation, a biopsy operation, an endomicroscopy operation, an optical biopsy operation, a clinical examination of a patient, and combinations thereof. In one implementation, putting electrodes **158**, **160**, and **162** of exemplary CDP **102**

in contact with exemplary portion **262** of living tissue **260** may include inserting electrodes **158**, **160**, and **162** of exemplary CDP **102** in portion **262** of living tissue **260** with an insertion depth between about 3 mm and about 5 mm.

In an exemplary embodiment, portion **262** of living tissue **260** may be in liquid form or solid form. In further detail, in an exemplary embodiment, portion **262** may comprise at least one of a liquid sample suspicious to be cancerous, a solid sample suspicious to be cancerous, and combinations thereof.

In an exemplary embodiment, portion **262** of living tissue **260** may include at least one of a biopsied sample from a human or animal body, a sample resected from a human or animal body by surgery, a portion of living tissue **260** in a human or animal body near to skin, an exemplary portion **262** of living tissue **260** of a human or animal body that may be accessible during surgery (tumor removal surgery) or biopsy operation, a suspicious mass to be cancerous in a human or animal body, a removed sample from a human or animal body by surgery, and combinations thereof.

Moreover, step **224** may include recording an electrochemical response from the portion of the living tissue, where the electrochemical response may include a cyclic voltammetry (CV) diagram with an oxidation current peak of hypoxic glycolysis chemical reaction in biological cells within the portion of the living tissue. In an exemplary implementation, step **224** may include recording a CV diagram with an oxidation current peak of hypoxic glycolysis chemical reaction from portion **262** of living tissue **260** utilizing exemplary CDP **102**. In an exemplary implementation, recording the electrochemical response from the suspicious sample (step **224**) may include recording the electrochemical response from exemplary suspicious sample **250** (FIG. **2**B) or exemplary portion **262** of living tissue **260** (FIG. **2**C). In an exemplary embodiment, the electrochemical response may be recorded using exemplary CDP **102** that is shown in FIGS. **1**E, **1**H and **1**I. In an exemplary embodiment, the electrochemical response may include a cyclic voltammetry (CV) diagram with an oxidation current peak of hypoxic glycolysis chemical reaction in biological cells within exemplary portion **262** of the living tissue **260**.

In an exemplary implementation, recording the electrochemical response from exemplary portion **262** of living tissue **260** may include connecting exemplary CDP **102** to an electrochemical stimulator-analyzer, applying a set of electrical potentials to exemplary CDP **102** using the electrochemical stimulator-analyzer, and recording a set of electrical currents respective to the applied set of electrical potentials from exemplary portion **262** of the living tissue **260** using the exemplary CDP **102** and the electrochemical stimulator-analyzer.

In an exemplary implementation, applying the set of electrical potentials to exemplary CDP **102** may include applying a sweeping range of electrical potentials between about −1 V and about 1 V to exemplary working electrode **158** or exemplary working electrode **108**. In an exemplary implementation, applying the set of electrical potentials to exemplary CDP **102** may include applying a sweeping range of electrical potentials between about −0.8 V and about 0.8 V to exemplary working electrode **158** or exemplary working electrode **108**. In an exemplary embodiment, the electrochemical stimulator-analyzer may comprise a potentiostat.

In detail, step **226** may include detecting a cancer-involving status of the portion of the living tissue based on the oxidation current peak. In an exemplary implementation, step **226** may include detecting a cancer-involving status of exemplary suspicious sample **250** (FIG. **2**B) or exemplary portion **262** of living tissue **260** (FIG. **2**C). In an exemplary implementation, detecting the cancer-involving status of portion **262** of living tissue **260** based on the oxidation current peak (step **226**) may include detecting a healthy state at portion **262** of living tissue **260** responsive to a value (an amount) of the oxidation current peak being smaller than a first threshold value, detecting a cancerous state at portion **262** of living tissue **260** responsive to the value of the oxidation current peak being larger than a second threshold value, and detecting a moderately cancer-involved state at the portion **262** of living tissue **260** responsive to the value of the oxidation current peak being between the first threshold value and the second threshold value.

In an exemplary implementation, exemplary method **220** utilizing exemplary CDP **102** may be utilized for in-vivo cancer diagnosis within all tissues in a human or animal's body. In an exemplary implementation, exemplary method **220** utilizing exemplary CDP **102** may be utilized for in-vivo cancer diagnosis of all cancerous tumors, in which hypoxia glycolysis may be the main differential mechanism between the phenotypes of healthy, precancerous and cancerous cells. In an exemplary implementation, detecting the cancer-involving status of portion **262** of living tissue **260** based on the oxidation current peak (step **226**) may include detecting presence of human breast cancer in a portion of a breast tissue responsive to the value of the oxidation current peak being equal to 203 μA or more, detecting the healthy state at the portion of the breast tissue responsive to the value of the oxidation current peak being equal to 137 μA or less, and detecting a moderately breast cancer-involved state at the portion of the breast tissue responsive to the value of the oxidation current peak being between 137 μA and 203 μA.

In an exemplary implementation, detecting the cancer-involving status of portion **262** of living tissue **260** based on the oxidation current peak (step **226**) may include detecting presence of cervical cancer in a portion of a cervical tissue (cervix) responsive to the value of the oxidation current peak being equal to 145 μA or more, detecting the healthy state at the portion of the cervical tissue (cervix) responsive to the value of the oxidation current peak being equal to 115 μA or less, and detecting a moderately cervical cancer-involved state (or a suspicious-involved state) at the portion of the cervical tissue (cervix) responsive to the value of the oxidation current peak being between 115 μA and 145 μA.

FIG. **2**I shows an exemplary implementation of detecting the cancer-involving status of portion **262** of living tissue **260** based on the oxidation current peak (step **226**), consistent with one or more exemplary embodiments of the present disclosure. In detail, detecting the cancer-involving status of portion **262** of living tissue **260** based on the oxidation current peak (step **226**) may include generating a set of reference current peak values (step **270**), looking up the oxidation current peak within the generated set of reference current peak values (step **272**), and detecting the cancer-involving status in portion **262** of living tissue **260** (step **274**).

In detail, step **270** may include generating a set of reference current peak values. FIG. **2**J shows an exemplary implementation of generating the set of reference current peak values (step **270**), consistent with one or more exemplary embodiments of the present disclosure. In an exemplary implementation, generating the set of reference current peak values (step **270**) may include recording a set of CV diagrams from a plurality of samples of living tissues using the electrochemical probe (i.e., CDP **102**) (step **280**), measuring a set of reference current peaks respective to the

recorded set of CV diagrams for each sample of the plurality of samples of living tissues (step **282**), determining status of each sample by applying a pathological assay to each sample (step **284**), and assigning the determined status of each sample to the respective measured reference current peak (step **286**). In an exemplary implementation, generating the set of reference current peak values (step **270**) may include calibrating exemplary CDP **102** for an exemplary living tissue similar to living tissue **260**. In such implementation, the plurality of samples of living tissues may include a plurality of samples of living tissues from the same organ, for example, breast tissue, of a plurality of human or animal bodies.

The determined status may include one of a healthy state, a cancerous state, and a moderately cancer-involved state, based on result of the applied pathological assay. In an exemplary implementation, detecting the cancer-involving status in portion **262** of living tissue **260** (step **274**) may include detecting the healthy state for portion **262** of living tissue **260** responsive to the oxidation current peak being in a first range of the generated set of reference current peak values assigned as being of the healthy state, detecting the cancerous state for portion **262** of living tissue **260** responsive to the oxidation current peak being in a second range of the generated set of reference current peak values assigned as being of the cancerous state, and detecting the moderately cancer-involved state for portion **262** of living tissue **260** responsive to the oxidation current peak being in a third range of the generated set of reference current peak values assigned as being of the moderately cancer-involved state.

In an exemplary implementation, the whole process of exemplary method **200** which may include, putting the array of VAMWCNTs of exemplary sensor **102** in contact with the suspicious sample (step **202**), recording the electrochemical response from the suspicious sample (step **204**), and detecting the cancerous state in the suspicious sample (step **206**) may be carried out in less than about 30 seconds. Similarly, in an exemplary implementation, steps **222**-**226** of exemplary method **220** which may include putting electrodes **158**, **160**, and **162** of exemplary CDP **102** in contact with exemplary portion **262** of living tissue **260** (step **222**), recording the electrochemical response from exemplary portion **262** of living tissue **260** (FIG. **2**C) (step **224**), and detecting the cancerous state in **262** of living tissue **260** (step **226**) may be carried out in less than about 30 seconds.

In an exemplary implementation, conducting cancer diagnosis process of exemplary method **220** which may further include replacing a previously used sensing part **154** with a new sensing part **154** may take place in less than about 40 seconds. In an exemplary implementation, conducting cancer diagnosis process of exemplary method **220** which may include replacing a previously used sensing part **154** with a new sensing part **154**, inserting exemplary CDP **102** including the new sensing part **154** into a target tissue by inserting new sensing part **154** into a target location within the target tissue, recording a CV response with a current peak from the target location, and detecting cancerous state of the target tissue may take place in less than about 40 seconds. For example, replacing a previously used sensing part **154** with a new sensing part **154**, inserting exemplary CDP **102** including the new sensing part **154** into portion **262** of living tissue **260** by inserting new sensing part **154** into portion **262** of living tissue **260**, recording a CV response with a current peak from portion **262** of living tissue **260**, and detecting cancerous state of portion **262** of living tissue **260** may take place in less than about 40 seconds.

In an exemplary implementation, replacing the previously used sensing part **154** may include removing the previously used sensing part **154**, and connecting the new (fresh) sensing part **154** to handle **152**. In an exemplary implementation, replacing the previously used sensing part **154** may take a time interval of less than about 20 sec. In an exemplary implementation, recording the CV response with the current peak from a target location (i.e., portion **262** of living tissue **260**) may be carried out in about 15 sec or less due to synchronized real-time processing.

Accordingly, in an exemplary embodiment, methods **200**, and **220**, provide a quick and efficient approach to instantaneously detect a tissue's cancerous state, including indicating presence of cancer. For example, exemplary CDP **102** may be utilized through exemplary methods **200**, and **220** for real-time high-accurate detecting cancer-involved margins in a patient's body. In such implementations, exemplary methods **200**, and **220** may be applied on at least one exemplary portion of a living tissue that may be suspicious to contain a cancerous tumor. In one implementation, exemplary methods **200**, and **220** may be applied before a tumor removal surgery, during a tumor removal surgery, after a tumor removal surgery, and combinations thereof. In an exemplary implementation, exemplary CDP **102** may be utilized through exemplary methods **200**, and **220** at suspicious margins around a dissected tumor after the tumor removal surgery to determine whether the suspicious margins are cancerous or not.

In an exemplary implementation, electrochemical system **100** may be utilized for cancer diagnosis via exemplary method **200**. FIG. **3**A shows a schematic view of exemplary electrochemical reactions involved on sensor **102** including exemplary VAMWCNTs **130** as shown in FIGS. **1**D and **1**G, consistent with one or more exemplary embodiments of the present disclosure. Presence of H_2O_2 active molecule released during hypoxia glycolysis in a suspicious sample may be the main trigger of the electrochemical reactions. Hence, the chemical reaction occurring on the working electrode **108** including VAMWCNTs **130** may include:

$$\text{L-Lactate} + O_2 \xrightarrow[\text{Oxidase}]{\text{L-Lactate}} \text{Pyruvate} + H_2O_2 \qquad \text{Eq. 1}$$

$$H_2O_2 \rightarrow O_2 + 2H^+ + 2e^- \text{ response reaction of the } CDP \qquad \text{Eq. 2}$$

When the hypoxia glycolysis (Eq. 2) is activated (the concentration of O_2 is less than 5%) in cancer cells, increased reactive oxygen species (ROS) generated by mitochondria, would significantly enhance the cathodic peak of an electrochemical response measured from the suspicious sample which could be sharply detected by VAMWCNTs **130** electrodes. It may be known that the lactate released by hypoxic tumor cells during their glycolysis may not be discharged as a waste product, but may be taken up by oxygenated tumor cells as energy fuel in which Lactate is converted to pyruvate and H_2O_2 by LDH-B and then enters the mitochondria for OXPHOS to generate ATP. Similar to this process, the lactate released from hypoxic tumor cells may be used herein in electrochemical assay to trace the concentration of lactate due to the intensity of the H_2O_2 produced during LADH (Eq. 1) and released electrons due to the intensity of H_2O_2 oxidation reaction (Eq. 2).

FIG. **3**B shows a schematic overview of mitochondrial electron and proton fluxes in hypoxia, consistent with one or more exemplary embodiments of the present disclosure.

During normaxia, electrons released from reduced cofactors (NADH and $FADH_2$), flow through the redox centers of the respiratory chain (r.c.) to molecular oxygen (dotted lines), to which a proton flux from the mitochondrial matrix to the intermembrane space is coupled (grey arrows). Protons then flow back to the matrix through the F0 sector of the ATP synthase complex, driving ATP synthesis. ATP is carried to the cell cytosol by the adenine nucleotide translocator (grey arrows). Under moderate to severe hypoxia, electrons escape the r.c. redox centers and reduce molecular oxygen to the superoxide anion radical before reaching the cytochrome c (black arrows). Under these conditions, to maintain an appropriate $\Delta\psi m$, ATP produced by cytosolic glycolysis enters the mitochondria where it is hydrolyzed by the F1F0 ATPase with extrusion of protons from the mitochondrial matrix (black arrows). So, the mechanism of H_2O_2 detection by the VAMWCNTs **130** electrodes in hypoxia glycolysis may be based on released ion species during reduction of $NADH^+$, generation of ROS and production of superoxide anion radical by reducing molecular oxygen before reaching to cytochrome c. The amount of released charged species and increased current transferred by VAMWCNTs **130** electrodes may be correlated with the concentration of the lactate and subsequently H_2O_2 which resulted in ROS generated during hypoxia glycolysis.

Example 1: Fabrication of CNT Based Electrochemical Chip for In Vitro Assays

In this example, exemplary CNT based electrochemical chips was fabricated for in vitro assays. First, silicon wafer (p-type <100>) substrates were cleaned through standard RCA #1 method ($NH_4OH:H_2O_2:H_2O$ solution and volume ratio of 1:1:5 respectively). Then, the cleaned substrates were rinsed in deionized (DI) water and dried by air. A thin layer of SiO_2 with a thickness of about 200 nm was grown by wet oxidation furnace on the surface of the silicon wafer, as a passivation layer. Nickel (Ni) catalyst layer for CNT growth with a thickness of about 9 nm was coated on SiO_2 by E-beam evaporation system at a temperature of about 120° C. with depositing rate of about 0.1 Angstroms/s. Afterwards, Ni-covered samples were located in a direct current plasma enhanced chemical vapor deposition (DC-PECVD) system to grow vertically aligned multi-walled carbon nanotubes (VAMWCNT). The growth process has three steps, including annealing, graining and growth. At first, the sample was annealed at a temperature of about 680° C. in an H_2 environment with a flow rate of about 35 standard cubic centimeters per minute (sccm) for about 30 minutes. During the graining, the surface was plasma hydrogenated for about 5 minutes with the intensity of about 5.5 $W \cdot cm^{-2}$ which results in the catalyst graining and formation of Ni nano-sized islands. In the growth step a plasma of C_2H_2 and H_2 mixture with flow rates of about 5 sccm and about 35 sccm were introduced to the chamber for about 15 minutes. Finally, CNT's were characterized with field emission scanning electron microscopy (FESEM). The length of CNTs ranged from about 2.5 to about 5 μm and the diameter of CNTs ranged from about 50 nm to about 70 nm.

FIG. **4** shows the FESEM image of the VAMWCNTs array on a portion of an exemplary fabricated CNT based electrochemical chip, consistent with one or more exemplary embodiments of the present disclosure. The CNTs were multi-walled carbon nanotubes with high purity and a presence of nickel on the top side of the CNTs could be related to the tip-growth mechanism. The CNT has been used as the work, counter and reference electrodes in exemplary fabricated CNT based electrochemical chips. The active area of the work, counter and reference electrodes were about 100 mm^2, 100 mm^2, 50 mm^2, respectively. The CNT based electrochemical chips were connected to a potentiostat by conductive wires bonded to the pads of the potentiostat.

Example 2: Fabrication of Cancer Diagnostic Probe (CDP) for In Vivo Assays

In this example, the tips of sterile steel needles were coated by Ni catalyst layers similar to that was described in EXAMPLE 1 for CNT based electrochemical chips with the assistance of E-Beam coating system. A fixture was designed and fabricated to hold the needles both in E-Beam and DC-PECVD systems to limit the growth of CNTs just in the tips of the needles. Then, the CNT grown needles were attached to electrical connectors with three pins by a conductive paste. Just tips of the needle were extended from the connectors up to about 1 cm. The probe was reinforced with a homemade holder and connected to a readout system by a noiseless cable which handled all three electrodes.

FIGS. **5**A-**5**D show FESEM images of a tip of a needle electrode of an exemplary fabricated cancer diagnostic probe (CDP) coated with an array of VAMWCNTs on the tip and exemplary portions **501**, **502** and **503** of the tip, consistent with one or more exemplary embodiments of the present disclosure. FIG. **5**A illustrates a FESEM image of the tip of a needle electrode of an exemplary fabricated cancer diagnostic probe (CDP) coated with the array of VAMWCNTs on the tip, consistent with one or more exemplary embodiments of the present disclosure. FIG. **5**B illustrates a FESEM image of portion **501** of the tip, consistent with one or more exemplary embodiments of the present disclosure. FIG. **5**C illustrates a FESEM image of portion **502** of the tip, consistent with one or more exemplary embodiments of the present disclosure. FIG. **5**D illustrates a FESEM image of portion **503** of the tip, consistent with one or more exemplary embodiments of the present disclosure.

Example 3: CV of H_2O_2 Contained Lactate Solution

In this example, the cyclic voltammetry (CV) diagram of L-lactic acid solution individually were recorded by exemplary electrochemical sensors including working electrodes (WEs) fabricated from platinum (Pt), Gold (Au), amorphous glassy carbon (GC) and carbon nanotube (CNT).

FIG. **6**A shows the CV diagrams of L-lactic acid solution individually recorded by electrochemical sensors fabricated from platinum (Pt) (curve **620**), Gold (Au) (curve **630**), amorphous glassy carbon (GC) (curve **640**), and carbon nanotube (CNT) working electrodes (WEs) (curve **650**), consistent with one or more exemplary embodiments of the present disclosure. It may be observed that the detected cathodic peak by CNT WE was so sharper (about 1500 μA) in similar concentration of H_2O_2 with respect to other electrodes (about 717, 5.7 and 0.8 μA in Au, Pt and GC electrodes, respectively). CNT greatly transfer the released charges from oxidized H_2O_2 beneath the nanotubes in media solution. Hence, CNT arrays were used as electrodes of exemplary sensors in the present disclosure.

FIG. **6**B shows the CV diagrams of solutions with various concentrations of lactate (and subsequently H_2O_2) recorded by electrochemical sensors with CNT arrays working electrode, consistent with one or more exemplary embodiments of the present disclosure. CV diagrams were recorded for

solutions with a lactate concentration of about 0.025 mM (CV diagram **602**), 0.05 mM (CV diagram **604**), 0.1 mM (CV diagram **606**), and 0.3 mM (CV diagram **608**). CNT working electrode presented a well concentration depended increased response to the presence of lactate molecules in the solutions ranged from about 0.025 mM (CV diagram **602**) to about 0.3 mM (diagram **608**).

FIG. **6**C shows the CV diagrams of H_2O_2 contained lactate solution with a lactate concentration of about 0.3 mM (CV diagram **614**) in comparison with two cell culture solutions RPMI (CV diagram **610**) and DMEN (CV diagram **612**) recorded by electrochemical sensors with CNT arrays working electrode, consistent with one or more exemplary embodiments of the present disclosure. It may be observed that RPMI and DMEN cell culture solutions show less electrochemical responses in comparison with H_2O_2 contained lactate solution. The RPMI presented no electrochemical responses in the voltage attributed to the lactate detection. As a result, RPMI could be applied as cellular and tissue culture media with a negligible false positive response.

Example 4: Electrochemical Responses of Different Cell Lines

In this example, electrochemical sensing of H_2O_2 produced during Lactate/Pyruvate hypoxic glycolysis was verified in four different phenotypes of breast cell lines ranged from normal to malignant stages, including: MCF10 A, MCF-7, MDA-MB-231, and MDA-MB-468. Breast cancer cell lines (MCF10A, MCF-7, MDA-MB-231, MDA-MB-468) were obtained and were maintained at 37° C. (5% CO_2, 95% air) in RPMI medium supplemented with 5% fetal bovine serum, and 1% penicillin/streptomycin. The fresh medium was replaced every other day. All cell lines were tested and found negative for Mycoplasma contamination. The cells were detached from the plates by trypsin and counted by neobar laam.

FIG. **7** shows the CV responses of normal (MCF10A: CV diagram **702**) and different grades of cancerous (MCF7: CV diagram **706**, MDA-MB231: CV diagram **708**, and MDA-B468: CV diagram **710**) breast cells' solution media cultured for about 48 hours in comparison with standard H_2O_2 contained lactate solution with a lactate concentration of about 0.3 mM (CV diagram **712**) and RPMI (CV diagram **704**) in individual sensing wells of exemplary fabricated sensor in EXAMPLE 1 herein above, consistent with one or more exemplary embodiments of the present disclosure. Lactate production due to hypoxic glycolysis would be well detectable after about 48 hours of incubation in cancer cell lines. The CV diagrams of FIG. **7** show that the intensity of oxidation peak, located at the position of H_2O_2 electrochemical response, significantly increased with the progression in invasive grades of cancer cells in which hypoxia glycolysis would be enhanced.

Referring to FIG. **6**B and FIG. **7**, sharp difference in electrochemical peaks of H_2O_2 contained lactate solution was observed from about 0.025 mM to about 0.05 mM which could be applied to calibrate cancer cells' media from normal ones. Because the electrochemical responses of cancer cells' media solution was equal to the response range of H_2O_2 contained lactate solution with the concentration of more than about 0.05 mM meanwhile such response in normal cells was equal to the response range of the H_2O_2 contained lactate solution with the concentration of less than about 0.025 mM.

Moreover, similar responses were recorded from the culture media of colon, prostate, liver, lung, mouth, neural and hematopoietic cell lines in normal and cancer phenotypes with invasive and moderate grades by electrochemical sensing of H_2O_2 produced during Lactate/Pyruvate hypoxic glycolysis for some other types of colon, neural, prostate, liver, mouth, hematopoietic and lung cell lines. Colon (COR-L 105, SW-480, HT-29), Hematopoietic (1301, LCL-PI 1), Liver (HEP G2), Lung (QU-DB, MRC-5), Mouth (KB), Neuron (BE(2)-C, LAN-5), Prostate (PC-3, Du-145) cell lines were obtained and were maintained at 37° C. (5% CO_2, 95% air) in RPMI medium supplemented with 5% fetal bovine serum, and 1% penicillin/streptomycin. The fresh medium was replaced every other day. All cell lines were tested and found negative for Mycoplasma contamination. The cells were detached from the plates by trypsin and counted by neobar laam.

FIGS. **8**A-**8**G shows the CV responses of the solution media of different normal and cancerous cell lines in various phenotypes including Colon (COR-L 105 **802**, SW-480 **803**, HT-29 **804**) in FIG. **8**A, Hematopoietic (1301 **805**, LCL-PI 1 **806**) in FIG. **8**B, Liver (HEP G2 **807**) in FIG. **8**C, Lung (QU-DB **808**, MRC-5 **809**) in FIG. **8**D, Mouth (KB **810**) in FIG. **8**E, Neuron (BE(2)-C, LAN-5) in FIG. **8**F, and Prostate (PC-3 **813**, Du-145 **814**) in FIG. **8**G cell lines in comparison with Reference diagram **801** for H_2O_2 contained lactate solution with a lactate concentration of about 0.3 mM, consistent with one or more exemplary embodiments of the present disclosure. The current peaks in cancerous samples were observably increased. The H_2O_2 based oxidative peaks of cancer media solutions were sharper than that in normal cells. Grade dependent increase was observed in H_2O_2 peaks of cancer cells with sharp difference between normal and cancer phenotypes in all of the cell lines. This reveal the increased hypoxia glycolysis in cancer cells with respect to that in normal cells. A great correlation was observed between the cells' phenotypes and their lactate based H_2O_2 electrochemical responses.

Example 5: In Vitro Diagnosis of Cancer in Samples by Electrochemical Tracking of Hypoxia Glycolysis in Secretion of the Samples

In this example, the electrochemical responses of 6 breast tissues removed by biopsy (core needle biopsy (CNB)) or surgery from 6 of suspicious patients to cancer were analyzed using exemplary CNT based electrochemical chip. The size of the removed samples was similar (with the non-dehydrated weight of about 25 mg). The electrochemical responses were compared with cytopathological analysis done by Hematoxylin and Eosin (H & E) staining of the 6 breast tissues. Each resected sample was maintained in RPMI for about 24 hours before analyzing by exemplary CNT based electrochemical chip to be ensured from the lactate release in hypoxic tumors. Before pathological assaying, each resected sample was fixed in Formaline. For electrochemical analysis of hypoxia glycolysis in secretion of the samples, live spices from CNB or surgically removed samples were cut in similar specimens and directly transferred through sensing wells of exemplary CNT based electrochemical chip containing RPMI-1640 without any preprocessing. About 24 hours after maintaining the samples in incubator, about 200 μl of the culture media was dropped to individual sensing wells and the cathodic current of electrochemical responses of H_2O_2 were recorded in CV profile.

FIGS. **9**A-**9**F show the cytopathological results (H&E images) (top side) and electrochemical responses (bottom side) of the breast tissues removed by biopsy or surgery from 6 suspicious patients to cancer, consistent with one or more exemplary embodiments of the present disclosure. The electrochemical responses were calibrated based on the reference H_2O_2 contained lactate solution with a lactate concentration of about 0.3 mM as used for cell lines in EXAMPLE 4 above. The intensity of oxidation peak and released electrons strongly correlated to the lactate produced by hypoxia glycolysis in cancer cells. A well correlation could be observed between increased H_2O_2 dependent current peak and cancer transformed morphology of the tissues. A great match observed between the quantified electrochemical response and pathological result of the samples in which the normal and hyperplasic tissues expressed low levels of H_2O_2 related current peak meanwhile the cancerous tissues exhibited high levels of H_2O_2 related electrochemical peaks. Accordingly, FIGS. **9**A-**9**C show results obtained from non-cancerous samples and FIGS. **9**D-**9**F show results obtained from cancerous samples.

Similar electrochemical responses of 5 more samples, including live spices from CNB or surgically removed samples, were obtained using exemplary CNT based electrochemical chip. FIG. **10** shows a columnar diagram of electrochemical responses of the breast tissues removed by biopsy or surgery from 11 suspicious patients to cancer, consistent with one or more exemplary embodiments of the present disclosure. Referring to this figure, two regimes **1002** and **1003** of responses were achieved due to the trace of hypoxia glycolysis based on LADH in comparison with a reference state **1001** of a H_2O_2 contained lactate solution with a lactate concentration of about 0.3 mM. In regime 1 indicated by **1002**, the oxidation peaks were ranged from about 933.9 μA to about 1068.9 μA, and in regime 2 indicated by **1003**, the oxidation peaks were ranged from about 269.6 μA to about 718 μA. The pathological results showed a well correlation with this determination. The samples presented high levels of hypoxia related oxidative peaks (categorized in regime 1) were verified as cancer in their H&E assays. Nests of distinguished tumoral cells in H&E images of those patients could be observed in FIGS. **9**D-**9**F. Such responses were observed in the H_2O_2 contained lactate solution with the concentration of more than about 0.05 mM (FIG. **6**B). Samples with low levels of lactate (regime2) were diagnosed as non-cancer with different types of benign cancer patients such as hyperplasia (peak: 556.5 μA) in FIG. **9**B, lactational changes (peak: 718 μA), and so on. These electrochemical responses were equal to the peak determined in H_2O_2 contained lactate solution with the concentration of less than about 0.025 mM (FIG. **6**B). Comparative columnar diagram presented in FIG. **10** would elaborate the difference in lactate based electrochemical response between normal and cancer tissues.

Example 6: Standard Colorimetric Lactate Assay Kit

As the released H_2O_2 concentration have a direct correlation with lactae concentration, to further investigate the accuracy of exemplary electrochemical method described above, the results of both cell lines (described in EXAMPLE 4) and patients' samples (described in EXAMPLE 5) were compared by standard colorimetric lactate assay kit. Although this method is so time consuming and expensive with complicated multi sequential steps, it was conducted to check the reliability of lactate concentration based cancer diagnosis measured by exemplary CNT based electrochemical chip. Comparative responses versus reference H_2O_2 contained lactate solution for both electrochemical and Lactate Kit assays are presented in Table 1 and Table 2.

TABLE 1

Comparative responses of CNT based electrochemical chip and standard Lactate Kit Assay on 4 different phenotypes of Breast cell lines.

Cell line	Electrochemical sensor: Relative Current (%)	Lactate kit: Relative Lactate Concentration (%)
Reference lactate solution	100	100
MCF 10A	31.1	31.1
MCF-7	52.9	56.3
MDA-MB-231	69.5	70.9
MDA-MB-468	91.5	91.5

TABLE 2

Diagnostic results of 11 patients suspicious to breast cancer determined by H&E, Lactate kit, and the cathodic peaks of released H_2O_2 from the cells measured by CNT based electrochemical chip assays, respectively.

Patient ID	Type of Tissue	H & E Result	Lactate Kit Result (%)	CNT Electrochemical Sensor (%)
Reference lactate solution	—	—	100	100
1	Normal	Non Cancer	22.2	22.2
2	Normal	Left Hyper Plasy	42.3	42.3
3	Normal	Lactational Change	59.1	59.2
4	Normal	Adenosis benign glandular prolifration	53.8	53.7
5	Normal	Hyperplasy and inflammation	45.9	45.9
6	Suspicious to Cancer	Lympho vascular invasion	88.1	88.2
7	Suspicious to Cancer	Cancer	77.2	77.2
8	Suspicious to Cancer	Cancer	85.5	85.4
9	Suspicious to Cancer	Cancer	80.5	80.5
10	Suspicious to Cancer	Cancer	85.1	85.2
11	Suspicious to Cancer	Cancer	62	62.2

A correlation was observed between the responses of the CNT based electrochemical chip and kit which revealed the accuracy of CNT based electrochemical chip in lactate based cancer detection as shown in Table 1 and Table 2. The raw values recorded by Lactate kit and electrochemical sensing wells were presented in these tables. In summary, tracing the

hypoxia glycolysis (correlated with lactate concentration) in the interstitial fluid of biopsy sample by electrochemical assay with suitable electrode (such as CNT) exhibited a high correlation with their pathological states and may be used as a new method in cancer diagnosis.

Example 7: Integrated Assay on the Tip of the Needles of Cancer Diagnostic Probe (CDP) for Real-Time Cancer Detection Both In Vitro and In Vivo

To extend the application of exemplary label free electrochemical method of the present disclosure in real-time and precise detection of the tumor tissues during interventional sonography or surgery, exemplary CDP fabricated by growth of carbon nanostructures on the tip of the sterile steel needles as described in EXAMPLE 2 was used herein. Such integrated system contains three carbonated needles as working electrode (WE), counter electrode (CE), and reference electrode (RE). The needles were rinsed by PBS, Ethanol 70% and DI water followed by drying in N_2 ambient and UV sterile to prevent from any detachment and remaining the residues of the nanotubes in the tissue. CV responses were taken immediately after squeeze of exemplary CDP into the breast cancerous and normal tissues that indicated sharp increase in the current peak of the CDP with CNT covered electrodes interacted by cancer tissue. The important point is that the diagnosis was completed in live time based on monitoring the lactate concentration of the tissues inner domain.

FIG. **11**A shows CV response of exemplary CDP with all three needles covered by VAMWCNTs immediately after connection to the tissues, consistent with one or more exemplary embodiments of the present disclosure. It may be observed that reversible shapes with symmetric anodic and catholic peaks were obtained in CV responses. Distinguishable response between normal and cancer tissues may be observed.

FIG. **11**B shows CV response of exemplary CDP with only working electrode covered by VAMWCNTs immediately after connection to the tissues, consistent with one or more exemplary embodiments of the present disclosure. Quality of the peaks were degraded when replacing the RE and CE by steel needle. The intensity and symmetry of the responses were degraded in the sensor with just CNT covered WE (CE and RE were steel needles).

FIG. **11**C shows CV response of exemplary CDP with non-CNT covered by needles immediately after connection to the tissues, consistent with one or more exemplary embodiments of the present disclosure. There may be observed a noisy response without any distinguishable electrochemical peak. When all of the electrodes were non CNT covered needles, the responses were completely degraded and not distinguishable between normal and cancer tissues. This revealed the important role of CNT in selective interaction and charge transfer from the H_2O_2 released during transformation of lactate to pyruvate.

FIGS. **12**A-**12**E show CV responses recorded by exemplary CDP (needle based electrochemical sensor) from the resected tissues from five patients among 50 individual patients suspicious to breast cancer at the bottom side of FIGS. **12**A-**12**E in comparison with images obtained by conventional pathological methods (H&E) at the top side of FIGS. **12**A-**12**E, consistent with one or more exemplary embodiments of the present disclosure. Patients respective to FIGS. **12**A-**12**C have normal/non-cancerous (FIG. **12**A), hyperplasic (FIG. **12**B), and adenosis glandular proliferative tissues (FIG. **12**C). Patients respective to FIGS. **12**D and **12**E have cancer tissues. Electrochemical current peaks of cancer tissues are sharply (more than about 150 μm) higher than benign ones with a strong correlation by the abundance of distributed cancer cells. The CV responses recorded from the normal and cancer tissues of these 50 individual patients by CNT covered needle sensors (CDP) greatly detected the hypoxic glycolysis just in cancerous samples due to cathodic peaks of H_2O_2 (FIGS. **12**A-**12**E). Meanwhile, while the response time of CDP was less than about 1 minute after the tissue resection, diagnosis by conventional pathological methods (H&E) requires at least several hours for sample fixation and staining procedures. The ratio of cathodic peaks of reference H_2O_2 contained lactate solution vs. non-cancerous tissues were more than three times (FIGS. **12**A-**12**C) while such ratio was less than one time in cancerous tissues (FIGS. **12**D and **12**E).

Table 3 shows the results recorded by exemplary CDP in comparison with the results obtained by H&E analysis from live resected tissues of 50 patients suspicious to breast cancer. They exhibited great correlations with the pathological results of the samples assayed by H&E method.

TABLE 3

Results recorded by exemplary CDP in comparison with the results obtained by H&E analysis from live resected tissues of 50 patients suspicious to breast cancer.

Patient ID	Oxidation Current Peaks (μA)	CDP (Cancer)	H&E (Cancer)
1	0	Negative	NO
2	46.6	Negative	NO
3	87	Negative	NO
4	316.5	Positive	YES (Cancer 90%, Normal 10%)
5	287.8	Positive	YES (Cancer 90%, Normal 10%)
6	22	Negative	NO
7	142.3	Positive	YES (Cancer 30%, Normal 70%)
8	150	Positive	YES (Cancer 30%, Normal 70%)
9	300	Positive	YES (Cancer 90%, Normal 10%)
10	13	Negative	NO
11	0	Negative	NO
12	101.5	Positive	YES (Cancer 30%, Normal 70%)
13	180.2	Positive	YES (Cancer 60%, Normal 40%)
14	289.4	Positive	YES (Cancer 90%, Normal 10%)
15	302	Positive	YES (Cancer 90%, Normal 10%)
16	274.2	Positive	YES (Cancer 90%, Normal 10%)
17	0	Negative	NO
18	142.8	Positive	YES (Cancer 30%, Normal 70%)
19	80	Negative	NO
20	32.5	Negative	NO
21	200	Positive	YES (Cancer 60%, Normal 40%)
22	188.2	Positive	YES (Cancer 60%, Normal 40%)
23	264.5	Positive	YES (Cancer 90%, Normal 10%)
24	23	Negative	NO
25	179.5	Positive	YES (Cancer 60%, Normal 40%)
26	55.2	Negative	NO
27	52	Negative	NO
28	77	Negative	NO
29	0	Negative	NO
30	201	Positive	YES (Cancer 60%, Normal 40%)
31	75.6	Negative	NO
32	155.8	Positive	YES (Cancer 30%, Normal 70%)
33	99.5	Positive	YES (Cancer 30%, Normal 70%)
34	305.5	Positive	YES (Cancer 90%, Normal 10%)
35	297.7	Positive	YES (Cancer 90%, Normal 10%)
36	112	Positive	YES (Cancer 30%, Normal 70%)
37	17.8	Negative	NO
38	40	Negative	NO
39	73	Negative	NO
40	290	Positive	YES (Cancer 90%, Normal 10%)
41	90	Positive	YES (Cancer 30%, Normal 70%)
42	330	Positive	YES (Cancer 90%, Normal 10%)
43	197.5	Positive	YES (Cancer 30%, Normal 70%)

TABLE 3-continued

Results recorded by exemplary CDP in comparison with the results obtained by H&E analysis from live resected tissues of 50 patients suspicious to breast cancer.

Patient ID	Oxidation Current Peaks (μA)	CDP (Cancer)	H&E (Cancer)
44	77.5	Negative	NO
45	25	Negative	NO
46	266.2	Positive	YES (Cancer 90%, Normal 10%)
47	0	Negative	NO
48	102.5	Positive	YES (Cancer 30%, Normal 70%)
49	310	Positive	YES (Cancer 90%, Normal 10%)
50	259.3	Positive	YES (Cancer 90%, Normal 10%)

FIG. **13** shows a summary of categorized regimes of CV responses recorded by exemplary CDP from the resected tissues from five patients among 50 individual patients suspicious to breast cancer that were presented in Table 3. It represents CV regimes along a spectrum from a completely non-cancerous state to cancerous state, consistent with one or more exemplary embodiments of the present disclosure. It may be seen that if the H_2O_2 cathodic peak (equal to oxidation current peak) of exemplary CV response recorded by exemplary CDP from a patient is less than 90 μA, the tissue is in non-cancerous state. On the other hand, if the CV response recorded by exemplary CDP from the tissue is in a range more than about 95 μA, there exists a cancerous state which may be more intensified by increasing the oxidation current peak. A range of oxidation current peak between 90 μA and 95 μA is the border range.

Example 8: In Vivo Analysis of Observable Tumor with Histologically Distinct Cancer Margin Before any Mastectomy

To determine if CDP would in real time identify an observable tumor in vivo, about 2.3×10^6 4 T1-derived cancer cells were implanted into the back of 10 female BALB/C mice, and the mice were maintained in individual groups with similar size of formed tumors with sharp histologically distinct patterns. After about 10 days, individual CDPs were externally squeezed into their cancerous and normal regions had been specified by sonography. The space between each assayed regions was about 3 mm. Also the mice under body were connected to ground potential such as done for any patient in surgery room.

FIG. **14**A shows a sonography image from a tumor side taken from an exemplary mouse tumorized by 4T1 breast cancer cell lines, consistent with one or more exemplary embodiments of the present disclosure. A tumor with average sizes with a length **1402** of about 2.24 cm and another length **1404** of about 1.60 cm could be observed in sonography image.

FIG. **14**B shows H&E image from the tumor side taken from exemplary tumorized mouse by 4T1 breast cancer cell lines, consistent with one or more exemplary embodiments of the present disclosure. FIG. **14**C shows H&E image from a normal/healthy side taken from exemplary tumorized mouse by 4T1 breast cancer cell lines, consistent with one or more exemplary embodiments of the present disclosure.

FIG. **14**D shows CV diagrams of normal and tumor regions/sides of exemplary tumorized mouse by 4T1 breast cancer cell lines calibrated by a Reference CV diagram from H_2O_2 contained lactate solution with a lactate concentration of about 0.3 mM obtained using exemplary CDP, consistent with one or more exemplary embodiments of the present disclosure. It may be observed that the lactate related peaks were about 3 times higher in cancer region (CV diagram **1406** and FIGS. **14**A and **14**B) versus normal ones (CV diagram **1408** and FIG. **14**C). Sharp lactate electrochemical peaks were observed in tumor locations by about three times higher current than that recorded from their normal regions

To more clearly clarify the impact of H_2O_2 monitoring in tumor growth and progression, tumor size effects on H_2O_2 related electrochemical peaks recorded by CDP were compared. A distinguishable increasing regime was observed in the intensity of current peak through increment in the tumor size. Moreover, Histopathological images taken from the normal and cancer regions detected by CDP confirmed this result. Hyper chromatic and irregular nucleus with increased nucleus/cytoplasm ratio may be observable in H&E images of cancer region.

Example 9: In Vivo Analyses of Suspicious Regions Before and During the Surgery

In this example, the ability of the CDP to distinguish suspicious regions to cancer in mice model was analyzed by the resolution of about 3 mm which could be translated to human model. Tissue samples that contained regions of invasive breast cancer adjacent to normal stroma were experimented.

Five tumorized mice by 4T1 breast cancer cell lines were checked by sonography. FIG. **15**A shows a sonography image from a tumor **1501** taken from an exemplary mouse tumorized by 4T1 breast cancer cell lines, consistent with one or more exemplary embodiments of the present disclosure. Approximate dimensions of the tumor could be observed in sonography image of FIG. **15**A.

Exemplary CDP was tested on tumor and suspicious regions of the five tumorized mice before (by squeezing through skin) and during the surgery on exemplary six regions. FIGS. **15**B and **15**C show exemplary six analyzed regions **1502-1507** of an exemplary tumorized mouse among the exemplary five tumorized mice before (FIG. **15**B) and during surgery (FIG. **15**C), consistent with one or more exemplary embodiments of the present disclosure. Six analyzed regions may include center **1502** of tumor **1501**, left side **1503** of tumor **1501**, right side **1504** of tumor **1501**, upside **1505** of tumor **1501**, bottom side **1506** of tumor **1501**, and also an exemplary normal side **1507** far from tumor **1501** all depicted in FIGS. **15**B and **15**C were analyzed consecutively before and during surgery using a CDP with an about 3 mm distance between needle electrodes.

Moreover, frozen H&E assay was used and rechecked by IHC method to be ensure from the precision of CDP results with respect to standard protocols. A tissue section of the sample including exemplary six regions analyzed by exemplary CDP was subjected to frozen H&E staining processes and evaluated by the pathologist. Exemplary tumor **1501** containing suspicious regions was removed and sent for frozen pathology and the H&E images taken from the center **1502** of tumor **1501** as well as its posterior **1505**, anterior **1506**, right **1504** and left **1503** laterals with the distance of about 3 mm from the histologically distinct region, were demanded by the CDP results as presented in Table 4. The results of CDP before and during surgery exhibited a perfect correlation. Ki67 based IHC assay confirmed the normal state of R5 and cancer involvement in R3 as classifier reference.

TABLE 4

Results recorded by exemplary CDP before and during surgery in comparison with the results obtained by H&E analysis from six suspicious regions of an exemplary tumorized mouse.

Region	CDP Before Surgery (Ox Current Peaks (μA))	CDP During Surgery (Ox Current Peaks (μA))	H&E frozen (Cancer)
1502 (Center)	Positive (169.104)	Positive (178.621)	Yes (Cancer 90%, Normal 10%)
1503 (Right)	Positive (94.773)	Positive (96.89)	Yes (Cancer 30%, Normal 70%)
1504 (Left)	Positive (122.643)	Positive (122.8)	Yes (Cancer 60%, Normal 40%)
1505 (Up)	Negative (30.397)	Negative (31.85)	No
1506 (Bottom)	Negative (0)	Negative (0)	No
1507 (Normal)	Negative (0)	Negative (0)	No

As represented in Table 4, it was distinguished from H&E analyzes that center **1502** was diagnosed by frozen histopathology as cancer tissue, whereas regions **1505** and **1506** were diagnosed as normal stroma. Region **1504** was in the margin between the cancer and normal stroma tissue regions, presenting about 40% tumor tissue and about 60% normal stroma tissue. Region **1503** was a suspicious region without any tumor margins but the trace of distributed cancer cells would be observed between stroma. Tumoral cells would be distinguished due to their hyper chromic nuclei (triangular arrows in H&E images of regions **1503** and **1504**). Tabled result shows the CDP obtained for regions **1502** and **1504** presented significant hypoxic lactate peaks meanwhile lower but detectable meaningful levels of the H_2O_2 was recorded for region **1503**. No detectable trace of any peak was measured for region **1506**. The CDP response obtained for **1507**, diagnosed as reference normal stroma tissue, presented no H_2O_2 peak similar to that observed for **1506**.

The CDP response obtained for regions **1504** and **1506** were then evaluated by Ki67 IHC as an independent validation set. The expression of Ki67 has been reported to be correlated with tumor cell proliferation and growth in routine pathological investigation and used as a diagnostic marker. Ki67 based IHC classifier identified no trace of cancer proliferation in region **1506** (as the normal stroma) and showed different intensities of filtrated cancer cells in region **1504**. Similar results were obtained for 5 other animal models with suspicious regions in anterior, posterior, right and left laterals of their tumors.

In addition, exemplary CDP exhibited a fine distinguishable response in interaction with another type of cancer tumors (MC4L2) as cancer cells with lower invasive grades than 4T1 as experimented on mice models. Tumors formed by the injection of about 5×10^5 MC4L2 cells (mice primary breast cancer cell lines) were analyzed by exemplary CDP on 5 mice.

FIG. **16** shows comparative diagram of CDP responses in interaction with normal (curve **1601**), non-metastasized tumor (curve **1602**) and metastatic tumor (curve **1603**) recorded from individual mice, consistent with one or more exemplary embodiments of the present disclosure. Tracing the hypoxia glycolysis exhibited a strong correlation with the invasive state of the tumor. Results revealed sharply distinguishable responses between cancerous and normal regions. However the intensity of the response of MC4L2 tumors is lower than that was recorded for malignant tumor, it is observably higher than the response peak of normal tissue.

Furthermore, in this example, exemplary CDP was applied in finding the suspicious margins during tumor resection surgery in breast cancer patients. Not only the known normal domains were detected and set as reference point, but also suspicious margins of cancer and normal domains were precisely diagnosed in real-time and confirmed by histopathological assays. So, without requirement to frozen pathological process the surgeon can finish the surgery with insurance from precise resection of tumor without any additional mastectomy from the peripheral tissues.

FIGS. **17A-17C** shows CV responses obtained by applying exemplary CDP in detection of suspicious margins during breast cancer surgery for a known normal region (FIG. **17A**) that was checked as calibrating data, and two suspicious margins (FIGS. **17B** and **17C**) that were precisely diagnosed as cancerous (FIG. **17B**) and normal (FIG. **17C**) domains by CDP in real-time, consistent with one or more exemplary embodiments of the present disclosure. The results obtained by exemplary CDP were confirmed by H&E analysis. FIGS. **17D-17F** shows H&E results after the surgery for the known normal region, and two suspicious margins, consistent with one or more exemplary embodiments of the present disclosure.

These results show that the diagnostic information obtained by exemplary CDP can be used to detect cancer in marginal suspicious regions with rare distribution of cancer cells filtrated between normal stroma in less than about 20 seconds during the surgery or biopsy of live animal as well as human models without any requirement to tissue resection and preparation for frozen pathology. Even it may detect the accurate location of cancer involved regions before surgery in superficial tumors. The precision of this method is as well as reported for H&E from the assayed regions.

Example 10: Pathological Classification of Current Peaks Obtained by the Exemplary Fabricated CDP

In this example, current peaks of 258 human fresh samples prepared from 74 breast cancer patients (Biopsied or surgically removed) were recorded utilizing exemplary CDP **102**. 258 human fresh samples were tested immediately after dissection from the body (with the non-dehydrated weight of about 15-25 mg and size of up to about 1 cm^2. All three integrated needle electrodes of exemplary CDP **102**, assembled on the head probe (the exemplary sensing part **154**), were entered into a target tissue of the 258 human fresh samples at the same time. The whole process which may include replacing a previously used sensing part **154** by removing the previously used sensing part **154** and connecting a new sensing part **154** (about 20 sec), entering exemplary CDP **102** to the target tissue by inserting new sensing part **154** into a target location within the target tissue, and

recording a CV response with a current peak from the target location (about 15 sec due to synchronized real-time processing) would take place in less than about 40 seconds. The permanent pathological diagnostic results of the samples, which were re-checked by three histological slides from each sample, were a set of reference data in probable scalability of the recorded CV responses.

Meaningful results were observed after comparing an experimental categorization of samples through their CDP recorded current peaks with their categorization through their H&E pathological diagnoses. Table 5 shows CDP current peak results of 258 fresh samples from 74 patients in association with pathological diagnosis based on pathological classification (DIN, LIN and FEL). Additionally, FIG. **18** shows H&E images **1802-1818** from nine exemplary samples associated with nine exemplary categories in Table 5, consistent with one or more exemplary embodiments of the present disclosure.

TABLE 5

CDP current peak results of 258 fresh samples from 74 patients in association with pathological diagnosis based on pathological classification (DIN, LIN and FEL).

Pathological Diagnosis (classification system)	Pathological scoring for re-excising recommendation (warning state)	Ranges of recorded CDP peak current (μA)	Number of tested samples	Number of the matched samples in CDP ranges
Fatty breast tissue (FEL)	Negative	0-40	15	14
Sclerosing adenosis (DIN)	Negative	83-115	11	8
FCC with CCC (DIN)	Negative	110-117	19	17
Moderate usual ductal hyperplasia (DIN)	Negative	117-137	12	10
Florid ductal hyperplasia (DIN)	Negative (moderate risk)	150-170	10	8
Stroma + one focus of ADH (DIN)	Negative (moderate risk)	175-196	5	4
Stroma + two or more foci of ADH; DIN1b (DIN)	positive	203-260	31	28
Stroma + one foci of DCIS; DIN1c (DIN)	positive	231-290	24	21
IDC >5%	positive	360 and more	19	19

It was observed that 26 samples among 258 samples were normal breast stroma, including fatty breast tissues and simple fibroadenoma, which all showed current peaks in a range of about 0-83 μA as shown in Table 5. Image **1802** of FIG. **18** shows H&E image from an exemplary sample including fatty breast tissue (FEL) as a normal breast tissue with a current peak between about 0 μA and about 40 μA, consistent with one or more exemplary embodiments of the present disclosure. 18 samples were non proliferative fibrocystic changes (FCC) which all of them showed current peaks in a range of about 53-111 μA. 10 samples were mild usual ductal hyperplasia (UDH) which all of them showed current peaks in a range of about 83-110 μA. 11 samples were sclerosis adenosis (SA) which 8 of them showed current peaks in a range of about 86-115 μA. Image **1804** of FIG. **18** shows H&E image from an exemplary sample including sclerosis adenosis (SA) with a current peak between about 83 μA and about 115 μA, consistent with one or more exemplary embodiments of the present disclosure. 12 samples were moderate UDH which 10 of them showed current peaks in a range of about 120-137 μA. 19 samples were FCC with columnar cell changes (CCC) (some of them also had one foci suspicious to atypical ductal hyperplasia (ADH)) which 17 of them showed current peaks in a range of about 110-173 μA. Image **1806** of FIG. **18** shows H&E image from an exemplary sample including fibrocystic changes (FCC) with columnar cell changes (CCC) with a current peak between about 110 μA and about 117 μA, consistent with one or more exemplary embodiments of the present disclosure. Image **1808** of FIG. **18** shows H&E image from an exemplary sample including Moderate usual ductal hyperplasia (DIN) with a current peak between about 117 μA and about 137 μA, consistent with one or more exemplary embodiments of the present disclosure. Image **1810** of FIG. **18** shows H&E image from an exemplary sample including Florid ductal hyperplasia (DIN) with a current peak between about 150 μA and about 170 μA, consistent with one or more exemplary embodiments of the present disclosure. Image **1812** of FIG. **18** shows H&E image from an exemplary sample including stroma with one focus of atypical ductal hyperplasia (ADH) with a current peak between about 175 μA and about 196 μA, consistent with one or more exemplary embodiments of the present disclosure. In summary, normal breast (e.g. breast fatty tissue), UDH (e.g. FCC lesions) and DIN1a (e.g. FCC with CCC and a small foci of ADH) showed response peak ranges from about 0 μA to about 196 μA which were negatively scored by CDP.

Moreover, 31 samples showed involvement to two or more foci of ADH which 28 of them showed peak currents in a range of about 203-250 μA. Image **1814** of FIG. **18** shows H&E image from an exemplary sample including stroma with two or more foci of ADH (DIN1b) with a current peak between about 203 μA and about 260 μA, consistent with one or more exemplary embodiments of the present disclosure. 24 samples showed involvement to low grade ductal carcinoma in-situ (DCIS), from about 10% to about 45% of the histological pattern, which 21 of those samples showed current peaks in a range of about 250-360 μA. Image **1816** of FIG. **18** shows H&E image from an exemplary sample including stroma with one foci of ductal carcinoma in-situ (DCIS) (DIN1c) with a current peak between about 231 μA and about 290 μA, consistent with one or more exemplary embodiments of the present disclosure. 12 samples were invasive ductal carcinoma (IDCs) with distributions between 5-55% of histological pattern, which all of them showed current peaks in a range of about 610-800 μA. 2 samples were phylloids tumor which both showed peak currents more than about 260 μA. Just 10 samples were found with lobular based atypia/neoplasia; 4

of those samples were invasive lobular carcinoma (ILC) with extensive distribution which all showed current peaks in a range of about 380-465 μA. 4 samples were atypical lobular hyperplasia (ALH) which showed current peaks between in a range of about 257-270 μA. 2 other samples were lobular carcinoma in-situ (LCIS) which both showed current peaks of about 290 μA. Image **1818** of FIG. **18** shows H&E image from an exemplary sample including invasive ductal carcinoma (IDC) with a current peak more than about 360 μA, consistent with one or more exemplary embodiments of the present disclosure.

Considering the above pathological results and current peaks of the samples together, a classification on CV responses recorded by exemplary CDP **102** was proposed based on pathological diagnosis. The lowest cut-off for pathologists on diagnosing a margin as positive (dissection is mandatory) is presence of at least two foci of ADH. Therefore, a border line at about 203 μA was proposed as a cut-off current for positive scoring exemplary CDP **102**. Samples consisting of ADH with more than two foci, DCIS and IDCs most often showed peak currents higher than about 203 μA while other samples consisting of one foci of ADH, UDH and FCC lesions showed peak currents lower than about 196 μA. Hence, the responses of exemplary CDP **102** were found to be classifiable based on newest edition of ductal intraepithelial neoplasia (DIN), lobular intraepithelial neoplasia (LIN) and fibro-epithelial lesion (FEL) systems reported by world health organization (WHO). FIG. **19** shows classification of current peaks recorded by exemplary CDP **102** after examining more than 250 samples in consistence with pathological diagnosis, consistent with one or more exemplary embodiments of the present disclosure. It may be observed that samples with positively scored levels of glycolytic related H_2O_2 peaks were verified as ADH, DCIS, IDC and metastatic lymph nodes in their H&E assays showed more than about 203 μA (as the cut-off) in CDP response peaks. Samples with current peaks lower than about 196 μA were negatively scored by CDP as neither cancerous nor pre-cancerous tissue with different types of benign states such as usual ductal hyperplasia, adenosis, fibrosis and non-proliferative fibrocystic changes. Most of the abnormal samples were found in DIN classification (as the mostly occurred types of breast diseases such as IDC, DCIS, ADH and UDH). CDP peak responses were scored with a defined cut-off between free and involved margins (at 203 μA), respectively assigned as "Negative" and "positive". Such scoring would consider any pathological involvement to atypical, pre-invasive and invasive lesions in margin checking. Also, a warning regime in negative regions was defined in this classification. These samples with current peaks between about 137 μA and about 196 μA may be classified in this region. Surgeons need to be aware on these lesions through presence of complex fibroadenoma, complex SA or single focus of atypia. Although these lesions are not pathologically high risk pre-neoplasia, they ought to be reported and considered through some guidelines. DIN1b (e.g. two or more foci of ADH), DIN1c (e.g. low grade-DCIS), DIN2 (e.g. intermediate DCIS), DIN3 (e.g. high grade DCIS) and IDC lesions showed response peaks in the ranges between 203 to more than 600 μA which were positively scored by CDP. Based on this example, pathologically validated diagnostic scores of exemplary CDP **102** were defined for 258 breast tissue samples with sensitivity of about 95% and specificity of about 92% respectively. Such results may be achieved by CNT covered sensing needles of exemplary CDP **102** which may provide selective interaction with released H_2O_2 from abnormal tissues with no post recording perturbation on morphology and distributions of the sterilized CNT-covered needles.

Example 11: Real-Time In-Vivo Scoring of External Margins (EMs) and Internal Margins (IMs) by CDP During Breast Cancer Surgery in Human Models

In this example, exemplary prepared CDP **102** was utilized through exemplary method **200** as a real-time diagnostic tool to find involved body side margins (named IMs) during human cancer surgery. In this regard, exemplary prepared CDP **102** was applied in real-time finding of suspicious IMs and EMs during lumpectomy and/or mastectomy of 127 patients with different types of breast tumors in different steps of treatment. 14 patients were excluded from the survey and 113 patients (107 female and 6 male) were included. All of the tests were done under the license of Ethics Committee with the informed consent of candidate patients. The sensing needles (i.e., exemplary working electrode **158**, counter electrode **160** and reference electrode **162**) were entered into the margins up to a depth of about 4 mm and a stopping specimen was embedded on exemplary head **166** to prevent from further entrance of the needles. A distance between the exemplary three electrodes was about 3 mm. Hence, more than about 30 mm^3 of exemplary portion of breast tissue was exposed to exemplary CDP **102** during each test. Depending on a surgeon's opinion, up to 12 breast margins (6 EMs on dissected tumor and 6 IMs in cavity side of a patient (including posterior, anterior, superior, inferior, medial and lateral) were intraoperatively checked by exemplary CDP **102** for each patient. The EMs on dissected tumor were diagnosed (scored) by CDP and the tested lesions were sent for frozen pathology. Subsequently, the IMs in cavity side (in the body of the patient) were checked by exemplary CDP **102** and similarly the tested lesions were considered by standard frozen pathology. Finally, all of EMs and IMs were diagnosed (scored) by exemplary CDP **102** and tested by frozen pathology, were individually evaluated by permanent pathology as reference standard diagnosis based on pathological classifications of breast tumors. Also, when a permanent histological pattern was suspicious for pathologist between two different diagnoses (e.g. UDH and ADH), IHC would be recommended by her/him. Totally, 895 individual EMs and IMs were intra operatively scored by CDP and diagnosed by pathology.

FIG. **20**A shows an image resulted from frozen H&E (top-side image **2002**), an image resulted from permanent H&E (middle-side image **2004**), and a CV response recorded by exemplary CDP **102** (bottom-side image **2006**) for the anterior IM of a patient (ID 18), consistent with one or more exemplary embodiments of the present disclosure. It may be observed that real-time CV response recorded by exemplary CDP **102** positively scored the margin, and both frozen and permanent H&E confirmed involvement of invasive ductal carcinoma for this patient.

FIG. **20**B shows an image resulted from frozen H&E (top-side image **2008**), an image resulted from permanent H&E (middle-side image **2010**), and a CV response recorded by exemplary CDP **102** (bottom-side image **2012**) for a suspicious margin inside the body of the patient (anterior margin of patient ID 46), consistent with one or more exemplary embodiments of the present disclosure. It may be observed that real-time CV response recorded by exemplary CDP **102** positively scored the margin, and the removed specimen showed negative result for malignancy in frozen analyses meanwhile the permanent H&E showed the

papillary lesion with Atypia region, which must be removed by surgeon. This example may show the significant role of using exemplary CDP **102** for high-accurate cancer diagnosis.

FIG. **20**C shows an image resulted from frozen H&E (top-side image **2014**), an image resulted from permanent H&E (middle-side image **2016**), and a CV response recorded by exemplary CDP **102** (bottom-side image **2018**) for a suspicious margin inside the body of the patient (posterior IM of the same patient ID 46), consistent with one or more exemplary embodiments of the present disclosure. It may be observed that real-time CV response recorded by exemplary CDP **102** negatively scored the margin, which was confirmed by both frozen and permanent H&E as usual hyperplasia.

FIG. **20**D shows an image resulted from frozen H&E (top-side image **2020**), an image resulted from permanent H&E (middle-side image **2022**), and a CV response recorded by exemplary CDP **102** (bottom-side image **2024**) for Sentinel Lymph Node (SLN) of patient ID 18, consistent with one or more exemplary embodiments of the present disclosure. It may be observed that real-time CV response recorded by exemplary CDP **102** negatively scored the margin, whereas it was diagnosed as reactive lymphoid hyperplasia by both H&E assays.

Regarding EXAMPLES 10 and 11 described hereinabove, a matched clinical diagnostic categorization between the pathological results of the tested tissues and response peaks obtained by exemplary CDP **102** was proposed based on pathological classification (ductal intraepithelial neoplasia (DIN), lobular intraepithelial neoplasia (LIN) and fibro epithelial lesion (FEL)) with the latest reported modifications. CDP scoring ability in intra-operative margin detection was verified on more than 890 human in-vivo clinical breast samples with sensitivity of about 97% and selectivity of about 94%. The ability of exemplary CDP **102** and exemplary method **200** in non-invasive and real-time diagnosis of internal margins with pathological values (from high-risk benign to pre-invasive and invasive cancer lesions) may make exemplary CDP **102** a distinct intra-operative tool with simple and small handheld equipment to increase the prognostic factor of the cancer patients.

Example 12: Real-Time Tracking of Hypoxia Glycolysis in Conization Samples for Cervical Intraepithelial Neoplasia (CIN) Detection

In this example, exemplary methods **200** and **220** utilizing exemplary CDP **102** were applied to precisely diagnose the cervical intraepithelial neoplasia (CIN) cells in cone biopsy samples in real-time in order to improve pathological evaluations to find any missed CIN (I to III) or other high-risk dysplasia in cone biopsy samples. Electrochemical assays according to method **220** utilizing CDP **102** were carried out on in-vitro human fresh cervical samples prepared from 30 patients' candidate for conization through the history of abnormal cells present in their pap smear results. CV studies were done using DC voltage, and no AC frequency was applied. The potential was swept in the range from about −0.8 to about +0.8 V, using a scan rate of about 100 mV s^{-1}. Hematoxylin and Eosin (H&E) staining was used as staining procedure in histopathology assays. Hypoxia related H_2O_2 ionic currents from the in-vitro human fresh cervical samples prepared from 30 patients were recorded. Hypoxia glycolysis metabolism of fresh cervical tissues was monitored immediately after dissection from the body (with a non-dehydrated size of up to 6 cm^2). In each sample, at least three points on all over the tissue were recorded and inked the measured locations. Next, the tissues held in formalin and sent for standard pathological evaluation (dehydration, block preparation from the tissues, preparing a thin layer slide from the block, and H&E staining of the slides). The permanent pathological diagnostic results of samples were carried out independently from considering the inked locations. After the declaration of pathological results, the block of samples was re-molded and re-blocked from the surface in which the trace of inked points (points tested by exemplary CDP **102**) could be observable. Again, the H&E slide preparation processes were carried out, and the pathological diagnosis of inked regions was declared. This second pathological evaluation was assumed as the reference for responses recorded by exemplary CDP **102**.

FIG. **21** shows a visually summarized comparison between current peak values of recorded CV responses utilizing exemplary CDP **102** via exemplary methods **200**, and **220** for in-vivo cancer diagnosis within a living tissue, and CIN pathological classification, consistent with one or more exemplary embodiments of the present disclosure. Coherent results were achieved after categorizing the values of recorded current peaks from the samples and comparing them with the H&E diagnosis of the inked samples. As may be observed from FIG. **21**, current peak values of the recorded CV diagrams from the samples were categorized in three ranges of a first range **2100** assigned as being at healthy state, a second range **2200** assigned as being at cancerous state, and a third range **2300** assigned as being at a suspicious state. Among 30 samples, 9 samples were non-CIN tissues (healthy tissues) including chronic cervicitis and benign flat condyloma tissues, which all showed current peaks in the first range **2100** as being between about 0 μA and about 115 μA, and their healthy state was confirmed by H&E results as is exemplary shown in images **2102** (Chronic cervicitis) and **2104** (flat condyloma). Nineteen samples were low grade cancerous and high-grade cancerous, including CIN I (image **2202**), CIN II (image **2204**), and CIN III (image **2206**) with neoplastic mitotic cells, in which all samples showed current peaks above about 145 μA within the second range **2200**. By considering the pathology reports of tested regions utilizing exemplary CDP **102**, a CIN based scoring of CV responses was proposed. The lowest cut-off for pathologists to declare a positive diagnosis of a cone biopsied sample may be the presence of low-grade CIN I or neoplastic mitotic cells in upper layers of basal cells. The current peak of about 115 μA was the lowest value recorded for an involved sample. Hence, it was proposed as a cut-off current for positive scoring of CV recorded responses. Samples with current peaks in the third range **2300** between about 115 μA and about 145 μA were assigned as suspicious samples to be cancerous being at a gray zone, for which re-evaluation by pathology is recommended.

As described and shown hereinabove, exemplary methods **200**, and **220**, and exemplary CDP **102** may be utilized to lively and selectively determine a value of H_2O_2 released from cancer or atypical cells, through reverse Warburg effect and hypoxia assisted glycolysis pathways. The determined value of released H_2O_2 may be a high-accurate parameter for cancer detection in any solid or liquid suspicious mass that may be cancerous. Although the pathology method may be a gold standard of cancer diagnosis, it needs to prepare a lot of H&E slides to reach a perfect diagnosis without any false negatives as well as time consuming pathology procedures. Accordingly, exemplary methods **200**, and **220** and exemplary CDP **102** may be applied as a more accurate and faster

diagnostic tool in comparison with pathology assays, or as a complementary diagnostic tool for pathology assays in order to reach fast and accurate cancer detection.

While the foregoing has described what are considered to be the best mode and/or other examples, it is understood that various modifications may be made therein and that the subject matter disclosed herein may be implemented in various forms and examples, and that the teachings may be applied in numerous applications, only some of which have been described herein. It is intended by the following claims to claim any and all applications, modifications and variations that fall within the true scope of the present teachings.

Unless otherwise stated, all measurements, values, ratings, positions, magnitudes, sizes, and other specifications that are set forth in this specification, including in the claims that follow, are approximate, not exact. They are intended to have a reasonable range that is consistent with the functions to which they relate and with what is customary in the art to which they pertain.

The scope of protection is limited solely by the claims that now follow. That scope is intended and should be interpreted to be as broad as is consistent with the ordinary meaning of the language that is used in the claims when interpreted in light of this specification and the prosecution history that follows and to encompass all structural and functional equivalents. Notwithstanding, none of the claims are intended to embrace subject matter that fails to satisfy the requirement of Sections 101, 102, or 103 of the Patent Act, nor should they be interpreted in such a way. Any unintended embracement of such subject matter is hereby disclaimed.

Except as stated immediately above, nothing that has been stated or illustrated is intended or should be interpreted to cause a dedication of any component, step, feature, object, benefit, advantage, or equivalent to the public, regardless of whether it is or is not recited in the claims.

It will be understood that the terms and expressions used herein have the ordinary meaning as is accorded to such terms and expressions with respect to their corresponding respective areas of inquiry and study except where specific meanings have otherwise been set forth herein. Relational terms such as first and second and the like may be used solely to distinguish one entity or action from another without necessarily requiring or implying any actual such relationship or order between such entities or actions. The terms "comprises," "comprising," or any other variation thereof, are intended to cover a non-exclusive inclusion, such that a process, method, article, or apparatus that comprises a list of elements does not include only those elements but may include other elements not expressly listed or inherent to such process, method, article, or apparatus. An element proceeded by "a" or "an" does not, without further constraints, preclude the existence of additional identical elements in the process, method, article, or apparatus that comprises the element.

The Abstract of the Disclosure is provided to allow the reader to quickly ascertain the nature of the technical disclosure. It is submitted with the understanding that it will not be used to interpret or limit the scope or meaning of the claims. In addition, in the foregoing Detailed Description, it can be seen that various features are grouped together in various implementations. This is for purposes of streamlining the disclosure, and is not to be interpreted as reflecting an intention that the claimed implementations require more features than are expressly recited in each claim. Rather, as the following claims reflect, inventive subject matter lies in less than all features of a single disclosed implementation. Thus, the following claims are hereby incorporated into the Detailed Description, with each claim standing on its own as a separately claimed subject matter.

While various implementations have been described, the description is intended to be exemplary, rather than limiting and it will be apparent to those of ordinary skill in the art that many more implementations and implementations are possible that are within the scope of the implementations. Although many possible combinations of features are shown in the accompanying figures and discussed in this detailed description, many other combinations of the disclosed features are possible. Any feature of any implementation may be used in combination with or substituted for any other feature or element in any other implementation unless specifically restricted. Therefore, it will be understood that any of the features shown and/or discussed in the present disclosure may be implemented together in any suitable combination. Accordingly, the implementations are not to be restricted except in light of the attached claims and their equivalents. Also, various modifications and changes may be made within the scope of the attached claims.

What is claimed is:

1. An electrochemical probe for in-vivo measurement of H_2O_2 oxidation within a living tissue, comprising:

a sensing part comprising:

a working electrode comprising a first biocompatible conductive needle;

a counter electrode comprising a second biocompatible conductive needle;

a reference electrode comprising a third biocompatible conductive needle,

wherein each needle of the first, second, and third needles comprises a sensing tip, each sensing tip comprising:

a catalyst layer deposited on the sensing tip; and

an array of vertically aligned multi-walled carbon nanotubes (VAMWCNTs) grown on the catalyst layer, a length of between 3 and 5 mm of the array being configured to:

be put in contact with the living tissue for 1 second or less; and

sense a cyclic voltammetry (CV) response based on the first, second, and third needles being connected to a potentiostat device; and

an electrode holder holding the first, second, and third needles, the first, second, and third needles being attached to a first end of the electrode holder; and

a handle, comprising:

an insertion part configured to facilitate insertion of a length of between 3 and 5 mm of the sensing tips of the first, second, and third needles into the living tissue, a second end of the electrode holder being attached to a first end of the insertion part;

a releasing button placed on a surface of the insertion part in proximity of the first end of the insertion part, the releasing button being configured to release the sensing part from the first end of the insertion part for replacing the sensing part;

a handle head located at a second end of the insertion part; and

a switch located on the handle head, the switch configured to:

connect the electrochemical probe to the potentiostat device; and

disconnect the electrochemical probe from the potentiostat device.

2. The electrochemical probe of claim 1, wherein each catalyst layer comprises a layer of Nickel (Ni) with a thickness of less than 10 nm.

3. The electrochemical probe of claim 1, wherein:

each array of VAMWCNTs comprises VAMWCNTs with a length of between 0.5 μm and 10 μm, and

each array of VAMWCNTs comprises VAMWCNTs with a diameter of between 20 nm and 100 nm.

4. The electrochemical probe of claim 1, wherein each of the sensing tips has a diameter between 100 μm and 200 μm and a length between 0.3 cm and 1 cm.

5. The electrochemical probe of claim 1, wherein the first, second, and third needles are attached at the first end of the electrode holder apart from each other by a distance between 1 mm and 5 mm.

* * * * *